Mechanisms of sustained resistance towards Th1-mediated experimental liver injury

Dissertation

Zur Erlangung der Würde des Doktorgrades der Naturwissenschaften des Fachbereichs Biologie, der Fakultät für Mathematik, Informatik und Naturwissenschaften der Universität Hamburg

vorgelegt von

Benjamin Andreas Claaß

aus Rotterdam

Hamburg 2013

Genehmigt vom Fachbereich Biologie
der Fakultät für Mathematik, Informatik und Naturwissenschaften
an der Universität Hamburg
auf Antrag von Frau Professor Dr. G. TIEGS
Weitere Gutachterin der Dissertation:
Priv.-Doz. Dr. M. BRELOER
Tag der Disputation: 19. September 2013

Hamburg, den 05. September 2013

Professor Dr. C. Lohr
Vorsitzender des
Fach-Promotionsausschusses Biologie

Date: 07/24/2013

Miss Ellen Gardner
915 Oakcrest Street #9,
Iowa City,
Iowa,
52240,
USA

University of Iowa, Bsc Biomedical Engineering 2010 - June 2014

I, Ellen Gardner, testify that I have fully read over the doctoral thesis of Benjamin Claaß and declare that the English written is clear and free of grammatical errors.

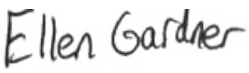

Full name

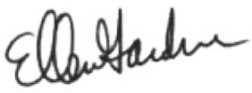

Signature

Contents

List of publications

Journal articles

Wintges K, Beil FT, Albers J, Jeschke A, Schweizer M, Claass B, Tiegs G, Amling M, Schinke T (2013). Impaired bone formation and increased osteoclastogenesis in mice lacking chemokine (C-C motif) ligand 5 (Ccl5). *Journal of Bone and Mineral Research*; doi: 10.1002/jbmr.1937. (Electronically published ahead of print)

Erhardt A, Wegscheid C, Claass B, Carambia A, Herkel J, Mittrücker HW, Panzer U, Tiegs G (2011). CXCR3 deficiency exacerbates liver disease and abrogates tolerance in a mouse model of immune-mediated hepatitis. *Journal of Immunology*; 186(9), 5284-93

Sharp FA, Ruane D, Claass B, Creagh E, Harris J, Malyala P, Singh M, O'Hagan DT, Pétrilli V, Tschopp J, O'Neill LA, Lavelle EC (2009). Uptake of particulate vaccine adjuvants by dendritic cells activates the NALP3 inflammasome. *Proceedings of the National Academy of Sciences of the USA*; 106(3), 870-5.

Abstracts of congress presentations

Claass B, Erhardt A, Tiegs G (2013). Induction of Sustained Tolerance towards Experimental ConA Hepatitis Depends on CD4+ T and NKT Cells. *Zeitschrift für Gastroenterologie*; 51(1) (Abstract P5.08)

Claass B, Erhardt A, Tiegs G (2012). Induction of sustained tolerance towards experimental ConA hepatitis depends on CD4+ T and NKT cells. *Immunology*; 137 (Suppl. 1), 503-504 (Abstract P0995)

Claaß B, Erhardt A, Tiegs G (2012). Re-programming of Kupffer Cells for immune regulation in response to ConA-induced liver injury. *Zeitschrift für Gastroenterologie*; 50(1) (Abstract P4.16)

Claass B, Erhardt A, Tiegs G (2011). Immune regulation in response to ConA-induced liver injury is mediated by regulatory T cells induced in dependence of IFNgamma. *Zeitschrift für Gastroenterologie*; 49(1) (Abstract P4.11)

Claass B, Erhardt A, Tiegs G (2010). Conversion of naïve T cells into regulatory T cells after tolerance induction in the murine liver. *Zeitschrift für Gastroenterologie*; 48(1) (Abstract P4.10)

Further congress presentations

Claass B, Erhardt A, Sparwasser T, Tiegs G (2010). Liver tolerance is mediated by activation of naturally occurring regulatory T cells (nTregs) in the model of concanavalin A hepatitis in mice. 40th Annual Conference of the German Society of Immunology, Leipzig

Claass B, Erhardt A, Tiegs G (2009). Conversion of naïve T Cells into regulatory T Cells after tolerance induction in the murine liver. Falk Workshop "Immunology and Liver Disease", Hanover

List of Abbreviations

αGalCer	α-galactosylceramide
AIH	autoimmune hepatitis
ALT	alanine aminotransferase
ASK1	apoptosis-signaling kinase-1
APC	antigen-presenting cell
ATP	adenosine triphosphate
BH	Benjamini-Hochberg
cAMP	cyclic adenosine monophosphate
caspase	cystein-aspartic protease
CD	cluster of differentiation
Con A	Concanavalin A
CT	threshold cycle
CTLA-4	cytotoxic T-lymphocyte-associated protein 4
CV	central vein
DC	dentritic cell
DD	death domain
DEREG	depletion of regulatory T cell
DNA	deoxyribonucleic acid

ELISA	enzyme-linked immunosorbent assay
FADD	Fas-associated protein with death domain
FasL	Fas ligand
Foxp3	forkhead box P3
GCK	germinal center kinase
GRE	gradient echo
H&E	hematoxilin and eosin
HSC	hepatic stellate cell
ICER	inducible cAMP early suppressor
ICS	intracellular cytokine staining
IFNγ	interferon-γ
IκB	inhibitor of κB
IKK	inhibitor of κB kinase
IL-2	interleukin-2
im-DILI	immune-mediated drug-induced liver injury
IL-10R	IL-10 receptor
iNKT	invariant NKT cells
IPEX	immunodysregulation polyendocrinopathy enteropathy X-linked syndrome
IVC	individually ventilated cage
i.p.	intraperitoneal
i.v.	intravenous

JNK	c-Jun N-terminal kinase
KC	Kupffer cell
KEGG	Kyoto Encyclopedia of Genes and Genomes
LN	lymph node
LPS	Lipopolysaccharide
LSEC	liver sinusoidal endothelial cell
mAB	monoclonal antibody
MEKK1	mitogen-activated protein kinase/extracellular signal regulated kinase kinase kinase-1
MHC	major histocompatibility complex
MIP-2α	macrophage inflammatory protein 2α, also termed CXCL2
MKK7	mitogen activated protein kinase kinase 7
MNC	mononuclear cell
mRNA	messenger RNA
MRI	magnetic resonance imaging
NEMO	NFκB essential modulator
neutrophil	neutrophil granulocyte
NFκB	nuclear factor κ-light-chain-enhancer of activated B cells
NK cell	natural killer cell
NKT cell	natural killer T cell
p38-MAPK	p38 mitogen-activated protein kinase
PAMP	pathogen-associated molecular pattern

PCR	polymerase chain reaction
PD-1	programmed cell death protein 1
PD-L1	PD-1 ligand 1, also termed B7-H1
PD-L2	PD-1 ligand 2, also termed B7-H2
PGE_2	Prostaglandin E_2
PBS	phosphate buffered saline
PRR	pattern-recognition receptor
PT	portal tract
RAG	recombination activating gene
RBC	red blood cell, erythrocyte
real-time RT-PCR	semi-quantitative real-time RT-PCR
RF	radio frequency
RIP	serine/threonine kinase receptor-interacting kinase
RNA	ribonucleic acid
ROS	reactive oxygen species
RT	room temperature
RT-PCR	reverse transcription PCR
SCID	severe combined immunodeficiency
STAT1	signal transducer and activator of transcription-1
T2w	T2-weighted
TCR	T cell receptor
TGFβ	tumor growth factor-β

Th cell	T helper cell
TLR	Toll-like receptor
TNFα	tumor necrosis factor-α
TNFR	TNF receptor
Tr1	type 1 regulatory T cell
TRADD	TNFR type 1-associated death domain protein
TRAF2	TNF receptor-associated factor 2
Treg	regulatory T cell
TSE	turbo-spin-echo
qT2st	quantitative T2*-relaxometry

List of Tables

List of Figures

1 Introduction

1.1 Liver anatomy and physiology

The liver fulfills pivotal functions regarding metabolism and detoxification in the human system. Its essential role is demonstrated by the fact that the liver is responsible for 20% of total body oxygen consumption and receives about 25% of the cardiac output during resting state although it accounts for only about 2% of body mass [Vollmar & Menger, 2009]. The liver is located in the upper quadrant of the abdomen separated from lung and heart via the diaphragm. In general, the liver is separated into four lobes: the right lobe, left lobe, quadrant lobe and caudate lobe. A more modern division established by Couinaud separates the liver into 8 segments regarding the branching pattern of the hepatic artery, portal vein and bile ducts (see fig. 1.1A) [Crawford & Burt, 2012; Couinaud, 1957].

Similar to the nomenclature of the lobes, there are diverse compartmentalization models of these lobes into smaller functional subunits. Two general compartmentation models are widely accepted and currently used. The first separates the parenchyma into hexagonal subunits termed lobules. Following this nomenclature, the portal tracts which consist of a portal vein, hepatic artery and bile duct occupy three of the 6 apices of the hexagon. The center of the lobule is shaped by the central vein [Crawford & Burt, 2012]. The second nomenclature subdivides the liver lobes into functional subunits termed liver acini regarding the way of blood supply and thus, this nomenclature highlights the progressive decline of oxygen concentration and nutrients along the sinusoids (see fig. 1.1B). The area most proximal to the portal tracts, from where blood is supplied to the parenchyma, is termed zone 1. The area neighboring the central vein, from where blood leaves the liver, is termed the terminal zone 3. Between zone 1 and zone 3, the midzonal area zone 2 is located [Rappaport et al., 1954].

Special discontinuous capillaries, the liver sinusoids, are surrounded by a fenestrated

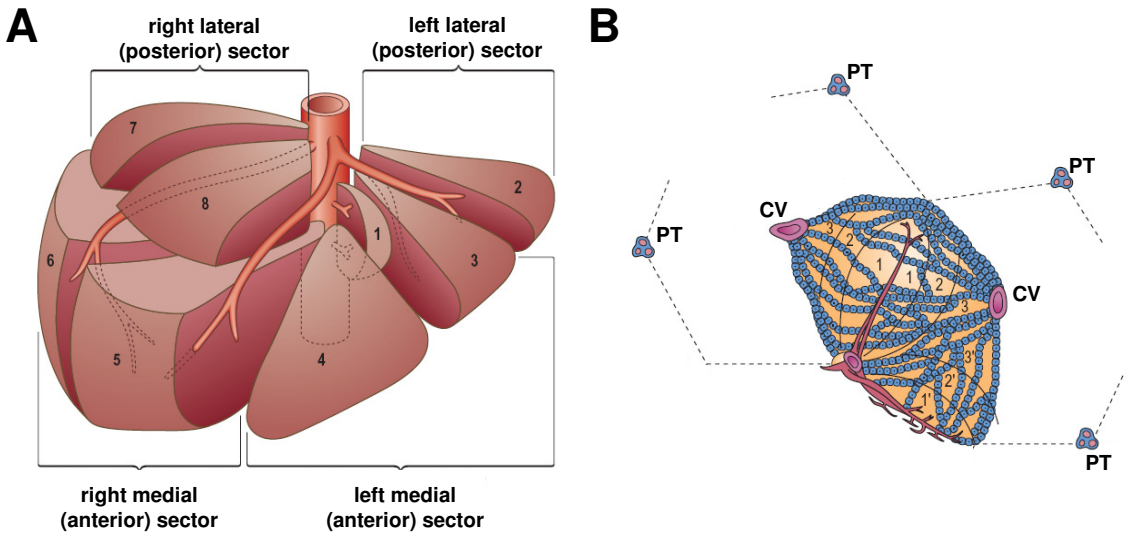

Source: [Crawford & Burt, 2012]

Figure 1.1: *Liver anatomy and microanatomy:* A) Liver segmentation according to Couinaud: Caudate lobe (1); left lobe: medio-superior (2), medio-inferior (3), latero-superior (4a), latero-inferior (4b, also known as quadrate lobe); right lobe: medio-inferior (5), latero-inferior (6), latero-superior (7) and medio-superior (8). B) Liver acinus describing the zonal arrangement of hepatocytes: liver sinusoids supplying the parenchyma with blood are fed from portal tracts and blood is transported from zone 1, via zone 2 and zone 3 into central veins. Oxygen concentration and nutrients decline progressively along zones. The dashed line shows the hexagonal organization of the classical liver lobule. PT=portal tract, CV=central vein.

monolayer of liver sinusoidal endothelial cells (LSECs) and provide the liver parenchyma with blood-derived oxygen and nutrients. The sinusoidal space, also termed space of Disse, lies between the endothelial layer of the sinusoids and the hepatocytes. Here is where hepatocytes make contact with plasma. The space of Disse is also where hepatic stellate cells (HSCs, also termed Ito cells) reside. In the quiescent state, these cells store vitamin A and retinol ester. HSCs can be activated upon liver damage and contribute to liver fibrogenesis [Crawford & Burt, 2012]. The liver resident macrophages, termed Kupffer cells (KCs), are located within the sinusoidal lumen. Here they are perfectly located to scan the passing blood for pathogens and debris that they phagocytose [Böttcher et al., 2011]. The sinusoids are furthermore populated by dentritic cells (DCs), which are typically found around central veins and portal tracts [Crawford & Burt, 2012]. Finally, compared to other organs, the liver sinusoids are occupied by a special composition of lymphocytes, including cells of the innate (NK and NKT cells) and adaptive (B and T

cells) immune system [Racanelli & Rehermann, 2006].
The liver receives dual blood supply [Vollmar & Menger, 2009]: It receives oxygen-enriched blood from the hepatic artery and gut-derived, nutrient-rich blood from the portal vein. Thus, liver sinusoids are fed with blood by branches of these vessels, arterioles and venules that run through the portal tracts. This blood supply of sinusoids underlies complex regulation. In general, about one third is supplied via the hepatic arterial system, whereas two thirds are supplied via the portal venous system. The blood flow rate in sinusoids can be controlled by sphincters composed of sinusoidal cells at the inlet and outlet of the sinusoids. Arterial blood flow can be furthermore controlled by contractile smooth muscle sphincters in the walls of arterioles. Therefore, blood in the sinusoids can be of arterial origin, venous origin, or a mixture of both depending on the activity of respective sphincters. Apart from sphincters, blood supply of single sinusoids can be controlled by LSECs themselves, which can vary the diameter of sinusoids by swelling or contracting in response to vasoactive substances. Moreover, Kupffer cells (KCs) and HSCs might play an important role in regulation of blood flow rate in the sinusoid [Vollmar & Menger, 2009].
Liver function seems to be heterogeneously distributed along the liver sinusoid [Crawford & Burt, 2012]. For example, it has been shown that periportal hepatocytes have a higher capacity for gluconeogenesis and fatty acid metabolism, whereas centriloblular hepatocytes have higher capacities for detoxification. This zonation is reflected in gene expression patterns of hepatocytes which differ depending on their position along the sinusoid. However, gene expression might be varied depending on metabolic or hormonal state. The zonal heterogeneity is not only characterized by differences in hepatocyte function, but moreover, by other components of the liver tissue. The course of sinusoids, for example, appears more tortuous with a narrower lumen in the periportal areas whereas pericentral sinusoids appear straighter and broader. Additionally, the fenestrae of LSECs are greater in number and diameter in the centrilobular region. KCs in periportal areas appear larger with more heterogeneous lysosomes and seem to be more active in phagocytosis than in pericentral areas, where they appear smaller and seem to be more active in cytokine production [Crawford & Burt, 2012; Malarkey et al., 2005]. From an immunological point of view, this anatomical location of highly phagocytotic KCs appears reasonable, because it provides a first line of defense against gut-derived potentially pathogenic molecules.

1.2 The immunological milieu of the liver

Via the portal vein gut-derived harmless nutrients, but also toxins and pathogens, like microbial constituents with an immunogenic potential, reach the liver. Consequently, cells in the liver are constantly challenged with so-termed pathogen-associated molecular patterns (PAMPs) that are recognized by pattern-recognition receptors (PRRs), like Toll-like receptors (TLRs). Engagement of PRRs typically results in the initiation of immune responses. In the liver, however, a rather anti-inflammatory milieu predominates under physiological conditions, i.e. induction of tolerance towards antigens is favored instead of inflammatory immune responses in the liver [Böttcher et al., 2011].
First evidence for the tolerance inducing capacities of the liver came from transplantation studies in pigs where it was shown that liver allografts were accepted across major histocompatibility complex (MHC) mismatch without immunosuppression, whereas skin, kidney and heart transplants were rapidly rejected [Tiegs & Lohse, 2010]. Moreover, co-transplantation of livers protected donor-specific skin, kidney and heart allografts but not third-party allografts from rejection. Later studies confirmed these observations in rodents. Even in humans, lung and kidney allograft survival was improved in patients that received livers of the same donor [Tiegs & Lohse, 2010]. Since then, remarkable knowledge about liver resident cells and their involvement in immunological regulation has been gained.

1.2.1 Lymphocyte populations in the liver

Lymphocytes make up 25% of non parenchymal cells in the liver and are of a specific composition. T cells account for about 63% of lymphocytes [Racanelli & Rehermann, 2006]. Conventional $\alpha\beta$ T cell receptor positive $CD8^+$ and $CD4^+$ T cells recognize their antigen in a classical MHCI- or MHCII- dependent manner, respectively. Activation of these cells is mediated by stimulation of their T cell receptor plus co-stimulation by CD28 binding to CD80 or CD86. Co-inhibitory molecules, like cytotoxic T-lymphocyte-associated protein 4 (CTLA-4) which also binds CD80 and CD86, or programmed cell death protein 1 (PD-1) which binds PD-1 ligand 1, also termed B7-H1 (PD-L1) and PD-1 ligand 2, also termed B7-H2 (PD-L2), might counterregulate T cell activation [Chen & Flies, 2013]. $CD8^+$ T cells are cytotoxic T lymphocytes that, upon activation, are able to kill target cells. $CD4^+$ T cells are known as T helper cells and are able

to guide an immune response either towards a cell-mediated cytotoxic response (Th1) or into a humoral response (Th2 cells) depending on their cytokine secretion. A Th1 response is characterized by high secretion of IFNγ, whereas Th2 cells rather produce IL-4, IL-5, IL-13 and IL-10 [Berger, 2000]. Other $CD4^+$ Th subsets exist, like Th17 cells and different subsets of T cells with regulatory functions (see section 1.3). Th17 cells produce large amounts of IL-17, but also IL-21 and IL-22. They are involved in clearance of pathogens and in the onset of tissue inflammation in autoimmune diseases [Korn et al., 2009]. In the liver, $CD4^+$ T cells are usually outnumbered by $CD8^+$ T cells, i.e. the ratio of $CD4^+$ T cells to $CD8^+$ T cells is inverted in comparison to the ratio in most other organs and peripheral blood [Racanelli & Rehermann, 2006].
Besides these conventional $CD4^+$ and $CD8^+$ T cells, unconventional T cells comprising $\gamma\delta$ T cell receptor expressing T cells ($\gamma\delta$ T cells), T cells expressing NK cell markers in addition to their T cell receptor (NKT cells), and others are extraordinarily frequent [Gao et al., 2008]. Unconventional $\gamma\delta$ T cells and NKT cells have a restricted T cell receptor repertoire and recognize conserved non-peptide antigens that are presented by MHC related molecules. Activation of $\gamma\delta$ T cells occurs even in the absence of T cell receptor stimulation and their effector functions include cytotoxicity and release of immunomodulatory cytokines [Bonneville et al., 2010]. NKT cells are highly abundant in the liver and comprise up to 30% of the liver lymphocyte population. NKT cells express NK cell markers and semi-invariant $\alpha\beta$ T cell receptors, i.e. their T cell receptor α chains usually contain the variable (V) and joining (J) segments, Vα14Jα18 in mice and Vα24Jα18 in humans, paired with a limited repertoire of β chain elements. They recognize glycolipids of microbial or mammalian origin presented by CD1d [Godfrey et al., 2010]. Activation of NKT cells induces a quick release of large amounts of cytokines like IFNγ and IL-4 but moreover, NKT cells are able to lyse target cells by death receptor engagement via FasL expression or by release of cytotoxic mediators from their granules including perforin and granzyme. Thus, NKT cells are able to efficiently modulate the immune response against invading pathogens, toxins and food antigens from portal venous blood [Swain, 2010]. Moreover, together with NK cells, which are also enriched in the liver sinusoids, they seem to play a key role in the removal of circulating tumor cells and in the killing of virus infected cells [Gao et al., 2008].

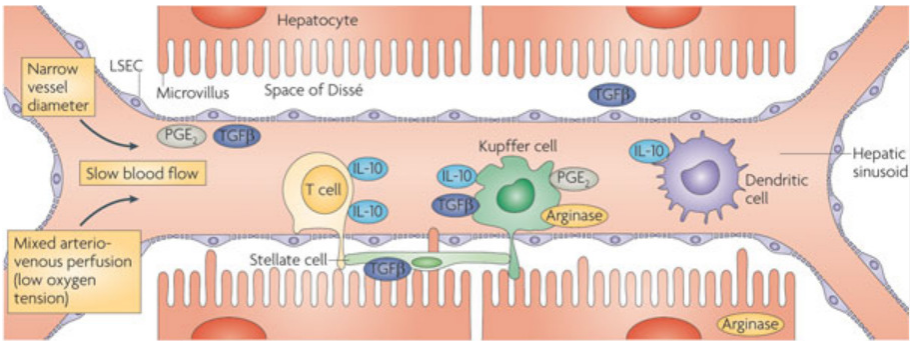

Source: [Thomson & Knolle, 2010]

Figure 1.2: *The anti-inflammatory milieu of the liver sinusoid:* Low blood flow and the fenestrated sinusoidal endothel allows the resident professional and non-professional APCs to interact with lymphocytes. Under non-inflammatory conditions all APCs, i.e. hepatocytes, LSECs, HSCs, KCs and DCs use a variety of mechanisms to induce a tolerogenic milieu.

1.2.2 Immmunological regulation by liver resident professional and non-professional antigen presenting cells

Hepatocytes account for about 60% to 80% of cells in the liver and their primary tasks are metabolism and detoxification [Böttcher et al., 2011]. On their apical site they build the bile canaliculi. On their basolateral site they are equiped with microvilli. These are membraneous protursions that might even squeeze through openings of the endothelial layer allowing the hepatocytes to contact the sinusoidal lumen. This enables the hepatocytes to efficiently take up molecules directly from plasma or after transcytosis from LSECs but also, to interact with lymphocytes residing in the sinusoids. Hepatocytes express MHCI molecules and are able to prime $CD8^+$ T cells, which under non-inflammatory conditions results in elimination of $CD8^+$ T cells due to lack of costimulation. During inflammation, hepatocytes are also able to express MHCII molecules enabling them to interact with Th cells. This interaction, however, leads to inhibition of the IFNγ-mediated Th1 response and favors the induction of Th2 responses. Expression of arginase by hepatocytes might deplete local L-arginine, which is essential for T cell function. Moreover, hepatocytes are able to induce anti-inflammatory regulatory T cells (Tregs), a cell population that is able to suppress inflammation by diverse mechanisms and is critical to maintain tolerance towards self antigens in the periphery [Böttcher et al., 2011]. Taken together, hepatocytes seem to have an important impact

on the generation of the tolerance-inducing liver milieu.
As phagocytes, KCs highly contribute to the clearing function of the liver by phagocytosis of particles like cellular debris bigger than 230 nm in diameter [Elvevold et al., 2008; Böttcher et al., 2011]. In a non-inflammatory liver state, KCs do not express MHCII or costimulatory molecules and favor suppression of immune cells by secretion of anti-inflammatory molecules like Prostaglandin E_2 (PGE_2). Moreover, they are able to activate Tregs and thereby stimulating further IL-10 production. In contrast, upon liver inflammation, KCs might be activated by TLR agonists and upregulate MHCII and costimulatory molecules enabling KCs to activate $CD4^+$ T cells and also $CD8^+$ T cells. As part of the innate immune system, KCs also possess immune effector functions including release of cytokines like TNFα, production of reactive oxygen species (ROS) and activation of the complement system [Böttcher et al., 2011]. Recently, it has been suggested that KC function might be compartmentalized to two different KC subpopulations, one highly phagocytotic active, ROS producing population, and one less phagocytotic active, cytokine secreting population, that contribute differently to liver immunology [Kinoshita et al., 2010].
Another important modulator of liver immunology are hepatic dendritic cells, which are enriched in the liver compared to other nonlymphoid organs [Böttcher et al., 2011]. However, hepatic DCs express rather low levels of MHCII and costimulatory molecules and thus, like other APCs in the liver, might rather favor suppression of T cells upon interaction with these. In comparison to splenic DCs, the inflammatory response of liver DCs is weaker and their maturation seems to be hindered upon TLR ligation [Böttcher et al., 2011].
HSCs have been shown to be able to express MHC class I and II molecules as well as CD1d and costimulatory but also coinhibitory molecules. Thus, although up to now poorly investigated, they might also contribute to liver immunological regulation. *In vitro* studies suggested that HSCs can prime $CD8^+$ T cells and activate NKT cells and induce immune responses [Böttcher et al., 2011].
LSECs account for up to 50% of the non-hepatocyte cell populations in the liver [Racanelli & Rehermann, 2006]. Besides accomplishing the exchange of molecules in plasma and hepatocytes passively, by building a leaky endothelium, and actively, by transcytosis, LSECs form together with KCs and DCs the reticular endothelial system of the liver which clears the system from toxins, pathogens and degradation products. LSECs are very active in endocytosis and take up soluble molecules to a size of about 230 nm

[Böttcher et al., 2011; Elvevold et al., 2008]. Furthermore, unlike any other endothelial cell, LSECs are able to modulate immune responses by expression of MHCII molecules and costimulatory molecules. Like in other liver APCs, expression of MHCII molecules and costimulatory molecules is very low under non-inflammatory conditions and expression of co-inhibitory molecules like PD-L1 is increased. Thus, LSECs induce tolerance upon interaction with T cells. Moreover, LSECs are very potent in the expansion of the Treg population and they might counteract DC-dependent T cell activation. However, under certain circumstances like very high antigen exposure or virus infection the tolerance inducing phenotype of LSECs can be lost enabling LSECs to prime T cells for proinflammatory responses [Böttcher et al., 2011].

1.3 T cells with regulatory functions

Tregs represent a mainly $CD4^+$ T cell population that is specified for suppression of immune responses [Josefowicz et al., 2012; Schmidt et al., 2012]. In the mouse, they can be identified by constitutive expression of CD25 and by their lineage specific transcription factor Foxp3 (forkhead box P3). In humans, however, Foxp3 might also be expressed by conventional T cells. Tregs are essential for systemic tolerance in mice and men and dysfunction of X-chromosome encoded Foxp3 results in severe autoimmune disease with multiple symptoms resulting in the 'scurfy' phenotype in mice and the immunodysregulation polyendocrinopathy enteropathy X-linked syndrome (IPEX) in humans [Josefowicz et al., 2012; Schmidt et al., 2012].
It has been demonstrated that Tregs can gain expression of transcription factors that are usually specific for certain T cell effector lineages [Barnes & Powrie, 2009]. For example, it has been demonstrated that IFNγ induces T-bet expression in Tregs [Koch et al., 2009]. In naïve conventional T cells, IFNγ induces STAT1-dependent T-bet and IL-12Rβ2 expression, which results in IL-12- and STAT4-dependent differentiation into IFNγ secreting proinflammatory Th1 cells [Afkarian et al., 2002; Mullen et al., 2001]. In Foxp3 expressing Tregs, however, the expression of the genetic locus for the IL-12Rβ2 chain is epigenetically silenced and therefore the Th1 differentiation program is blocked in Tregs (fig. 1.3)[Koch et al., 2012]. T-bet expression though enables Tregs to express a Th1-like chemokine receptor pattern and thus, T-bet^+ Tregs are recruited to the same inflammatory sites as Th1 cells allowing for efficient local suppression of overshooting

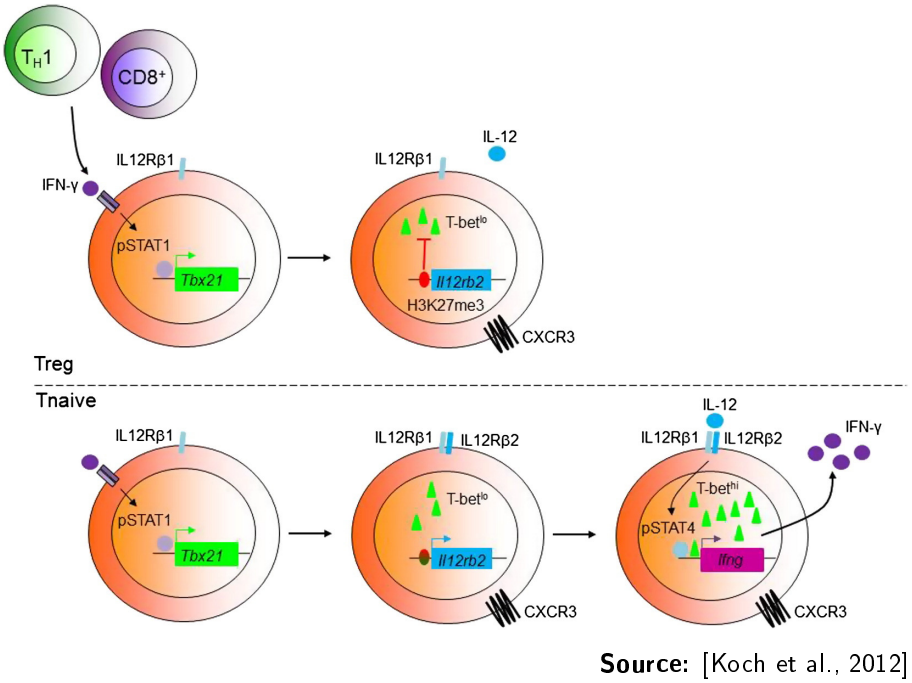

Source: [Koch et al., 2012]

Figure 1.3: *Induction of Th1-like Tregs:* IFNγ induces T-bet expression in Tcon and Tregs via a STAT1 dependent mechanism. This leads to IL-12R β2 expression in naïve T cells but not in Tregs because its genetic locus is epigenetically silenced. Thus, naïve T cells differentiate into proinflammatory Th1 cells while Tregs keep their suppressive characteristic but gain a Th1-like pattern of chemokine receptors which includes expression of CXCR3.

immune responses [Koch et al., 2009].

Tregs are equipped with multiple strategies to mediate immunosuppression [Schmidt et al., 2012]. First, Tregs secrete anti-inflammatory mediators like IL-10, IL-35 and tumor growth factor-β (TGFβ). Second, Tregs can suppress via contact dependent suppression mechanisms, e.g. CTLA-4 expressed on Tregs might interfere with antigen presentation by APCs. Third, Tregs are able to sequester the T cell stimulatory cytokine IL-2 via high expression of the IL-2 receptor α chain (CD25). Fourth, Tregs are able to produce high amounts of cyclic adenosine monophosphate (cAMP) and suppress conventional effector T cell activation in a manner of infectious tolerance. Tregs might 'infect' target cells with cAMP via direct contact and gap junctions thereby inducing expression of the inducible cAMP early suppressor (ICER), which functions as a suppressor e.g. at the IL-2 and IL-4 gene loci. Fifth, Tregs express the ectoenzymes CD39 and CD73 allowing for generation of adenosin from ATP, which also induces cAMP in target cells.

Sixth, Tregs might secrete cytolytic vesicles containing granzymes and perforin [Schmidt et al., 2012].
Besides Foxp3$^+$ Tregs, another CD4$^+$ T cell population with immunosuppressive potential has been discovered. These were termed Tr1 cells and are defined by high IL-10 secretion. They are furthermore characterized by lack of Foxp3 expression and high expression of TGFβ [Pot et al., 2011].

1.4 Inflammation induced liver injury

The hepatic immunologic milieu can be disturbed during liver disease. In many instances imbalanced innate and adaptive immune cells contribute to liver injury.
In autoimmune hepatitis (AIH) it is thought that infection of hepatocytes leads to their cytolysis by CD8$^+$ T cells and subsequent presentation of autoantigens together with expression of costimulatory molecules in the inflamed liver [Liberal et al., 2013]. Activated T cells stimulate proinflammatory responses e.g. by secretion of IFNγ and TNFα thereby stimulating innate immune cells. Under these conditions, liver resident CD4$^+$ T cells might also be activated in a MHCII dependent context enabling these cells to augment B cell activation and generation of autoantibodies. In addition to unwanted T cell activation, loss of counteracting immunosuppressive mechanisms might contribute to pathogenesis of AIH because there are studies showing reduced numbers of Tregs as well as reduced Treg function in AIH patients. Moreover, effector T cells from AIH patients might be less responsive to suppressive signals due to diminished expression of inhibitory molecules [Liberal et al., 2013].
Drugs can induce imbalanced hepatic immune responses culminating in immune-mediated drug-induced liver injury (im-DILI) [Adams et al., 2010]. Although the disease and its underlying mechanisms are highly diverse, a potential mechanism for im-DILI has been proposed. A given drug might be metabolized in the liver and an active metabolite conjugated to a host protein, most likely an enzyme responsible for disposal, might create a neoantigen. Upon cell damage this neoantigen might be recognized by B cells and also, upon presentation on MHC molecules, by T cells potentially leading to activation of these cell populations. This might result in adaptive immune-responses of an allergic or autoimmunologic manner against the drug or the host protein, respectively [Adams et al., 2010].

Alcoholic abuse or the metabolic syndrome might result in potentially hepatocellular-destructive lipid inclusions in hepatocytes a condition known as steatosis [Ian R. Mackay MD, 2007]. Although the lipid inclusions in itself are not necessarily injurious, it is often associated with inflammatory responses of the innate immune system that might co-activate cells of the adaptive immune system and result in chronic hepatitis, liver fibrosis and hepatocellular carcinoma [Ian R. Mackay MD, 2007].
In autoimmune mediated liver diseases like AIH, the specific auto-reactive immune response towards epitopes from proteins expressed in parenchymal cells determines parenchymal damage. For instance, presentation of the antigen on hepatocyte MHCI molecules can directly result in cytolysis by $CD8^+$ T cells [Liberal et al., 2013]. In other forms of liver disease, e.g. after warm and cold ischemia and reperfusion during liver resection and transplantation or endotoxemia, parenchymal liver damage might be determined by microvascular dysfunction. In these instances, KCs seem to initiate inflammation by high secretion of ROS upon activation, e.g. via TLR or complement receptor engagement [Vollmar & Menger, 2009]. KC derived ROS might primarily affect the liver sinusoidal endothelium, because oxidative stress was shown to induce intracellular gaps between LSECs and a reduction in the diameter of remaining fenestrations of LSECs [Cogger et al., 2004]. Furthermore, KC derived pro-inflammatory cytokines like TNFα, IL-6 and IL-1 contribute to subsequent leukocyte recruitment and adherence via induction of chemokines and cell adhesion molecules [Vollmar & Menger, 2009]. Through the increased permeability of the liver endothelium and recruitment of neutrophils, ROS production is augmented which results in close proximity of ROS and parenchyma. This process might lead to c-Jun N-terminal kinase (JNK) activation, which might mediate hepatocyte death. Furthermore, hepatocyte death might be induced by recruited lymphocytes via cytokine secretion, e.g. TNFα, and cytotoxic mediators, e.g. granzymes and perforin [Vollmar & Menger, 2009].

1.5 T cell mediated experimental hepatitis induced by Concanavalin A

In mice, hepatitis can be evoked by the injection of the plant lectin Concanavalin A (Con A) into the tail vein [Tiegs et al., 1992]. Con A functions as a T cell mitogen and activation of T cells probably involves engagement of the CD3 complex by Con A

[Kanellopoulos et al., 1985]. Most likely because of its accumulation in the liver sinusoids, Con A strongly stimulates $CD4^+$ T cell mediated inflammation in the liver with strong damage to the hepatocyte parenchyma that can be determined biochemically by highly increased activities of the hepatocyte specific enzyme alanine aminotransferase (ALT) in plasma [Gantner et al., 1995; Tiegs et al., 1992]. This model of experimental hepatitis shares several similarities with autoimmune hepatitis, these include [Gisa Tiegs, 2003]: First, both diseases are highly responsive to treatment with immunosuppressive drugs. Second, genetic predisposition of AIH is reflected by different susceptibility of mouse strains. Third, both diseases show prevalence of $CD4^+$ T cells. And fourth, in both diseases immunosuppression is observed upon remission [Gisa Tiegs, 2003]. Recently, even autoreactive antibodies were reported to occur and to peak 14 days after Con A challenge [Fujii et al., 2010]. However, because liver damage is manifested already several hours after intravenous (i.v.) Con A treatment, these antibodies most likely do not contribute to manifestation of liver disease. Despite these similarities, activation of the adaptive immune response is different in AIH compared to Con A induced hepatitis. In AIH, T cell activation is initiated via T cell receptor (TCR) engagement by specific epitopes whereas Con A induces a ploy clonal T cell response. Thus, the model of Con A induced experimental hepatitis does not completely reflect human liver disease. Nevertheless, the mechanisms resulting in hepatic parenchymal damage might also be involved in diverse human liver diseases and lessons can be learned about the complex regulation of the liver resident immune cells that might ultimately contribute to more specific therapeutical intervention.

1.5.1 Initiation of inflammation

Binding of Con A to liver sinusoids

After injection into the mouse tail vein Con A is transported via the blood circulation, i.e. Con A will be transported via the inferior vena cava into the right heart atrium and ventricle, from where it will first enter the pulmonary circulation. Only after having passed the pulmonary circulation Con A will enter into the aorta and systemic circulation via the left atrium and ventricle. Consequently, Con A will enter the liver via the hepatic artery or via the portal vein after having passed the intestinal capillary system. However, Con A seems to only accumulate in liver and bone marrow sinusoids and not in small vessel systems of any other organ [Gantner et al., 1995]. Therefore, the liver specificity

of Con A induced injury was suggested to result from its specific binding to LSECs and thus accumulation to the liver sinusoids.

Activation of T cells

Con A is a T cell mitogen and able to induce activation of T cells in the absence of APCs [Quintáns et al., 1989]. Activation of T cells has also been demonstrated to be a key event in Con A induced hepatitis because severe combined immunodeficient (SCID) and recombination activating gene (RAG) deficient mice that are both lacking T cells are completely protected against Con A doses that induce fulminant liver disease in wt mice [Tiegs et al., 1992; Kaneko et al., 2000]. Accordingly, it has been shown that the induction of hepatitis after Con A injection depends on $CD4^+$ T cells whereas $CD8^+$ T cells might play a minor role, because treatment with a depleting monoclonal antibody (mAB) against CD4 but not with a depleting mAB against CD8 protected from hepatitis [Tiegs et al., 1992]. Further investigations suggest that it is most likely the $CD4^+$ invariant NKT (iNKT) cell population that is responsible for initiation of liver inflammation because Vα14 deficient and CD1d deficient mice, which are both lacking iNKT cells, are protected against Con A induced hepatitis [Kaneko et al., 2000; Takeda et al., 2000]. Most likely, T and NKT cells initiate Con A induced inflammation by secretion of inflammatory mediators like IFNγ upon Con A stimulation *in vivo*. IFNγ was indeed shown to be critically involved in the onset of Con A induced liver injury because hepatitis is diminished in mice treated with a neutralizing anti-IFNγ antibody or in IFNγ deficient mice [Küsters et al., 1996; Mizuhara et al., 1996]. Therefore, Con A hepatitis is considered to be a Th1-driven inflammatory disease. In the early phase of disease, IFNγ might be responsible for induction of chemokine secretion and expression of adhesion molecules by liver resident cells including LSECs, KCs, and hepatocytes, which results in recruitment of inflammatory cells [Jaruga et al., 2004]. Moreover, IFNγ mediated activation of KCs might induce the release of large amounts of TNFα by these cells [Kawada et al., 1991]. TNFα is another cytokine that was shown to be essential for Con A induced liver disease and both, TNFα secreting KCs as well as TNFα secreting T and NKT cells, are equally indispensable for onset of liver damage [Grivennikov et al., 2005]. Besides these cell populations, neutrophil granulocytes (neutrophils) bind to the endothelium and invade the liver even before T cells and it has been demonstrated that they are critically involved in the onset of disease as well [Bonder et al., 2004].

1.5.2 Damage of Liver Parenchyma

In the Con A model, the mechanism by which hepatocytes are killed is not fully understood. Because TNFα deficiency, as well as TNF receptor I (TNFRI) or TNFRII deficiency, protect mice against Con A induced hepatitis, TNFα signaling is clearly involved [Küsters et al., 1997]. TNFα in combination with transcriptional inhibitors induces apoptosis in hepatocytes *in vitro* and *in vivo* and therefore it is thought that TNFα also contributes to liver damage by direct induction of death signaling in hepatocytes upon Con A challenge [Lehmann et al., 1987; Leist et al., 1994].
In principle, TNFRI signaling is initiated by assembly of the TNFR type 1-associated death domain protein (TRADD) with the intracellular death domain (DD) of the TNFR [Wajant et al., 2003]. This assembly will further recruit the TNF receptor-associated factor 2 (TRAF2) and the death domain containing serine/threonine kinase receptor-interacting kinase (RIP) and this complex results in the activation of three different pathways as reviewed e.g. by Wajant et al. [Wajant et al., 2003]: TRAF2 recruits the inhibitor of κB kinase (IKK) complex consisting of IKK1 and IKK2 (IKKα and IKKβ), the regulatory protein NFκB essential modulator (NEMO, also known as IKKγ), and chaperone proteins. RIP activates this complex which leads to phosphorylation and degradation of the inhibitor of κB (IκB). Thereby, the heterodimeric transcription factor nuclear factor κ-light-chain-enhancer of activated B cells (NFκB) is released and translocates to the nucleus where it enables transcription of various genes involved in cell survival, proliferation and inflammation. Moreover, TRAF2 is able to recruit and activate members of the germinal center kinase (GCK) family or to activate production of ROS. Thereby, the upstream kinases MEKK1 (mitogen-activated protein kinase/extracellular signal regulated kinase kinase kinase-1) and ASK1 (apoptosis-signaling kinase-1) are activated. Via additional kinases like MKK7 (mitogen activated protein kinase kinase 7) JNK and p38 mitogen-activated protein kinase (p38-MAPK) are activated. Depending on the cellular context, this pathway can be pro- or anti-apoptotic. Finally, TRADD is able to recruit the Fas-associated protein with death domain (FADD), which leads to autoproteolytic activation of the cystein-aspartic protease-8 (caspase 8). Active caspase 8 leads to apoptosis induction by cleavage and activation of downstream effector caspases. However, without inhibition of transcription death signaling by TNFRI is usually masked by NFκB dependent gene regulation.
Although a single study suggested caspase 8 involvement in hepatocyte death in the

model of ConA induced hepatic injury [Kaufmann et al., 2009], several studies reported that NFκB signaling as well as caspase 8 mediated activation of downstream effector caspases do not contribute to hepatocyte damage after Con A challenge but instead might play protective roles [Streetz et al., 2001; Maeda et al., 2003; Beraza et al., 2009; Liedtke et al., 2011]. Consequently, it was concluded that the third TNFα signaling pathway via JNK activation might be involved in death signaling in hepatocytes [Streetz et al., 2001; Maeda et al., 2003]. Surprisingly, more recent studies indicated that JNK signaling in hepatocytes is not essential for parenchymal damage after Con A challenge [Ni et al., 2008; Das et al., 2009]. In this regard, it is important to mention, that contribution of TNFα to hepatic damage specifically via TNFR signaling in hepatocytes has never been explicitly shown. Thus, it cannot be excluded that TNFα acts on cells other than hepatocytes.

It was demonstrated that preactivated T cells were able to kill hepatocytes in the presence of Con A *in vitro*. Interestingly, T cell mediated cytotoxicity against hepatocytes was perforin dependent but independent from TNFα [Watanabe et al., 1996]. *In vivo*, a role for Fas and FasL has been confirmed because FasL deficient gld/gld mice are completely protected from Con A induced hepatitis and Fas deficient lpr/lpr mice show at least reduced disease activity [Tagawa et al., 1998; Seino et al., 1997]. The role for NKT cells in Con A induced hepatitis depends on both, perforin and FasL expression, indicating that NKT cells are mainly responsible for these cytotoxic mechanisms after Con A challenge [Kaneko et al., 2000; Takeda et al., 2000]. However, as for TNFα signaling, clear *in vivo* evidence of direct destruction of hepatocytes by FasL or perforin is lacking.

Thus, Con A activated T cell cytotoxicity might target cells other than hepatocytes, e.g. the liver endothelial barrier. *In vitro* activated T cells kill LSECs in presence of Con A upon coculture, which was independent from TNFα signaling [Knolle et al., 1996]. Nevertheless, other studies reported TNFα and IFNγ dependent impairment of the liver microcirculation upon Con A challenge preceding the actual death of hepatocytes [Miyazawa et al., 1998]. A role for microcirculatory dysfunction in manifestation of Con A induced liver disease is furthermore supported by an investigation showing that KC derived ROS are involved in disease generation [Nakashima et al., 2008]. As described above, ROS heavily affect the liver sinusoidal endothelium which again might lead to increased permeability. On the one hand, this might facilitate migration of cytotoxic lymphocytes into the parenchyma. On the other hand, increased permeability

might also enhance leakage of ROS to the parenchyma and because ROS generation is most likely increased by recruited neutrophils after Con A challenge and because ROS can be hepatotoxic, this might provide an additional mechanism of Con A induced hepatic injury [Jaeschke, 2011].

1.5.3 Liver protective mechanisms in Con A hepatitis

Besides the anti-apoptotic effects of NFκB other hepato-protective mechanisms, especially potential regulators of inflammation, have been investigated in the model of Con A induced hepatitis. Although IL-6 is involved in recruitment of harmful neutrophils after Con A injection and thereby contributes to disease progression, IL-6 also mediates potentially protective signals in the healthy liver before and maybe immediately after Con A challenge [Malchow et al., 2011; Mizuhara et al., 1994; Tagawa et al., 2000]. Liver protection by IL-6 is most likely mediated by STAT3 signaling which might inhibit NKT cells and induce anti-apoptotic signals like Bcl-X_L in hepatocytes [Sun et al., 2004; Hong et al., 2002]. IL-22 is another cytokine that also signals via STAT3, but its receptor is not expressed on any immune cells but rather on parenchymal cells. IL-22 can be secreted by various T cell populations including unconventional $\gamma\delta$ T and NKT cells, which, as described above, are highly abundant in the liver [Wolk et al., 2010]. Indeed, IL-22 is secreted upon Con A challenge resulting in the induction of anti-apoptotic factors in hepatocytes and thus, IL-22 has a protective effect in Con A induced liver disease [Radaeva et al., 2004]. A very prominent anti-inflammatory role was shown for IL-10, which reduces injury to liver parenchyma most likely by downregulation of IFNγ and TNFα [Louis et al., 1997; Di Marco et al., 1999]. Moreover, it was shown that repeated injections of Con A into mice stimulate IL-10 secretion upon later injections which correlates with decreased ALT activities in plasma [Louis et al., 2000]. Later studies confirmed that IL-10 was indeed upregulated upon a second Con A challenge 8 days after a first Con A pretreatment [Erhardt et al., 2007; Ye et al., 2009]. In those studies, increased IL-10 levels were demonstrated to protect against hepatic damage and it was suggested that enhanced IL-10 levels were derived from KCs and Tregs or from Tr1 cells. A role for suppression of pro-inflammatory T cells by Tregs was also suggested by other studies. Wei et al. demonstrated higher abundance of Tregs in the liver shortly after Con A challenge and reported that Tregs protect against Con A induced liver injury by secretion of TGFβ [Wei et al., 2008]. Hegde et al. showed that cannabinoid treatment

shortly after Con A challenge increased absolute numbers of Tregs in livers and correlated with reduced liver injury [Hegde et al., 2008]. Finally, in a recent study, Erhardt et al. demonstrated that CXCR3 deficient mice exhibited reduced numbers of Tregs in their livers compared to wt mice and this correlated with enhanced liver damage upon Con A challenge [Erhardt et al., 2011]. Taken together, the model of Con A induced hepatitis can be used to understand mechanisms of liver destruction as well as to understand potentially protective mechanisms during immune-mediated inflammatory liver injury.

1.6 Aims of this study

Intravenous Con A injection induces hepatitis in mice and includes mechanisms of liver injury that also play a role in human hepatitides. Recently, it has been demonstrated by colleagues from this laboratory, that Con A pretreatment of mice results in resistance towards Con A rechallenge 8 days later as shown by significantly diminished ALT levels in plasma of rechallenged mice compared to levels of single Con A treated mice [Erhardt et al., 2007]. Proinflammatory cytokines IL-6, IL-2, IFNγ and TNFα were also decreased upon Con A challenge of Con A pretreated mice while IL-10 was upregulated. In the same study, liver protection was suggested to be mediated by immunosuppression via the anti-inflammatory cytokine IL-10. It could be shown that IL-10 secretion was dependent on presence of KCs and $CD25^+$ Tregs and that IL-10 deficient mice were not protected against Con A rechallenge 8 days after Con A pretreatment. Therefore, the authors of that study postulated that Tregs and KCs are able to inhibit liver inflammation by immunosuppression via secretion of IL-10. Preliminary data from this laboratory indicated that resistance towards Con A induced hepatic injury also occurs at later time points than 8 days after Con A pretreatment. However, in these settings IL-10 was less upregulated suggesting that IL-10 might play a minor role in resistance towards Con A induced hepatitis later after Con A pretreatment.
First, the inflammatory response to Con A was investigated in mice 14 days after Con A pretreatment. This was done by analyzing the systemic and hepatic cytokine profile via enzyme-linked immunosorbent assay (ELISA) and semi-quantitative real-time reverse transcription polymerase chain reaction (real-time RT-PCR), respectively. Potential sources of cytokines were determined by staining of intracellular cytokines and flow-cytometric analysis. Furthermore, it was tested if mechanisms that were postulated to

be protective in Con A hepatitis 8 days after Con A pretreatment might also play a role in protection 14 days after Con A pretreatment. This was done by antagonizing the anti-inflammatory cytokine IL-10 via a neutralizing mAB or via a mAB that blocks the IL-10 receptor (IL-10R). Experiments including depletion of Tregs or KCs were conducted to investigate a potential role for these cells in resistance towards Con A induced hepatic damage. To analyze a potential role for the entire $CD4^+$ T cell population, reconstitution experiments were performed in $RAG1^{-/-}$ mice, that are otherwise resistant to Con A induced hepatitis. Finally, it was investigated which processes involved in hepatodestruction are inhibited in Con A pretreated mice. Via immunohistology and FACS analysis it was analyzed if the livers of Con A pretreated mice are still targeted upon Con A rechallenge. Moreover, it was tested if liver microcirculation is intact upon Con A challenge of Con A pretreated mice. Finally, microarray analyses from liver tissue were performed to detect potential suppression of gene expression involved in inflammatory conditioning of the liver or to detect inhibition of liver detrimental signaling pathways.

2 Materials and methods

2.1 Materials

2.1.1 Technical equipment

Table 2.1: Technical equipment

equipment	**supplier**
7.0T MRI ClinScan	Bruker, Ettlingen
ATILON ATL-423-I millgram lab balance	Acculab Sartorius, Göttingen
C1000™ Thermal Cycler with CFX96™ Real-Time PCR Detection System	BioRad, München
Casy® Cell Counter	Roche, Basel CH
Centrifuge 5417R	Eppendorf, Hamburg
Centrifuge 5810R	Eppendorf, Hamburg
CK40 microscope	Olympus, Hamburg
COBAS Integra® 400 plus	Roche, Basel CH
Cobas c111	Roche, Basel CH
Cobas Mira	Roche, Basel CH
Eppendorf Research® Plus Pipettes	Eppendorf, Hamburg
BD LSR Fortessa™	BD Biosciences, Heidelberg
FACS Canto™ II	BD Biosciences, Heidelberg
G3013 Comfort	Liebherr, Biberach an der Riss
GeneChip® Scanner 3000 7G	Affimetrix, Santa Clara, USA
HandyStep® electronic Repeating Pipette	BRAND GmbH, Wertheim

Table 2.1 – continued from previous page

equipment	**supplier**
IKA Magnetic Stirrer RCT	Janke und Kunkel, Staufen
KC10 coagulation instrument	Amelung, Lemgo
DM IRE2 confocal microscope	Leica, Wetzlar
MDF U53V -86°C Freezer	Sanyo, München
Microm CryoStar Cryostat	Thermo Fisher Scientific, Hamburg
MSC Advantag Clean Bench	Thermo Fisher Scientific, Hamburg
MyCycler™	Thermal Cycler BioRad, München
NanoDrop® ND-1000	PEQLAB Biotechnologie GmbH, Erlangen
Pressure pad	SA Instruments, New York, USA
QuadroMACS™ Separator	Miltenyi Biotec, Bergisch Gladbach
TE124S Analytical Weight Scale	Sartorius, Göttingen
Tecan Infinite® M200	Tecan, Crailsheim
Tecan M8/2R ELISA washer	Tecan, Crailsheim
Vortex Mixer	Heidolph, Schwabach

2.1.2 Consumables

Table 2.2: Consumables

consumable	**supplier**
Nunc 96 well microtiter plate, black	ThermoFisher, Hamburg
ABgene PCR tubes	ThermoFisher, Hamburg
canulaes (hollow needles)	B.Braun Melsungen AG, Melsungen
Pre-Separation Filters (30 µm)	Miltenyi Biotec, Bergisch Gladbach
MACS® Separation Colums (LD, LS, MS)	Miltenyi Biotec, Bergisch Gladbach
Microlon® 600 high binding microplates	Greiner Bio-one GmbH, Frickenhausen
BD Falcon™ Cell Strainer (100 µm)	BD Biosciences, Heidelberg

Table 2.2 – continued from previous page

consumable	**supplier**
Parafilm M®	American National Can. USA
Pipette tips (10 µl, 200 µl, 1000 µl)	Sarstedt, Nümbrecht
Pipette tips, sterile and RNAse free (10 µl, 200 µl, 1000 µl)	Sarstedt, Nümbrecht
Pipettes (2 ml, 5 ml, 10 ml, 25 ml)	Sarstedt, Nümbrecht
Positive Displacement Tips (500 µl, 2.5 ml, 5 ml 12.5 ml)	BRAND GmbH, Wertheim
Reaction tubes (1,5 ml, 2 ml)	Sarstedt, Nümbrecht
Reaction tubes (13 ml, 15 ml, 50 ml)	Sarstedt, Nümbrecht
Reaction tubes, sterile and RNAse free	(1,5 ml, 2 ml) Sarstedt, Nümbrecht
Sealing Tape, optically clear	Sarstedt, Nümbrecht
SuperFrost® microscope slides	ThermoFisher, Hamburg
Syringes	B.Braun, Melsungen AG, Melsungen
syringe filter (0.22 µm)	TPP, Trasadingen, CH
flow cytometer tubes	Sarstedt, Nümbrecht

2.1.3 Reagents and kits

Table 2.3: Reagents and kits

reagents and kits	**supplier**
ABgene Verso cDNA Kit	Thermo Scientific, Hamburg
Acetic acid	Roth, Karlsruhe
Agarose	Serva, Heidelberg
ALT reagents	Roche, Basel CH
anti-rat-IgG-Alexa546	Invitrogen, Carlsbad, USA
BM8 anti-F4/80	BioLegend, San Diego, USA
bovine serum albumin (BSA)	Serva, Heidelberg

Table 2.3 – continued from previous page

reagents and kits	**supplier**
Brefeldin A (BFA)	Sigma-Aldrich, Taufkirchen
calcium chlorid dihydrate (CaCl)	Sigma-Aldrich, Taufkirchen
$CD4^+CD25^+$ Regulatory T cell Isolation Kit	Miltenyi Biotec, Bergisch-Gladbach
clodronate liposomes	Nico van Rooijen, Vrije Universiteit, Amsterdam, The Netherlands
Collagenase	Serva, Heidelberg
Concanavalin A	Sigma-Aldrich, Taufkirchen
CD1d, APC-labeled, PBS57 loaded	Emory Vaccine Center, Yerkes, Emory University, Atlanta, USA
Dade® Innovin®	Siemens Healthcare Diagnostics Products GmbH, Marburg
D-glucose	Roth, Karlsruhe
Dimethylsulfoxid (DMSO)	Roth, Karlsruhe
diphteria toxin	Calbiochem, Merck, Darmstadt
di-sodiumhydrogenphosphatlydrate (Na2HPO4)	Roth, Karlsruhe
dNTPs (10mM)	Invitrogen GmbH, Darmstadt
EDTA	Roth, Karlsruhe
Ethanol	Roth, Karlsruhe
Ethidiumbromid	Roth, Karlsruhe
fetal calf serum (FCS)	Lonza, Cologne
Fixable Viability Dye eFluor® 506	eBiosciences, San Diego, USA
Formaldehyde, 37% solution	Roth, Karlsruhe
Foxp3 Staining Buffer Set	eBioscience, Frankfurt
GBSS	Sigma-Aldrich, Taufkirchen

Table 2.3 – continued from previous page

reagents and kits	**supplier**
GeneChip®	Affimetrix, Santa Clara, USA
Gibco® 2-Mercaptoethanol	Invitrogen, Darmstadt
Gibco® penicillin/streptomycin (100U/ml)	Invitrogen, Darmstadt
HemosIL™	Instrumentation Laboratory, Kirchheim, Germany
heparin-sodium-25000-ratiopharm®	ratiopharm, Ulm
HEPES	Roth, Karlsruhe
hydrochloric acid	Roth, Karlsruhe
Ionomycin	Sigma-Aldrich, Taufkirchen
Ketamin	Gräub Albrecht GmbH, Aulendorf
Lipopolysaccharide (LPS)	Sigma-Aldrich, Taufkirchen
MACS® $CD4^+$ T Cell Isolation Kit II	Miltenyi Biotec, Bergisch-Gladbach
magnesium chloride hexahydrate (MgCl)	Roth, Karlsruhe
magnesium sulfate hexahydrate (MgSO4)	Merck, Darmstadt
Fermentas Maxima™ SYBR Green/ROX Master Mix (2X)	Thermo Scientific, Hamburg
Methanol	Roth, Karlsruhe
Mouse IFNγ ELISA MAX™ Standard	BioLegend, San Diego, USA
Mouse TNFα ELISA MAX™ Standard	BioLegend, San Diego, USA
NucleoSpin® RNA II Kit	Machery & Nagel, Düren
Optiprep®	Sigma-Aldrich, Taufkirchen
Paraformaldehyd	Roth, Karlsruhe
PCR Buffer (10x)	Invitrogen, Darmstadt
Percoll	GE Healthcare, Glattbrugg/Zürich, CH
phorbol 12-myristate 13-acetate (PMA)	Sigma-Aldrich, Taufkirchen
potassium chloride (KCl)	Roth, Karlsruhe
potassium dihydrogen phosphate (KH2PO4)	Sigma-Aldrich, Taufkirchen

Table 2.3 – continued from previous page

reagents and kits	**supplier**
rDNAse	Machery & Nagel, Düren
recombinant IL-10	BD Pharmingen, Heidelberg
recombinant IL-2	BD Pharmingen, Heidelberg
recombinant- IL-6	BD Pharmingen, Heidelberg
RNeasy® Micro Kit	Machery & Nagel, Düren
RPMI Gibco®	Invitrogen, Darmstadt
Sedaxylan	WDT, Gabsen
sodium azide (NaN3)	Roth, Karlsruhe
sodium chloride (NaCl)	AppliChem, Darmstadt
sodium chloride solution 0.9%, isotone	B.Braun Melsungen AG, Melsungen
sodium dihydrogen phosphate dihydrate (NaH2PO4)	Roth, Karlsruhe
sodium hydrogencarbonate (NaHCO3)	Roth, Karlsruhe
sodium hydroxide	Roth, Karlsruhe
Streptavidin horseradish peroxidase (HRP)	R&D, Minneapolis, USA
Sucrose	Roth, Karlsruhe
sulforic acid (H2SO4)	Roth, Karlsruhe
s+16a nanobody	Institute of Immunology, University Hospital Hamburg-Eppendorf
TMB Substrate Reagent Set	BD Opteia, Heidelberg
Tris-Base	Sigma-Aldrich, Taufkirchen
Tris-HCl	Roth, Karlsruhe
Trypan blue	Sigma-Aldrich, Taufkirchen
Tween 20	Roth, Karlsruhe

2.1.4 Buffers and solutions

Table 2.4: Buffers and solutions

Buffer or solution	**recipe**
ELISA blocking solution	1% BSA
	5% Sucrose
	0.8 mM NaN3 (0,05%)
	in PBS
ELISA coating buffer	0.1 M Na2HPO4
	0.1 M NaH2PO4
	pH 8.2
ELISA diluent buffer	0.1% BSA
	0.05% Tween 20
	20 mM Tris
	150 mM NaCl
	pH 7.2-7.4
ELISA washing buffer	PBS
	0.05% Tween 20
HBSS	5.4 mM KCl
	0.3 mM Na2HPO4 x 7 H2O
	4.2 mM NaHCO3
	1.3 mM CaCl2
	0.5 mM MgCl2 x 6 H2O
	0.6 mM MgSO4 x 7 H2O
	137 mM NaCl
	5.6 mM D-glucose
	pH 7.4
PBS 137.9	mM NaCl
	6.5 mM Na2HPO4 x 2 H2O
	1.5 mM KH2PO4
	2.7 mM KCl
	pH 7.4
MACS buffer	PBS

Table 2.4 – continued from previous page

Buffer or solution	**recipe**
FACS buffer	0.5% BSA 2 mM EDTA PBS 1% BSA 15.4 mM NaN3 (0.1%)
Ketamin-Xylacin-Heparin	8% Sedaxylan 12% Ketamin 20% Heparin 5000 (IU/mL) 60% isotonic NaCl
collagenase solution	0,5 mg/ml collagenase in GBSS
Ammoniumchloride (NH4Cl) (RBC lysis solution)	19 mM Tris-HCl 140 mM NH4Cl pH 7.2
4% Paraformaldehyd	10% Formaldehyde 20% PBS- (5x) in H2O

2.1.5 Software

Table 2.5: Software

Software	**company**
Windows XP	Microsoft GmbH, Seattle, USA
MS Office 2003	Microsoft GmbH, Seattle, USA
GraphPad Prism v5	GraphPad Software, La Jolla, USA
BD FACS Diva v6.1	BD Biosciences, Heidelberg
Zotero	Roy Rosenzweig, Center for

Table 2.5 – continued from previous page

Software	**company**
	History and New Media, Fairfax, USA
Primer3	Whitehead Institute for Biomedical Research, Cambridge, USA
SPSS	IBM, New York, USA
Tecan Magellan v6.5	Tecan, Crailsheim

2.2 Methods

2.2.1 Mice

Housing

C57Bl/6J mice were obtained from the central animal facilities at the University Medical Center Hamburg-Eppendorf. All Knock-Out mice were on a C57Bl/6J background. Depletion of Regulatory T cell (DEREG) mice were a kindly gift from Tim Sparwasser, Hanover, and RAG1$^{-/-}$ from Oliver Steinmetz, Hamburg. All mice received human care according to the guidelines of the National Institute of Health and legal requirements in Germany. All mice were bred and held in individually ventilated cages (IVCs) under controlled conditions (20°C ± 2°C, 50% ± 5% relative humidity, 12-hour day/night rhythm) at the same animal facility and were fed standard laboratory chow.

Animal treatments

To induce hepatic inflammation in a mouse liver, Concanavalin A was dissolved in sterile PBS or sterile saline solution and was administered in a total volume of 10µl/g body weight into the tail vein of a mouse [Tiegs et al., 1992]. Control mice received 10µl/g solvent. Protection against hepatic parenchymal injury was induced by a low, sublethal dose of Con A injected i.v. fourteen days before Con A challenge. Doses of Con A treatments are specified in correspondent experiment protocols in the results chapter. DEREG mice were used for depletion of Tregs. Each DEREG mouse received

1µg Diphteria Toxin (DT) intraperitoneally (i.p.) dissolved in sterile PBS [Lahl et al., 2007]. Control mice received sterile PBS. To deplete mice of Kupffer Cells 100µl of a 7 mg/ml liposome-encapsulated dichloromethylene-bisphosphonate PBS solution (clodronate liposomes, provided by Nico van Rooijen, Vrije Universiteit, Amsterdam, The Netherlands) were injected intravenously [Van Rooijen & Sanders, 1994]. For reconstitution of $CD4^+$ cells in $RAG1^{-/-}$ mice, 0.5 x 10^6 enriched $CD4^+$ cells were injected i.v. in 200µl sterile PBS. IL-10 was neutralized and IL-10 receptor (IL-10R) was blocked by i.v. injection of 500 µg of specific mAB one hour before Con A pretreatment or Con A challenge.

Anesthesia

To sample material mice were anesthetized by i.v. administration of isotonic saline solution containing 10% ketamin (120mg/kg) and 2% xylazin (5mg/kg) as well as 800 U/ml heparin to protect blood from clotting. To sample plasma for prothrombin time measurement animals were anesthetized by 10% ketamin and 2% xylazin solution without heparin.

2.2.2 Sampling of material

Withdrawal of organs

Blood was drawn by cardial puncture after anesthesia. Plasma was obtained by centrifugation of blood at 14000 x g for 5 min. Subsequently, liver, liver-draining celiac lymph nodes (LN) and spleen were excised and kept in HBSS.

Isolation of leukocytes from spleen, lymph node, or blood

Single cell suspensions from spleen and lymph nodes were prepared by pressing organs through 100µm nylon meshes in HBSS. After centrifugation at 500 x g for 5 min, pellets of LN cells were resuspended in PBS and cell pellets of homogenized spleens were subjected to red blood cell (RBC) lysis by incubation in RBC lysis solution for 10 min at room temperature. Afterwards, splenocytes were washed and resuspended in PBS. 60µL of blood were subjected to RBC lysis, washed and resuspended in PBS.

Isolation of intrahepatic mononuclear cells

Liver leukocytes were separated from hepatic parenchymal cells via density gradient centrifugation as described previously [Liu et al., 2000]. Briefly, livers were pressed through 100µm nylon meshes in HBSS and centrifuged at 500 x g for 5 min. The cell pellet was resuspended in isotonic 36% Percoll/HBSS solution containing 100U/L heparin and centrifuged at 800 x g for 20 min. Thereafter, cells were subjected to RBC lysis as described above and washed in HBSS. Subsequently, the cell pellet was resuspended in cold PBS.

Enrichment of $CD4^+$ T cells

To enrich $CD4^+$ T cells, magnetic sorting of cells was performed by a negative selection procedure with usage of the MACS $CD4^+$ T Cell Isolation Kit II according to the manufacturer's protocol. In brief, splenocytes or liver mononuclear cells (MNCs) were labeled with a cocktail of biotinylated antibodies against the surface molecules CD8a, CD11b, CD11c, CD19, CD45R, CD49b, CD105, MHCII and Ter-119. Cells expressing these markers were then magnetically labeled by streptavidin coupled beads. Upon running the cell solution through a column placed into a magnetic field, all labeled cells were retained within the column, while unlabeled, mainly $CD4^+$ T cells were collected with the run-through.

Messenger RNA isolation

RNA from liver tissue was isolated with the help of the NucleoSpin® RNA II kit according to the manufacturer's protocol. RNA concentration was determined by photometric measurement via a NanoDrop® ND-1000.

2.2.3 Gene expression analysis

Reverse transcriptase reaction

One µg of RNA was transcribed to cDNA using oligoDT primers and the ABgene Verso™ RT-PCR Kit according to the manufacturer's protocol.

Semi-quantitative real time PCR

Semi-quantitative real time PCR was performed using the Absolute^{TM} QPCR SYBR Green Mix. One µl of cDNA was added to an aqueous solution of Absolute^{TM} QPCR SYBR Green Mix and primer pairs specific for the transcribed gene of interest. Primers were designed for detection of exon overlapping amplicons and were obtained from metabion, Martinsried (see table 2.6), and applied at a final concentration of 0,7 mM. For calculation of relative mRNA expression, the relative threshold cycle (ΔCT) was first calculated by normalization of CT values of the genes of interest to reference β-actin CT values for every sample. Relative quantification of sample mRNA content ($2^{\Delta CT}$) was then calculated as x-fold difference to corresponding control sample content.

Table 2.6: List of primers (T = annealing temperature, time = elongation time)

name	**sequence (5'→3')**	**T[°C]**	**time[s]**
β-actin 5'	TGGAATCCTGTGGCATCCATGAAA	56	16
β-actin 3'	TAAAACGCAGCTCAGTAACAGTCCG	56	16
IFNγ 5'	GAACGCTACACACTGCATC	56	12
IFNγ 3'	GAGCTCATTGAATGCTTGG	56	12
IL-2 5'	AACCTGAAACTCCCCAGGAT	58	12
IL-2 3'	TCATCATCGAATTGGCACTC	58	12
IL-6 5'	GCCTATTGAAAATTTCCTCTG	57	12
IL-6 3'	GTTTGCCGAGTAGATCTC	57	12
IL-10 5'	ATGCCTGGCTCAGCAC	58	16
IL-10 3'	GTCCTGCATTAAGGAGTCG	58	16
TNFα 5'	CGTCAGCCGATTTGCTATCT	60	12
TNFα 3'	CGGACTCCGCAAAGTCTAAG	60	12

2.2.4 Liver gene expression by microarray analysis

Messenger RNA was isolated as described in section 2.2.2. Microarray analysis was performed at the Institute of Clinical Chemistry with the help of Benjamin Otto and Kristin Klaetschke. First, RNA integrity was validated by a Bioanalyzer (data not shown). RNA was then turned into double stranded cDNA by reverse transcription. Afterwards, the cDNA was again transcribed *in vitro* into biotinylated cRNA. This cRNA was first fragmented and subsequently hybridized to the Affimetrix GeneChip®. Afterwards the array was washed and labeled with streptavidin-Cy5. Finally, the array was scanned by a GeneChip® Scanner.

Microarray statistics

The fluorescence intensities of every single gene spot were analyzed in the pairwise group comparisons described in table 2.7. Significant differences were examined by Benjamini-Hochberg (BH) corrected student's t-test.

Table 2.7: Microarray group comparisons

comparison 1	**comparison 2**	**comparison 3**	**comparison 4**
solvent/solvent vs Con A/solvent	solvent/solvent vs solvent/Con A	solvent/Con A vs Con A/Con A	Con A/solvent vs Con A/Con A

Heatmap

For the generation of heatmaps, gene spots were included that were significantly regulated upon at least one of the comparisons (2) and (4) from table 2.7 (BH corrected student's t test): (2) solvent pretreated, unchallenged mice (solvent/solvent) compared to solvent pretreated, Con A challenged mice (solvent/Con A) and (4) Con A pretreated, unchallenged mice (Con A/solvent) compared to Con A pretreated, Con A challenged mice (Con A/Con A). Furthermore, genes were filtered for cytokine or cytokine receptor genes and genes involved in apoptosis signaling according to pathways of the Kyoto Encyclopedia of Genes and Genomes (KEGG) [KEGG, b,a]. The median fluorescence intensity (MFI) of all samples was calculated for every regulated gene spot. Aberration from this median was calculated and colorcoded as shown in scales in respective figures. Single samples were clustered by similarity of gene expression patterns. Genes were clustered with respect to similarity of expression within samples.

2.2.5 Determination of plasma enzyme activities and cytokine plasma concentrations

Plasma samples were diluted in 0.9% NaCl solution and ALT activities were measured by a Cobas system (Roche).

Plasma cytokine levels were analyzed by sandwich ELISA using high-binding 96-well-microplates. ELISA was performed either according to the manufacturer's protocol (TNFα and IFNγ) or as described in the following (IL-2, IL-6, IL-10; for antibodies see

table 2.8): Coating buffer containing monoclonal antibody against the protein of interest was added to the wells of the microplate and incubated at 4°C over night. Afterwards, the plate was washed 3 times with washing buffer. This washing procedure was repeated for all following washing step. Standard dilutions containing 10, 50, 100, 200, 400, 800, or 2000 pg/ml of the protein of interest or samples diluted in reagent buffer were added to wells and incubated for either 2 hours at room temperature or at 4°C over night. Subsequently, the plate was washed again, and then incubated with a second biotinylated monoclonal antibody against the gene of interest for 2h at room temperature (RT). After another washing step, streptavidin-coupled Horse-Radish-Peroxidase was added to wells and incubated at RT for 25 minutes. The plate was washed again and subsequently, TMB enzyme substrate was added to the wells. After coloring of the standard row, sulfuric acid was added without washing the plate. Absorbances of single wells were determined at a wavelength of 450nm by Tecan infinite M200 with Tecan Magellan V6.5 software.

Table 2.8: IL-2, IL-6, and IL-10 ELISA antibodies

name	host	clone	supplier	conjugate	conc.	endconc.
IL-2 capture	rat	JES6-1A12	BD Pharmingen	none	0.5 mg/ml	3 µg/ml
IL-2 detection	rat	JES6-5H4	BD Pharmingen	biotin	0.5 mg/ml	1 µg/ml
IL-6 capture	rat	MP5-20F3	BD Pharmingen	none	0.5 mg/ml	4 µg/ml
IL-6 detection	rat	MP5-32C11	BD Pharmingen	biotin	0.5 mg/ml	5 µg/ml
IL-10 capture	rat	JES5-2A5	BD Pharmingen	none	1 mg/ml	8 µg/ml
IL-10 detection	rat	SXC-1	BD Pharmingen	biotin	0.5 mg/ml	1 µg/ml

2.2.6 Determination of Con A plasma concentration

Blood samples were taken from Con A FITC challenged mice by puncturing the orbital sinus and were centrifuged at 14000 x g for 5 min to obtain plasma. Plasma samples were diluted 1:20 in PBS. A standard curve was generated by diluting Con A-FITC in plasma to given concentrations and further 1:20 dilution of these in PBS. Two hundred µl of each diluted sample were added to a black microtiter plate and the fluorescence was measured by Tecan reader. Concentrations were calculated from fluorescences according to the standard curve.

2.2.7 Determination of plasma prothrombin time

Blood was equally citrated immediately upon sampling from the animal. Plasma prothrombin time was measured on a KC10 coagulation instrument that was calibrated with human citrated plasma from healthy individuals (HemosIL^{TM}). Coagulation of plasma was activated by 200 µl Dade®Innovin® which consists of recombinant human tissue factor, phospholipids and $CaCl_2$. For determination of sample prothrombin times, 100µl of citrated plasma were activated by 200 µl Innovin® and times until fibrin clot formation were measured.

2.2.8 Histology

The liver lobus quadratus was fixed in 4% formaldehyde in PBS immediately after withdrawal. Subsequent steps were performed with the help of Alexander Quaas and Mareike Sandmann in the Institute of Pathology. The lobus quadratus was embedded in paraffin and sections were made and stained with hematoxilin and eosin (H&E) in the Institute of Pathology.
To visualize Con A localization in liver sinusoids, the lobus caudatus was removed from mice 30 min after Con A-FITC treatment, incubated in a 15% sucrose/PBS solution on ice for an hour, and freezed in -80°C isopentane. The liver was sectioned into 12 µm thick slices on a CryoStar® cryostat and adsorbed to SuperFrost® slides. Tissue slices were fixed for 10 minutes in a solution of 50% methanol and 50% formaldehyde (37%). Afterwards, slides were washed in PBS, antibody against F4/80 diluted 1:100 in PBS was added and incubated over night. Subsequently, slides were washed again in PBS and stained with goat anti-rat-IgG-Alexa546 diluted 1:400 in PBS. Cover slips were mounted with fluorescent mounting medium and stained slides were analyzed on a Leica DM IRE 2 confocal microscope.

2.2.9 Flow cytometry

For flow cytometry, $1x10^6$ liver MNCs, splenocytes, blood cells, or LN cells were incubated with anti-CD16/CD32 antibodies in PBS to block unspecific binding of antibodies to Fc receptors. Subsequently, antibodies to surface molecules were added in PBS. If dead cells were stained, 100 µl of Fixable Viability Dye eFluor® 506 diluted 1:1000 in PBS were added and incubated at RT for 30 min. After surface or dead cell staining,

cells were washed in PBS and resuspended in FACS buffer for flow cytometry or, alternatively, cells were fixed and permeabilized for staining of transcription factors or intracellular cytokine staining (ICS).
For intracellular staining of the transcription factors Foxp3 and T-bet, cells were permeabilized by eBioscience Foxp3 Fixation/Permeabilization solution according to the manufacturer's protocol. Subsequently, cells were washed twice in eBioscience Permeabilization Buffer solution. Anti-Foxp3, anti-T-bet and anti-KI-67 were added in eBioscience Permeabilization Buffer solution and incubated for 30 min at 4°C. After two additional washing steps with eBioscience Permeabilization Buffer, cells were resuspended in FACS buffer. For staining of cytokines, liver MNCs or splenocytes were isolated from mice 15 minutes after blocking ART2 enzyme activity by injection of 30 µg s+16a nanobody (kindly gift from Friedrich Koch-Nolte and Bjoern Rissiek) and were stimulated with 50 pg/ml PMA and 500 ng/ml Ionomycin. After 30 min 1 µg/ml Brefeldin A was added to stop vesicular transport and secretion of cytokines. After totally 2.5 hours of stimulation, cells were washed and surface as well as dead cells were stained as described above. ICS was performed after staining of surface molecules and dead cells. Cells were incubated with formaldehyde diluted 1:10 in FACS buffer at RT for 20 min, washed in FACS buffer, and then permeabilized by a 0.01% solution of NP-40 substitute in FACS buffer at RT for 4 min. Subsequently, cells were washed and stained with antibodies against cytokines at 4°C over night. After a final washing step in FACS buffer, cells were resuspended in FACS buffer. Antibodies used in flow cytometry are specified in table 2.9. Staining of iNKT cells was performed in parallel to staining of surface molecules with the help of APC-labeled CD1d tetramers loaded with the α-galactosylceramide (αGalCer) analog PBS-57. Stained cells were analyzed on a FACS CantoII™ or FACS LSR Fortessa™ System from BD Biosciences with FACS Diva™ software.

2.2.10 Detection of hemoglobin via magnetic resonance imaging

Magnetic Resonance Imaging (MRI) is an imaging technique that is used to visualizes structures in humans and animals.
For MRI measurements the object is placed in a large static magnetic field, which induces spin polarization in all nuclei with a nuclear spin that is non-zero, and such results in macroscopic magnetization of the sample. The magnetization can be manipulated by the application of alternating electromagnetic fields. For a given external magnetic field,

Table 2.9: Anti-mouse antibodies for flow cytometric analysis

antigen	host	clone	supplier	conjugate	conc.	endconc.
CD16/CD32	rat	93	BioLegend	none	0.5 mg/mL	10 µg/mL
CD3	arm. Hamster	145-2C11	BioLegend	BV421	not specified	1:200
CD4	rat	RM4-5	BioLegend	BV711	not specified	1:200
CD4	rat	GK1.5	BioLegend	APC/Cy7	0.2 mg/mL	1 µg/mL
CD45	rat	30-F11	BioLegend	PerCP	0.2 mg/ml	0.67 µg/mL
CD8	rat	53-6.7	BioLegend	BV785	not specified	1:300
Foxp3	rat	FJK-16s	eBioscience	PerCP/Cy5.5	0.2 mg/mL	2 µg/mL
IFNγ	rat	XMG1.2	BioLegend	PE	0.2 mg/mL	1 µg/mL
Ki-67	rat	16A8	BioLegend	APC	0.2 mg/ml	2 µg/mL
NK1.1	mouse	PK136	BD Pharmingen	PE	0.2 mg/mL	1 µg/mL
NK1.1	mouse	PK136	BD Pharmingen	FITC	0.5 mg/mL	2.5 µg/mL
TNFα	rat	MP6-XT22	BioLegend	PE/Cy7	0.2 mg/mL	1 µg/mL
T-bet	mouse	4B10	eBioscience	PE	0.2 mg/mL	1 µg/mL

the excitation frequency is specific for each nuclide. MRI conventionally utilizes the magnetization of the non-zero spin nuclide most abundant in organic samples: hydrogen. At a static external magnetic field of 7.0 T, excitation of hydrogen nuclei is performed by the application of short radio frequency (RF) pulses ($\approx$ 300MHz). The system responds to this excitation by the emission of weak RF signals. These RF signals depend on the chemical environment of the nuclei, which results in image contrast between different kinds of tissue. To achieve spatial resolution and optimal contrast, a succession of different RF pulses and timed deformations of the static field (gradient pulses) are applied. The entirety of these pulses is called sequence.

Paramagnetic materials like iron atoms cause inhomogeneities of local magnetic fields. These can be detected by T2* sensitive image acquisition via so-called gradient echo (GRE) sequences. Areas with enhanced local field inhomogeneities show decreased T2* time and appear dark in a GRE MRI scan. Because highest iron concentrations are found in hemoglobin from RBC in humans and animals, blood accumulation can be measured by GRE sequences. MRI was performed in the Diagnostic and Interventional Radiology Department and Clinic with the help of Thomas Ernst and Harald Ittrich. The experiment was performed on a small animal MRI system at 7.0 T using a circularly polarized body coil with an inner diameter and resonator length of 40 mm. Mice were anesthetized by inhalation of about 2% isoflurane and 98% oxygen at a flow rate of 500 ml/min. Res-

piration rate was detected by a pressure pad. If necessary, isoflurane concentration was adjusted to maintain a constant respiration rate of 40 beats per minute (bpm). Mice were kept on a water heated pad to maintain body temperature during measurement. In general, respiratory-triggered MR sequences were acquired during respiratory resting in between breaths. All MR sequences were acquired in the axial plane with an image matrix of 192 × 192 and a slice thickness of 0.7 mm. Quantitative T2*-relaxometry (qT2st) of the liver tissue was performed using a fat-saturated GRE sequence. For anatomical orientation and visual assessment of liver damage a respiratory-triggered T2-weighted (T2w) turbo-spin-echo (TSE) sequence was performed with two concatenations in interleaved mode. Further sequence parameters are presented in table 2.10.

Table 2.10: MRI parameters (TR: repetition time; TE: echo time; FoV: field of view; ST: slice thickness; ETL: echo train length; ES: echo spacing; FA: flip angle; NSA: number of signal acquisitions; TA: acquisition time

	TR [ms]	**TE [ms]**	**Voxel Size**	**FoV [mm]**	**Slices**	**Gap [%]**
T2w TSE	∼ 1500	50	167x167x700	32.0	13	0
qT2st GRE	300	1.98...12.87	177x177x700	34.0	8	100
	ETL	**ES [ms]**	**FA[°]**	**NSA**	**TA [min]**	
T2w TSE	14	7.1	180	4	∼3	
qT2st GRE	12	0.99	25	8	11:31	

2.2.11 Statistics

In general, comparison between two groups were performed by student's t test. If data were not normally distributed, data were normalized by logarithmic calculus. Welch corrected student's t test was performed if unequal variances were determined by F test. If more then two groups were compared, One-Way-ANOVA was performed with Bonferroni's post-hoc test. Two-Way-ANOVA with Bonferroni's post-hoc test was performed for analysis of decline of Con A plasma concentration with the time variable matched to treatment variable.

3 Results

3.1 Sustained and robust protection from hepatitis induced by Con A 14 days after a single Con A pretreatment in the absence of immunosuppression

Erhardt et al. showed that tolerance towards Con A induced hepatitis is established within 8 days after a single sublethal Con A treatment [Erhardt et al., 2007]. This tolerance towards Con A was postulated to be mediated by IL-10 secreted by Tregs and KCs upon a second Con A challenge. Preliminary data suggested that resistance towards hepatic injury lasts at least for about 42 days. However, sustained resistance towards Con A induced liver injury seemed not to be associated with enhanced IL-10 concentrations in plasma suggesting that IL-10 might play a minor role in sustained resistance towards Con A induced liver injury. Therefore, the mechanism for protection against Con A induced liver injury at later time points than 8 days remains elusive. First, it was investigated at which time point after pretreatment prominent protection against Con A challenge first occurred in the absence of enhanced IL-10 plasma levels.

3.1.1 Sustained and robust protection from Con A-induced hepatitis 14 days after Con A pretreatment

Mice were pretreated with 10 mg/kg Con A or solvent. Subsequently, groups of solvent pretreated and Con A pretreated mice were injected with 14 mg/kg Con A 8, 10, 12, or 14 days later (Fig. 3.1). After Con A challenge, the difference of ALT activities in plasma between groups, that had been pretreated with solvent or Con A 8 days before, was not significant. In contrast, plasma ALT activities were significantly lowered in Con A

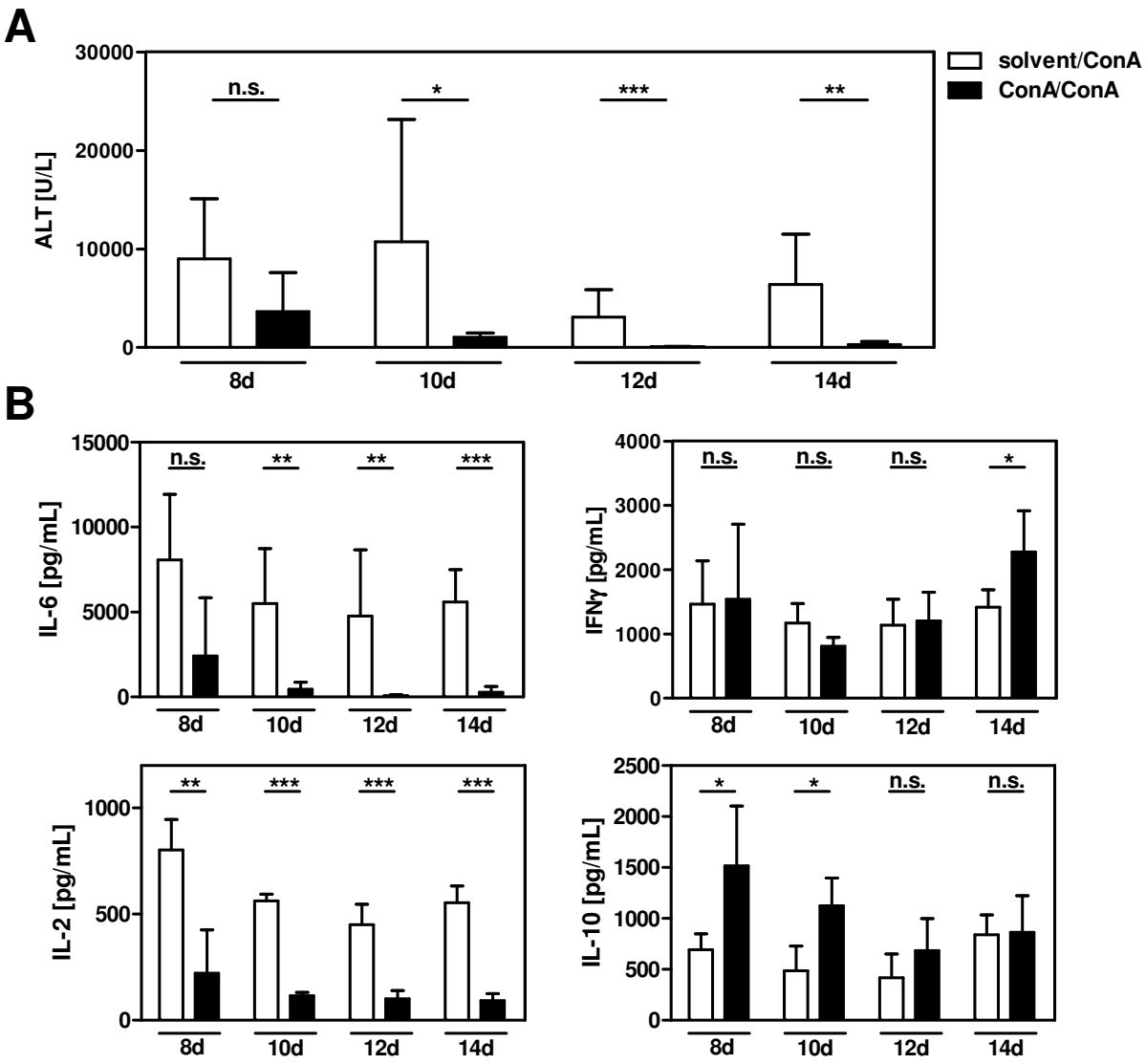

Figure 3.1: *Sustained robust protection against Con A induced hepatitis 14 days after Con A pretreatment:* C57BL/6J mice were treated with solvent or 10 mg/kg body weight Con A. Eight, 10, 12 or 14 days afterwards mice were treated with 14 mg/kg Con A. Mice were sacrificed 8 hours after the second treatment and plasma transaminase activities as well as plasma cytokine levels were determined. Data are given as mean ± SD (n=4 per group). Statistical analysis was performed by using student's t-test on logarithmized data of control groups and of respective Con A-pretreated groups at indicated time points (* $p \leq 0.05$; ** $p \leq 0.01$; *** $p \leq 0.001$; n.s., not significant).

pretreated mice compared to solvent pretreated mice when these were re-stimulated 10, 12 or 14 days after pretreatment. The most prominent decreases in ALT activities were seen in mice restimulated 12 to 14 days after Con A pretreatment and 14 days after

Con A pretreatment, IL-10 upregulation was abolished. This suggested robust protection against Con A induced liver damage 14 days after the first Con A treatment that was sustained in the absence of enhanced anti-inflammatory IL-10 upon Con A challenge.

3.1.2 Sustained resistance towards Con A induced hepatic injury despite hepatitis upon Con A challenge

Fourteen days after Con A pretreatment, mice showed sustained resistance towards Con A challenge despite the absence of enhanced IL-10 levels. The systemic and hepatic inflammatory response upon Con A challenge 14 days after pretreatment was thus analyzed in more detail. Mice were pretreated with solvent or 8 mg/kg Con A 14 days prior to Con A challenge with 9 mg/kg Con A (fig. 3.2A). As expected, Con A pretreated mice showed significantly lower ALT plasma activities compared to solvent pretreated mice 8 hours after Con A challenge. Furthermore, histological analysis of H&E stained liver sections revealed large necrotic areas in zone 2 of the liver acinus in solvent pretreated mice. In contrast, these necrotic areas were absent in Con A pretreated mice (fig. 3.2B). Noteworthy, many leukocytes were found in direct contact with the endothelium of central veins especially in samples from Con A pretreated mice indicating an ongoing hepatic endothelitis after Con A challenge even in protected mice (see asterisk in fig. 3.2B). Thus, fourteen days after Con A pretreatment Con A challenge culminates in liver inflammation without damage of the liver parenchyma indicating limited suppression of the Con A induced hepatic immune response.

3.1.3 Sustained resistance towards Con A induced hepatic injury without suppression of the Th1 associated cytokine milieu

It was reported that Con A challenge of mice 8 days after Con A pretreatment results in high plasma levels of anti-inflammatory cytokine IL-10 and rather low levels of pro-inflammatory cytokines IL-2, IL-6, and IFNγ in comparison to naïve control mice. Thus, immunoregulation was suggested to account for protection against Con A hepatitis in mice 8 days after Con A pretreatment [Erhardt et al., 2007]. Due to the presence of inflammatory foci in livers from Con A challenged mice 14 days after Con A pretreatment, inflammatory cytokines were determined in plasma 2 or 8 hours after Con A challenge of either solvent or Con A pretreated mice. In addition, cytokine expression was analyzed

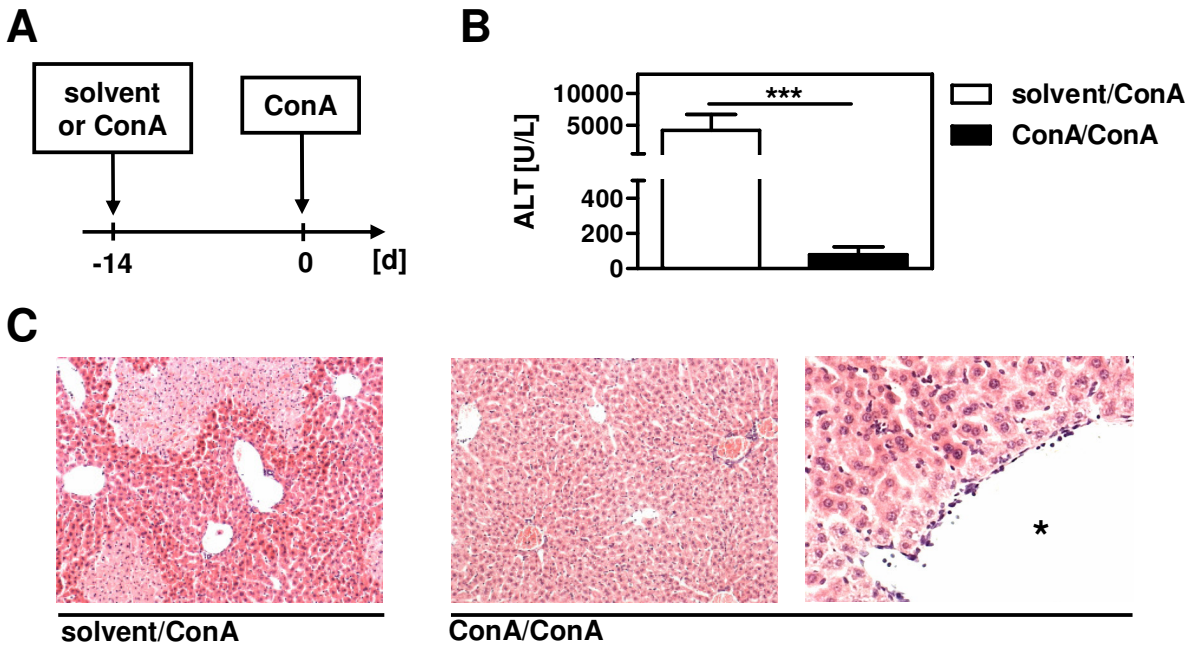

Figure 3.2: *Sustained resistance towards Con A induced hepatic injury despite occurrence of liver inflammation:* A) Treatment scheme: C57BL/6J mice were treated with solvent or 8 mg/kg Con A 14 days before Con A challenge with 9 mg/kg Con A. Mice were sacrificed 8 hours after Con A challenge. B) ALT activities were determined in plasma. C) Livers were fixed in formaldehyde, sectioned and stained with H&E. Asterisk indicates inflamed central vein. Data are presented as mean ± SD (n=5 per group). Statistical analysis was done on logarithmized data by student's t test (*** $p \leq 0.001$).

in liver tissue 8 hours after Con A challenge (fig. 3.3A). Two hours after Con A challenge plasma levels of TNFα, IL-6 and IL-2 were decreased in Con A pretreated mice compared to solvent pretreated controls (fig. 3.3A). IFNγ levels, however, were similar in these groups and IL-10 levels were below detection limit in both groups 2 hours after Con A challenge. TNFα is an early effector cytokine during Con A hepatitis and is below detection limit 8 hours after Con A challenge Sass et al. [2002]. However, Con A pretreated animals showed significantly reduced IL-2 and IL-6 plasma levels in comparison to solvent pretreated mice 8 hours after Con A challenge. In contrast, IFNγ levels were moderately and IL-10 levels were only very slightly increased in Con A pretreated mice (fig. 3.3B). In addition to plasma cytokine concentrations, cytokine expression was analyzed in liver tissue 8 hours after Con A challenge. The expression of TNFα was reduced in Con A pretreated mice. Consistent with findings from plasma, IFNγ expression was significantly upregulated in mice that were pretreated with Con A. Although not

significantly, IL-6 expression was moderately downregulated in Con A pretreated mice. IL-2 expression appeared downregulated in Con A pretreated mice. In contrast, IL-10 expression was slightly upregulated in Con A pretreated mice (fig. 3.3C). Together, these data indicate that sustained hepatic resistance towards Con A challenge 14 days after Con A pretreatment is independent from the suppression of the Th1 key effector cytokine IFNγ.

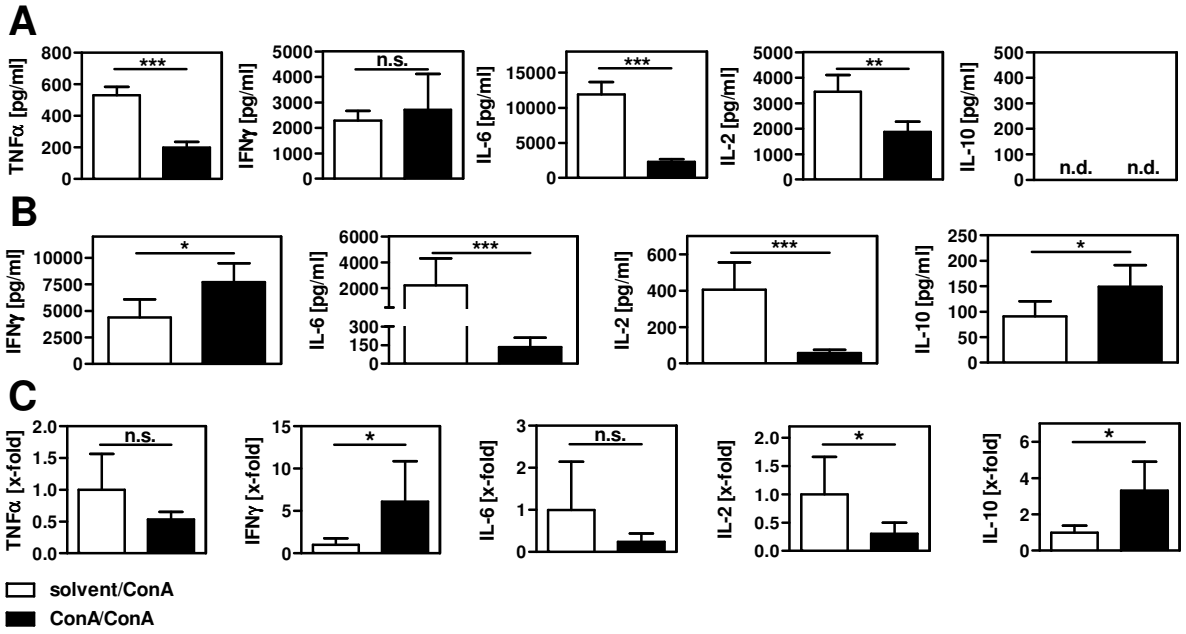

Figure 3.3: *Sustained resistance towards Con A induced hepatitis without suppression of the Th1 associated cytokine milieu:* Mice (n=5 per group) were treated as described in the prior section. Plasma cytokine concentrations were determined 2 hours after Con A challenge (A) or 8 hours after Con A challenge (B). Furthermore, expression of cytokines were determined in liver tissue 8 hours after Con A challenge (C). Data are presented as mean ± SD. Statistical analysis was done on logarithmized data by student's t test (* $p \leq 0.05$; ** $p \leq 0.01$; *** $p \leq 0.001$; n.s., not significant).

3.1.4 Predominant IFNγ and reduced TNFα secretion by liver lymphocytes from Con A pretreated mice

Resistance towards Con A induced hepatitis 14 days after pretreatment correlated with increased plasma levels of IFNγ and decreased plasma levels of TNFα. Therefore, it was investigated if this was the result of reprogrammed liver lymphocytes that resulted in an

altered cytokine secretion profile. For this purpose, mice were pretreated with solvent or 7 mg/kg Con A. Fourteen days afterwards, mice were sacrificed and liver MNCs and splenocytes were isolated. Fifteen minutes before sacrification, mice were treated with a llama derived recombinant s+16a single domain antibody against the ectoenzyme ADP-ribosyltransferase 2.2 (ART2.2). ART2 catalyzes transfer of ADP-ribose moieties from nicotine adenine dinucleotide (NAD) to target proteins and ART2 activity can result in apoptosis through ADP-ribosylation and activation of the P2X7 receptor [Seman et al., 2003]. NKT cells express high levels of the ART2 enzyme and, because its substrate NAD^+ is released from dead cells, NKT cells are very susceptible to apoptosis during isolation procedures where increased NAD^+ concentrations might occur (see fig. 4.1). Thus, inhibition of ART2.2, which can be accomplished by the s+16a nanobody, stabilizes the NKT cell population during isolation [Scheuplein et al., 2010]. After isolation, liver MNCs or splenocytes were stimulated with PMA and ionomycin *in vitro* and were then stained for FACS analysis and gated as shown in fig. 3.4. Frequencies of IFNγ^+ cells and TNFα^+ cells were determined among $CD4^+$ and $CD8^+$ T cells as well as among NKT and NK cells (fig. 3.5A and B). TNFα^+ cells were significantly less frequent among NKT, $CD4^+$ T cells, and $CD8^+$ T cells from livers of Con A pretreated mice. In general, very few NK cells from livers of both, solvent and Con A pretreated mice, were positive for TNFα. In contrast to TNFα, IFNγ^+ cells were significantly more frequent among $CD4^+$ and $CD8^+$ T cells from livers of Con A pretreated mice whereas they were equally frequent in NKT and NK cell populations from livers of solvent and Con A pretreated mice. In spleen, TNFα^+ cells were significantly diminished only in $CD4^+$ T cells from Con A pretreated mice and IFNγ^+ cells were significantly expanded only in $CD8^+$ T cells from Con A pretreated mice. In accordance with serum levels, lymphocytes and especially liver lymphocytes from Con A pretreated animals might predominantly secrete IFNγ. Taken together, these data indicate that liver lymphocytes, especially $CD4^+$ and $CD8^+$ T cells, are reprogrammed with respect to their capability of cytokine secretion after Con A pretreatment which might contribute to a modified immune response *in vivo* resulting in less harmful conditions for the liver parenchyma.

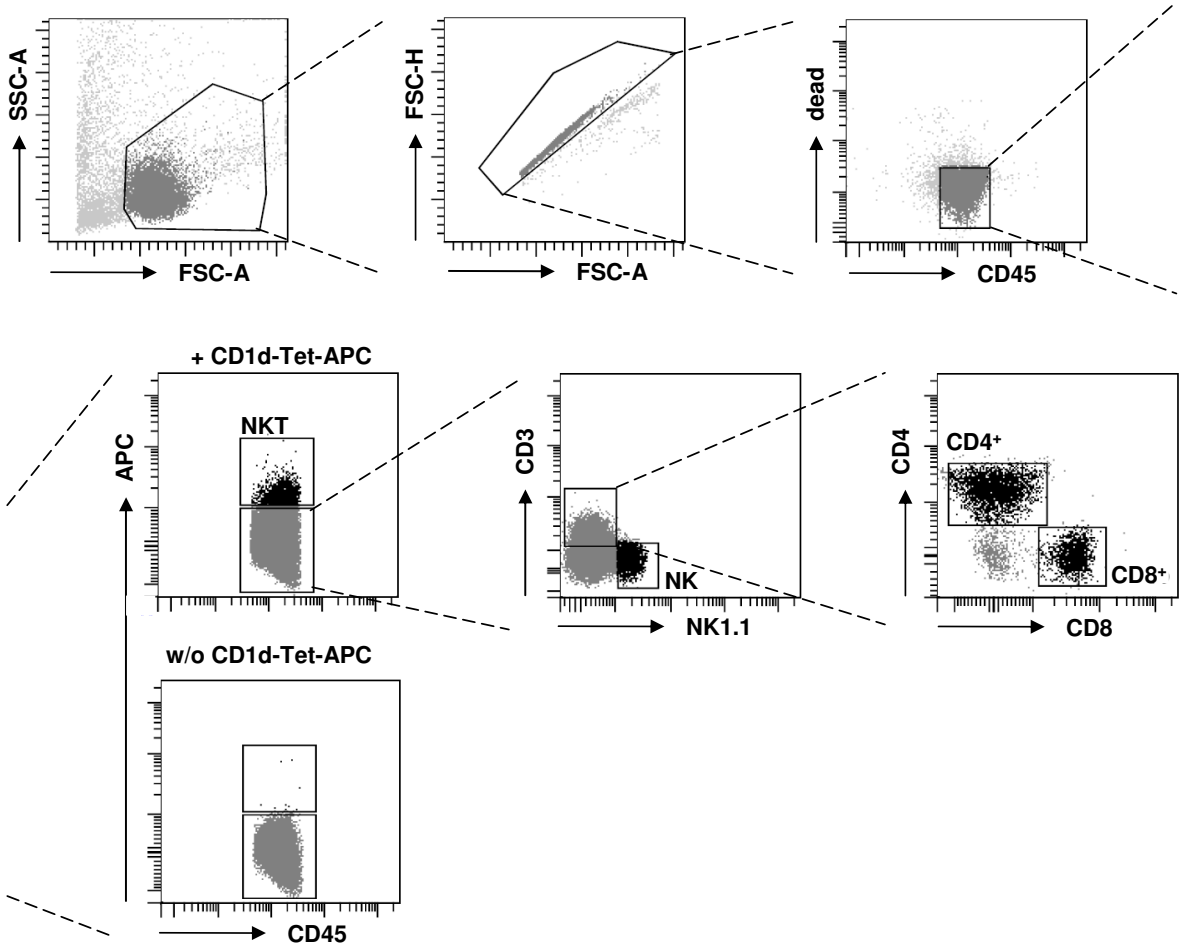

Figure 3.4: *Gating strategy for NKT, NK, CD4$^+$ T and CD8$^+$ T cells:* Liver MNCs or splenocytes were gated on living CD45$^+$ cells. NKT cells were identified as CD1d-tetramer$^+$ cells and the gate was adjusted in comparison to controls lacking CD1d-tetramer staining. NK cells were identified as CD1d$^-$NK1.1$^+$ cells. CD4$^+$ and CD8$^+$ T cells were gated from CD1d$^-$CD3$^+$ cells. NKT, NK, CD4$^+$ T and CD8$^+$ T cells are shown in black.

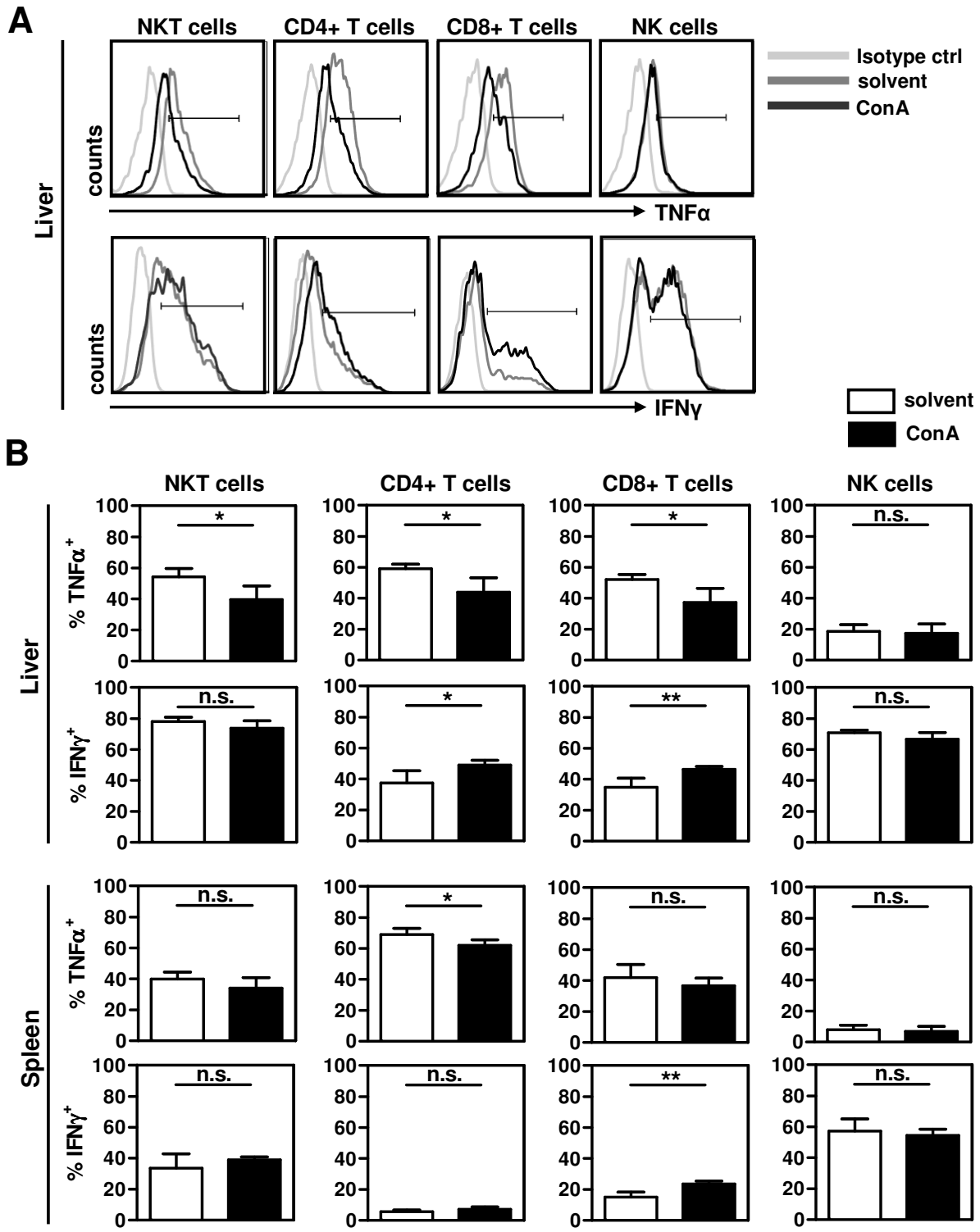
A
NKT cells
CD4+ T cells
CD8+ T cells
NK cells
Isotype ctrl
solvent
ConA
Liver
counts
TNFα
counts
IFNγ
solvent
ConA
B
NKT cells
CD4+ T cells
CD8+ T cells
NK cells
Liver
% TNFα+
% IFNγ+
Spleen
% TNFα+
% IFNγ+
n.s.
*
**

Figure 3.5: *Predominant IFNγ and reduced TNFα secretion in liver lymphocytes from Con A pretreated mice:* Mice (n=4 per group) were pretreated with solvent or 7 mg/kg Con A. After 14 days, mice were injected with s+16a llama derived single chain antibody to block ART2 activity and stabilize NKT cells. 15 minutes after s+16a injection, mice were sacrificed and Liver MNCs as well as splenocytes were isolated. After 2.5 hours stimulation with PMA and Ionomycin, cells were stained for intracellular cytokines. A) Histograms for quantification of TNFα$^+$ and IFNγ$^+$ cells among NKT, CD4$^+$ and CD8$^+$ T cells as well as among NK cells. B) Relative frequencies of TNFα and IFNγ among NKT, CD4$^+$ and CD8$^+$ T cells as well as NK cells in livers and spleens as determined by histograms in A. Data are presented as mean ± SD. Statistical analysis was performed by using student's t test (* $p \leq 0.05$; ** $p \leq 0.01$; n.s., not significant).

3.2 Role for IL-10 in sustained resistance towards Con A induced hepatic injury 14 days after pretreatment

IL-10 was postulated to mediate resistance towards Con A induced hepatitis 8 days after Con A pretreatment because Con A pretreatment could protect wt but not IL-10 deficient mice against hepatitis [Erhardt et al., 2007]. In contrast to findings from the study of Erhardt et al., the experiment described above revealed only slightly regulated IL-10 concentrations 8 hours after Con A challenge of mice that had been pretreated with Con A 14 days before. Thus, the IL-10 mediated immunosuppression for protection against hepatic damage might be differentially regulated in mice that had been pretreated with Con A 8 days before Con A challenge or mice that had been pretreated with Con A 14 days before Con A challenge. Therefore, it was analyzed if sustained resistance towards Con A induced hepatic injury 14 days after Con A pretreatment might occur independently from IL-10.

To identify the role for IL-10 signaling in protection against Con A induced liver injury 14 days after pretreatment, IL-10 signaling was neutralized by treatment of mice with anti-IL-10 or anti-IL-10R antibodies before Con A challenge (8 mg/kg) or before Con A pretreatment (7 mg/kg). Efficacy of IL-10 neutralization was tested by ELISA: Because the neutralizing anti-IL-10 antibody and the ELISA IL-10 detection antibody are derived from the same clone, efficacy of anti-IL-10 treatment is demonstrated by failure of IL-10 detection in plasma from anti-IL-10 treated animals 8 hours after Con A challenge. Efficacy of anti-IL-10R antibody is shown by accumulation of IL-10 in plasma

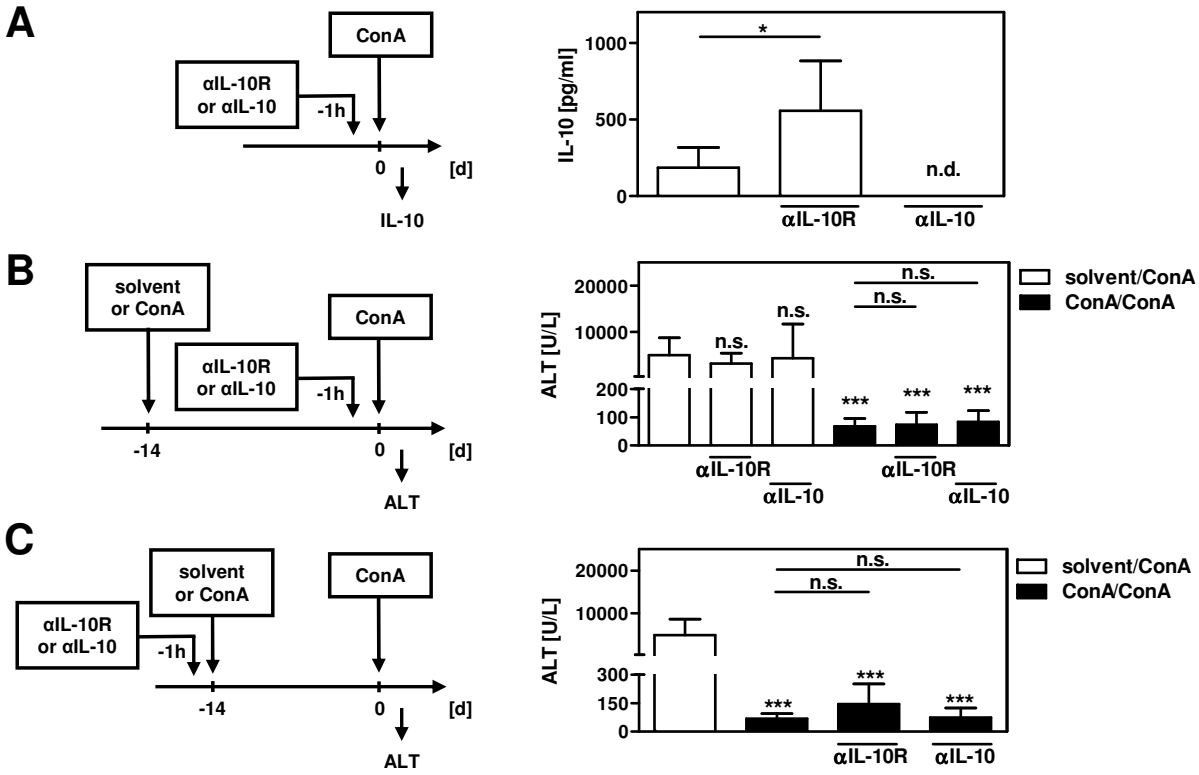

Figure 3.6: *Resistance towards Con A induced hepatic injury on day 14 is independent from IL-10 signaling:* Wt mice were challenged with 8 mg/kg Con A (A, B, C) fourteen days after solvent or Con A pretreatment (B, C). Cytokine concentrations (A) or ALT activities (B, C) were determined in plasma 8 hours after Con A challenge. A) Mice were injected i.v. with 500 µg anti-IL-10 antibody or anti-IL-10R antibody one hour before Con A challenge. B) Mice were injected with 500 µg anti-IL-10 or anti-IL-10R antibody one hour before Con A challenge. C) Mice were injected with 500 µg anti-IL-10 or anti-IL-10R antibody one hour before Con A pretreatment. Data are presented as mean ± SD (n=5 per group). Statistical analysis was done by student's t-test (A) or One-Way-ANOVA with Bonferroni's post-hoc test (B and C) on logarithmized data. Above bars statistics of the comparison of the specific bar to the respective solvent/Con A control without antibody treatment are indicated (* $p \leq 0.05$; *** $p \leq 0.001$; n.s., not significant).

taken from mice 8 hours after Con A challenge (fig. 3.6A). ALT activities in plasma were significantly decreased to nearly physiological levels if Con A pretreated mice were compared to solvent pretreated mice. Similarly, mice treated with anti-IL-10 or anti-IL-10R antibodies before Con A challenge showed nearly physiological levels of ALT activities if they had been pretreated with Con A and showed highly increased ALT activities in plasma if mice had been pretreated with solvent (fig. 3.6B). In mice treated with anti-IL-10 or anti-IL-10R antibodies before Con A pretreatment, ALT plasma activities were

also decreased to nearly physiological levels (fig. 3.6C). These data suggest that Con A pretreatment can lead to resistance towards Con A induced hepatic injury in the absence of IL-10 signaling upon Con A pretreatment and upon Con A challenge indicating that resistance 14 days after Con A pretreatment develops and is mediated independent from anti-inflammatory IL-10.

3.3 Role for Tregs in sustained resistance towards Con A induced hepatic injury

As described above abrogation of IL-10 signaling does not abolish resistance towards Con A induced hepatitis in mice 14 days after Con A pretreatment. Thus, IL-10 does not seem to be the main mediator of Con A induced sustained resistance towards Con A induced hepatitis. Hence, in opposite to the postulated mechanism of protection 8 days after Con A pretreatment [Erhardt et al., 2007], sustained resistance towards Con A might not depend on Tregs producing immunosuppressive IL-10. Therefore, a potential role for Tregs in protection against Con A induced hepatitis by other mechanisms was analyzed.

3.3.1 Sustained resistance towards Con A induced hepatic injury is independent from Tregs

To investigate if resistance towards hepatitis induced by Con A is mediated by Tregs, DEREG or wt mice were treated with solvent or Con A. Thirteen days afterwards, wt and DEREG mice were treated with DT. Twenty-four hours later mice were challenged with a second Con A treatment (fig. 3.7A). Treg frequencies in livers as well as plasma ALT activies were determined 8 hours after Con A challenge. Treg frequencies were highly decreased in DEREG mice compared to wt mice, suggesting efficient depletion of Tregs by DT (fig. 3.7B). DEREG and wt mice that received Con A for the first time showed highly increased ALT activities in plasma. In comparison, significantly reduced ALT levels were detected in plasma from Con A pretreated DEREG and wt mice (fig. 3.7C). Thus, resistance towards Con A induced hepatitis occurred in the absence of Tregs during a second Con A challenge. This disputes Tregs as the central mediators of hepatic protection in this model.

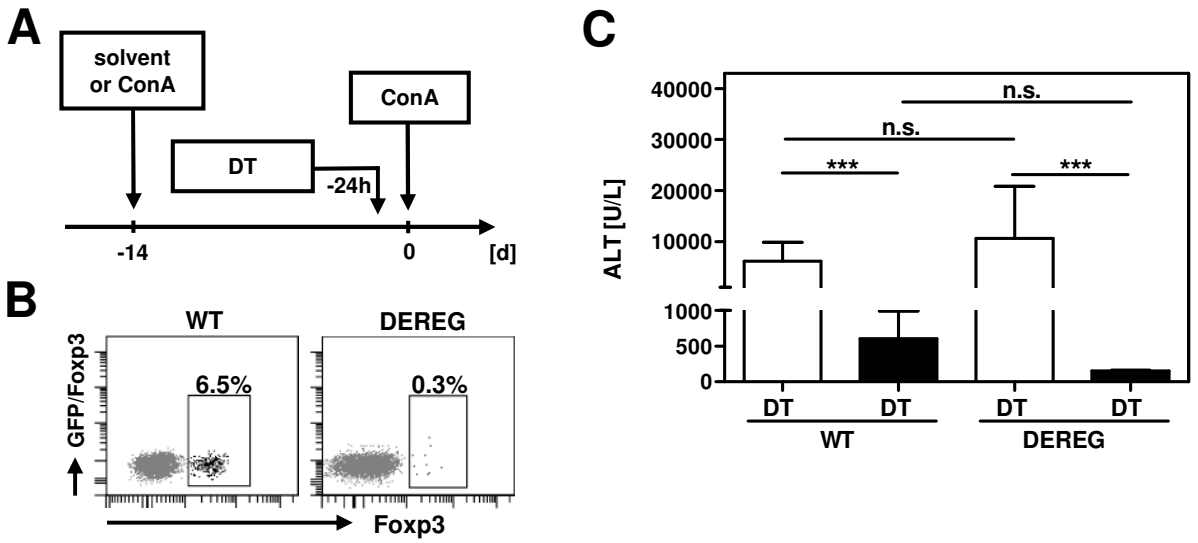

Figure 3.7: *Sustained resistance towards Con A induced hepatic injury is independent from Tregs:* A) Injection scheme: On day -14, wt or DEREG mice were treated with solvent or a first dose of Con A (7 mg/kg). Twenty-four hours before Con A challenge with 8 mg/kg (day 0) mice were treated with 1 µg DT. B) Frequencies of Tregs among $CD4^+$ T cells from the liver were determined by Foxp3 expression and GFP reporter protein expression via flow cytometry 8 hours after Con A challenge (day 0). C) ALT activities were determined in plasma. Data are presented as mean ± SD (n=4 per group). Statistical analysis was done by One-Way-ANOVA with Bonferroni's post-hoc test (*** $p \leq 0.001$; n.s., not significant).

3.3.2 Development and functional role of Th1-like Tregs during induction of sustained resistance towards Con A induced hepatic injury

Although Tregs might not directly protect against Con A induced hepatitis upon a second Con A challenge, they might still be involved in the induction of a hepatoprotective state that is developing after the first stimulus. Because it was reported that Tregs expand 24 hours after a single Con A injection, it was analyzed if the Treg phenotype changes during this increase of the Treg population [Erhardt et al., 2007]. Moreover, the functional role for this first Treg peak in later hepatic resistance towards repeated Con A challenges was investigated.

First of all it was analyzed if Tregs gain the Th1 expression pattern during the phase of Treg expansion in the first 24 hours after Con A stimulation. Liver MNCs, splenocytes, and cells from celiac lymph nodes were isolated 24 hours after solvent or Con A treatment (10 mg/kg), which was fatal for 3 out of 5 mice. Regulatory T cells were identified as

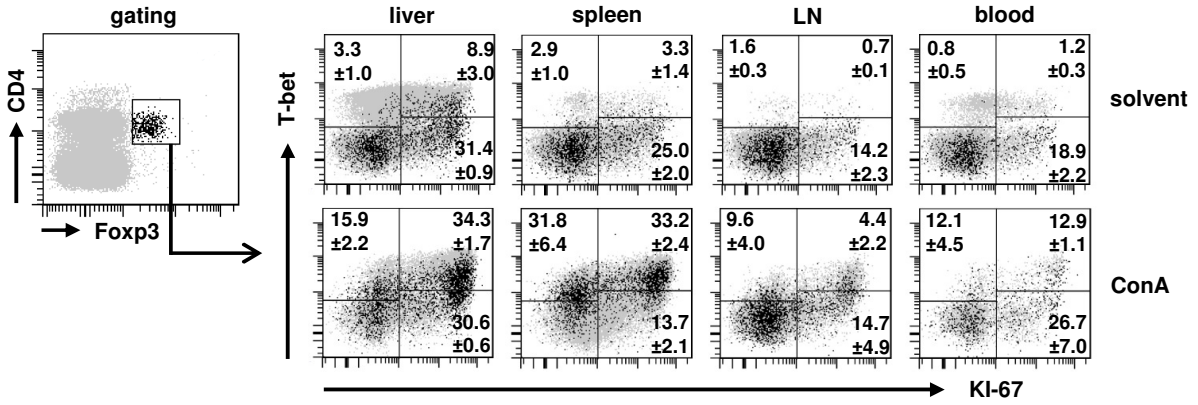

Figure 3.8: *Induction of a Th1 phenotype in Tregs within 24 hours after Con A challenge:* Wt mice were treated with solvent (n=5) or 10 mg/kg Con A (n=2). Twenty-four hours afterwards leukocytes were isolated from liver, spleen, liver-draining lymph-node and blood. Expression of intracellular markers Ki-67 and T-bet was analyzed in $CD4^+Foxp3^+$ Tregs. Numbers represent frequencies ± SD of the cells in the respective quadrant relative to $CD4^+Foxp3^+$ cells.

$CD4^+Foxp3^+$ cells (fig. 3.8). In comparison to untreated controls, T-bet expressing Tregs were more abundant in liver, spleen, liver-draining LN and blood from Con A treated mice (liver: 12.2% ± 4.0% T-bet^+ Tregs in solvent treated mice vs. 50.2% ± 3.9% T-bet^+ Tregs in Con A treated mice). Moreover, Tregs also showed higher expression levels for the proliferation marker KI-67 (liver: 40.4% ± 3.1% KI-67^+ Tregs in solvent-treated mice vs. 64.9% ± 2.3% KI-67^+ Tregs in Con A-treated mice).

Because functionally differentiated Tregs occur in the liver already 24 hours after a first Con A treatment, a possible early role for these Tregs in the establishment of liver protective mechanisms was investigated by depletion of Tregs from DEREG mice 24 hours before Con A pretreatment. First, it was tested if DT treatment depleted Tregs. $Foxp3^+$ Tregs were considerably diminished in liver, spleen, liver-draining LN and blood from DEREG mice. Thus, Tregs, including $CXCR3^+$T-bet^+Tregs, were efficiently depleted by DT treatment in DEREG mice 24 hours after Con A challenge (fig. 3.9A). To test the role for Tregs in induction of hepatoprotection, wt (GFP- DEREG littermates) and DEREG mice, that were treated with either PBS or DT before a solvent or Con A pretreatment (9 mg/kg), were challenged with a second dose Con A 14 days after pretreatment. Eight hours afterwards, ALT activities were determined in plasma of Con A challenged mice. Again, solvent pretreated DEREG mice showed significantly higher ALT activities than their Con A pretreated counterparts. Both, DT treated wt mice

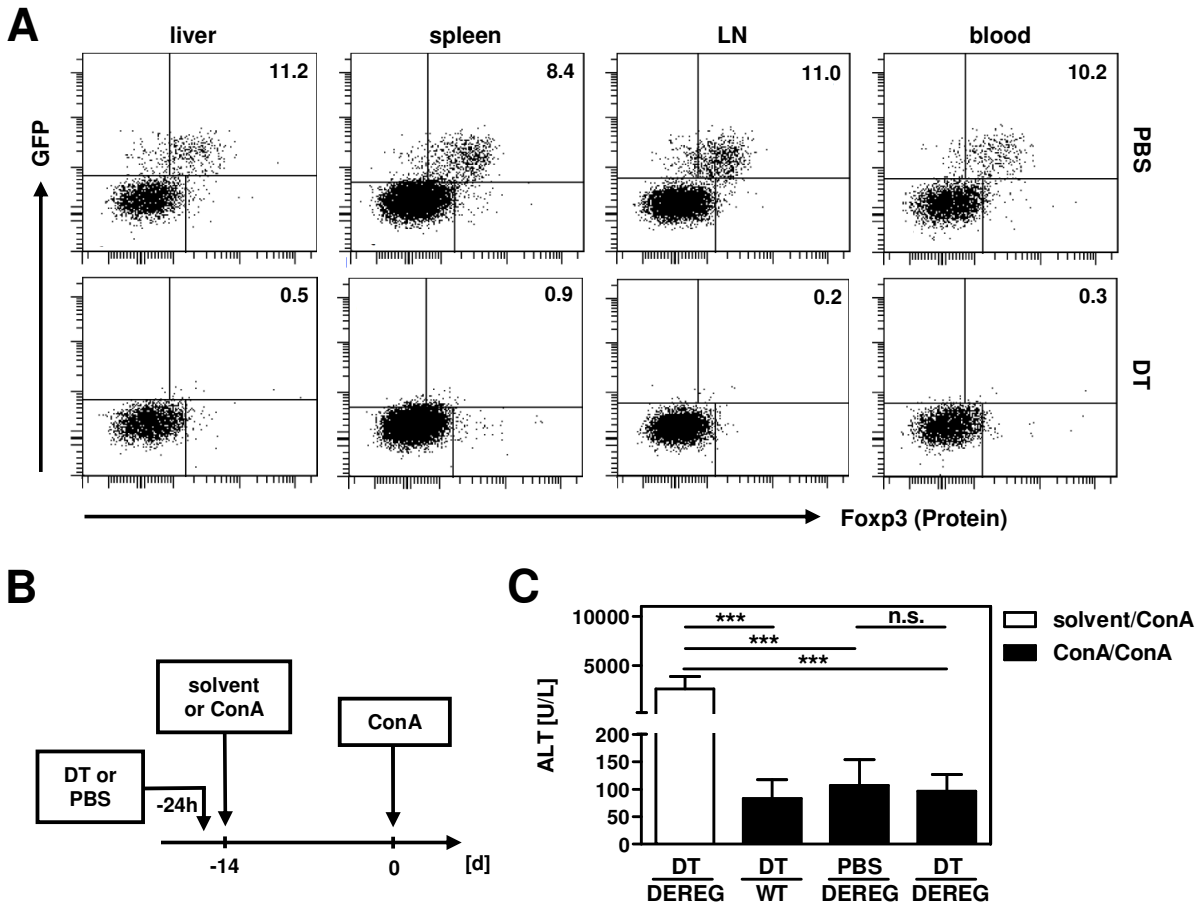

Figure 3.9: *Induction of resistance towards Con A induced hepatic injury in absence of Tregs:* A) DEREG mice were treated with PBS (n=2, upper 4 dot plots) or 1µg DT (n=3, lower 4 dot plots) 24 hours before 10 mg/kg Con A treatment. Twenty-four hours afterwards, mice were sacrificed and $CD4^+$ T cells were analyzed for Foxp3/GFP expression. Numbers in quadrants indicate mean percentage ± SD of $Foxp3/GFP^+$ among $CD4^+$ T cells. B and C: DEREG or wt mice were treated with 1 µg DT 24 hours before Con A pretreatment (9 mg/kg). Alternatively, DEREG mice were treated with PBS 24 hours before solvent or Con A pretreatment. Fourteen days after pretreatment all mice were challenged with 14 mg/kg Con A. B) Injection scheme. C) ALT plasma activities were determined 8 hours after Con A challenge. Data are presented as mean ± SD (n≥4 per group). Statistical analysis was done by One-Way-ANOVA with Bonferroni's post-hoc test (*** $p \leq 0.001$; n.s., not significant).

as well as DT treated and thus, Treg depleted DEREG mice showed the same plasma ALT activities and these were equal to activities in protected PBS and Con A pretreated DEREG mice (fig. 3.9B). These findings indicate that Tregs are not necessary for the induction of sustained resistance towards Con A challenge.

3.4 Involvement of CD4$^+$ T cells in induction of sustained resistance towards Con A induced hepatic injury

Depletion of Tregs before the first Con A injection did not abrogate resistance towards Con A hepatitis upon a second stimulus 14 days later. This suggested that Tregs do not induce liver resistance against Con A. CD4$^+$ T and NKT cells are essential for the onset of liver disease after a single Con A injection. Consequently, RAG1$^{-/-}$ mice do not develop hepatitis after injection of Con A doses used in this study (fig. 3.11). To investigate the role for CD4$^+$ T cells in induction of resistance towards Con A induced hepatitis, CD4$^+$ T cells were transplanted into RAG1$^{-/-}$ mice. It was first analyzed if transplantation of wt CD4$^+$ T cells could restore susceptibility towards Con A in RAG1$^{-/-}$ mice. Furthermore, it was tested whether resistance towards Con A hepatitis was inducible in RAG1$^{-/-}$ mice before CD4$^+$ T cell transplantation or after CD4$^+$ T cell transplantation.

3.4.1 Reconstitution of the CD4$^+$ T cell but not the NKT cell compartment in livers of RAG1$^{-/-}$ mice after adoptive transfer of wt CD4$^+$ T cells

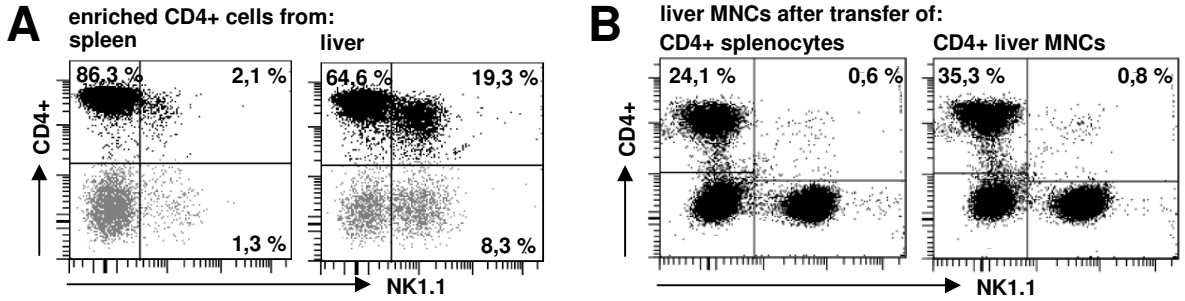

Figure 3.10: *Reconstitution of the CD4$^+$ T cell compartment in RAG1$^{-/-}$ mice:* A) CD4$^+$ T cells from spleen or liver were enriched by negative selection via MACS and stained for CD4 and NK1.1. B) Liver MNCs were isolated 14 days after adoptive transfer from CD4$^+$ T cells isolated as described in A and were stained for CD4 and NK1.1.

CD4$^+$ T cells were isolated from spleen or liver via magnetic separation (purity $\geq$ 90% or $\geq$ 70% from spleen or liver, respectively) and injected i.v. into RAG1$^{-/-}$ mice.

Frequencies of $CD4^+$ and $CD4^+NK1.1^+$ T cells were determined in liver 14 days afterwards (fig. 3.10B). Regardless of the fact if $CD4^+$ T cells were isolated from spleen or liver, $CD3^+CD4^+$ T cells in livers from $RAG1^{-/-}$ mice were mainly NK1.1 negative. This suggests that CD4 Th cells, but only very few NKT cells, repopulate the liver after adoptive transfer of splenic or liver wt $CD4^+$ T cells.

3.4.2 Liver susceptibility of $RAG1^{-/-}$ mice towards Con A after adoptive $CD4^+$ T cell transfer

$RAG1^{-/-}$ mice were reconstituted with splenic $CD4^+$ T cells. Fourteen days later, mice were treated with Con A (4 mg/kg) and ALT plasma activities were determined eight hours afterwards. Solvent and Con A treated naïve $RAG1^{-/-}$ mice showed ALT plasma activities in a physiological range. However, a slight but significant increase in ALT activities was found in plasma from $CD4^+$ transplanted, Con A treated animals (fig. 3.11).

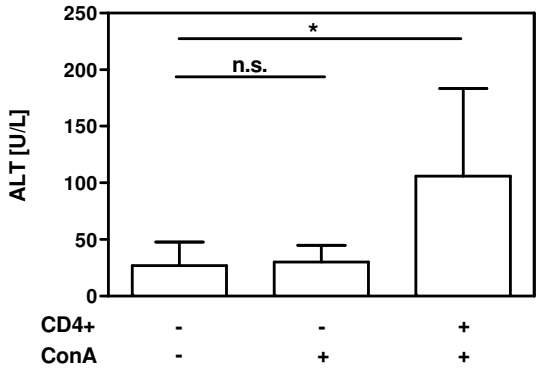

Figure 3.11: *Susceptibility of $RAG1^{-/-}$ mice towards Con A after adoptive transfer of $CD4^+$ T cells:* $RAG1^{-/-}$ mice were treated with 4 mg/kg Con A or solvent. Alternatively, $RAG1^{-/-}$ mice were reconstituted with splenic $CD4^+$ T cells and treated with 4 mg/kg Con A. Data are presented as mean ± SD ($n \geq 4$ per group). Statistics were analyzed by One-Way-ANOVA with Bonferroni's post-hoc test (* $p \leq 0.05$; n.s., not significant).

3.4.3 Resistance towards Con A induced hepatic injury after Con A pretreatment of $CD4^+$ T cell transplanted $RAG1^{-/-}$ mice

Splenic $CD4^+$ T cells were transferred into $RAG1^{-/-}$ mice. Fourteen days afterwards recipient mice were treated with solvent or Con A (3 mg/kg), which resulted in increased ALT activities in plasma of Con A treated animals 8 hours later (fig. 3.12A). Another fourteen days afterwards mice were treated with a second Con A dose (4 mg/kg). While ALT plasma activities were moderately increased in solvent pretreated mice, ALT

plasma activities were nearly at a physiological range in Con A pretreated mice 8 hours after Con A treatment (fig. 3.12B). The differences in ALT plasma activities were not significant. However, two additional experiments showed the same tendency. This suggests that Con A treatment of $CD4^+$ T cell transplanted $RAG1^{-/-}$ mice induces resistance towards later Con A injections. Additional to ALT plasma activities, systemic inflammation was assessed by cytokine plasma levels. IL-6 and IFNγ appeared slightly decreased in plasma from Con A pretreated animals if compared to solvent pretreated animals. In contrast, IL-10 levels appeared slightly increased in plasma from Con A pretreated animals. IL-2 levels were nearly equal in the two groups.

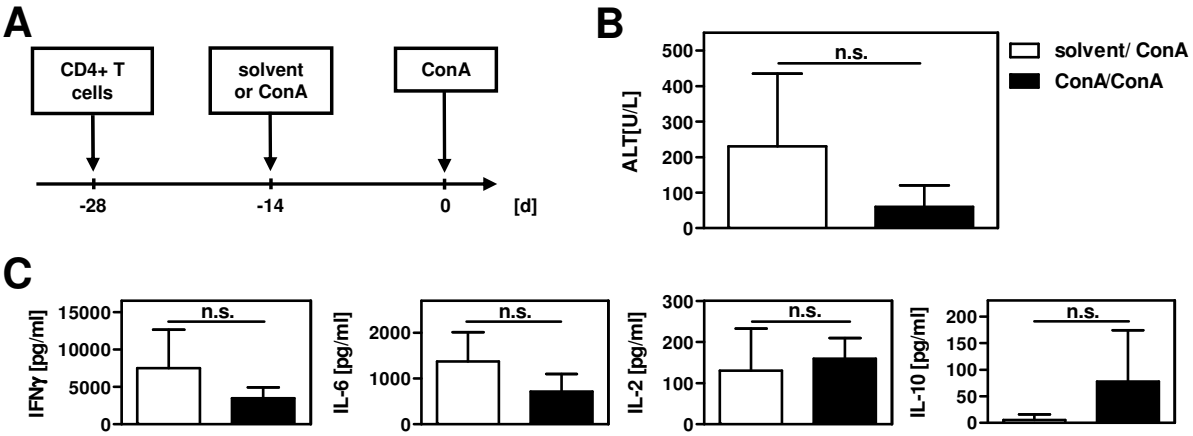

Figure 3.12: *Resistance towards Con A induced hepatic injury after Con A pretreatment of $CD4^+$ T cell transplanted $RAG1^{-/-}$ mice:* A) Injection scheme: MACS purified WT $CD4^+$ cells were transfered into $RAG1^{-/-}$ recipients at day -28. Fourteen days afterwards, reconstituted $RAG1^{-/-}$ mice were treated with solvent or 3 mg/kg Con A. At day 0, $CD4^+$ cell reconstituted and solvent or Con A pretreated mice were challenged with 4 mg/kg Con A. B) ALT plasma activities 8 hours after solvent or Con A pretreatment at day -14. C) ALT plasma activities 8 hours after Con A challenge at day 0. D) Plasma cytokine levels 8 hours after Con A challenge at day 0. Data are presented as mean ± SD (n≥3 per group). Statistical analysis was done by student's t-test on logarithmized (ALT) or original (cytokines) data (n.s., not significant).

3.4.4 Requirement of $CD4^+$ T cells during Con A pretreatment for the induction of liver resistance towards Con A

To test if the presence of $CD4^+$ T cells is necessary for the induction of resistance towards Con A hepatitis $RAG1^{-/-}$ mice or WT mice were treated with solvent or with

7 mg/kg Con A. After eight hours, ALT plasma activities increased only slightly in Con A challenged RAG1$^{-/-}$ mice and were still in a physiological range while ALT plasma activities were clearly increased in Con A challenged WT mice (fig. 3.13B). Three days later, splenic CD4^{+} T cells from naïve WT mice were transferred into RAG1$^{-/-}$ mice. Fourteen days after the transfer, RAG1$^{-/-}$ and WT mice were challenged with 3.5 mg/kg or 7 mg/kg Con A, respectively. Due to high morbidity of RAG1$^{-/-}$ mice, all animals were sacrificed 6 hours after Con A challenge. ALT plasma activities were in a pathological range in both, solvent and Con A pretreated RAG1$^{-/-}$ mice. In contrast, Con A pretreated WT mice showed significantly lower ALT levels than solvent pretreated WT mice. Together with the prior experiments these findings indicate that CD4^{+} T cells might be necessary for induction of resistance towards Con A induced hepatitis.

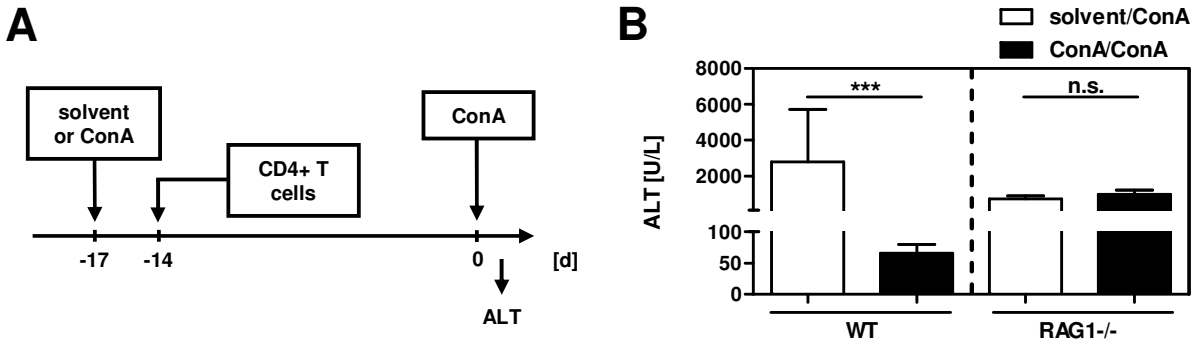

Figure 3.13: *Requirement of CD4^{+} T cells for the induction of liver resistance towards Con A:* A) Injection scheme: Wt or RAG1$^{-/-}$ mice were pretreated with solvent or 7 mg/kg Con A. Three days afterwards MACS purified CD4^{+} cells from naïve wt mice were transfered into RAG1$^{-/-}$ recipients. Fourteen days afterwards, wt mice were challenged with 7 mg/kg and reconstituted RAG1$^{-/-}$ mice were challenged with solvent or 3.5 mg/kg Con A. B) ALT plasma activities as determined 8 hours after Con A challenge. Data are presented as mean ± SD (n≥3 per group). Statistical analysis was done by student's t-test on logarithmized data (*** p≤0.001; n.s., not significant).

3.5 Role for Kupffer cells in the establishment of a milieu protecting against Con A induced hepatic injury

Besides Tregs, KCs were postulated to contribute to protection against Con A induced hepatitis by secretion of large amounts of IL-10 [Erhardt et al., 2007]. Macrophages can switch their phenotype from a proinflammatory type I, secreting large amounts of the pro-inflammatory cytokines TNF and IL-12 upon activation, to a rather anti-inflammatory type II, secreting large amounts of the anti-inflammatory cytokine IL-10. This led to the hypothesis that KCs might switch their phenotype to a stable antiinflammatory phenotype subsequently to Con A induced hepatitis.

3.5.1 Induction of resistance towards Con A induced hepatic injury in the absence of Kupffer cells

To investigate if KCs switch their phenotype and gain anti-inflammatory properties during the first Con A treatment, mice were treated with PBS or KC-depleting clodronate liposomes 48 hours before the first Con A injection. Eight hours afterwards some mice were sacrificed to validate depletion of KCs via histology. PBS treated mice showed F4/80$^+$ cells in liver tissue, whereas these were completely absent in mice treated with clodronate liposomes. Furthermore, blood was drawn and plasma ALT activities were determined 8 hours after solvent or Con A pretreatment. ALT activities in Con A treated mice were significantly increased compared to solvent treated mice. However, Con A treated mice depleted of KCs showed only very slightly increased ALT activities compared to KC depleted solvent control mice (fig. 3.14A). This confirmed the previous observation that KCs are indispensable for the onset of hepatitis after a single Con A injection [Schümann et al., 2000]. Fourteen days after Con A pretreatment, mice were challenged with a second Con A dose. Eight hours after the second Con A challenge, all solvent pretreated mice showed highly enhanced ALT activities. In contrast, low ALT plasma activities were detectable in Con A pretreated groups, irrespective of KC depletion before the first Con A treatment. Plasma cytokine levels for TNFα, IFNγ, IL-10 and IL-6 were equal in the solvent pretreated groups and among Con A pretreated groups plasma levels of these cytokines were equal, too. However, compared to the saline

pretreated groups, both Con A pretreated groups showed lower plasma levels of TNFα, IL-6, IL-10 and similar or very slightly reduced IFNγ plasma levels. These data suggest that resistance towards Con A induced hepatitis is established even in the absence of Kupffer Cells during the first Con A stimulus.

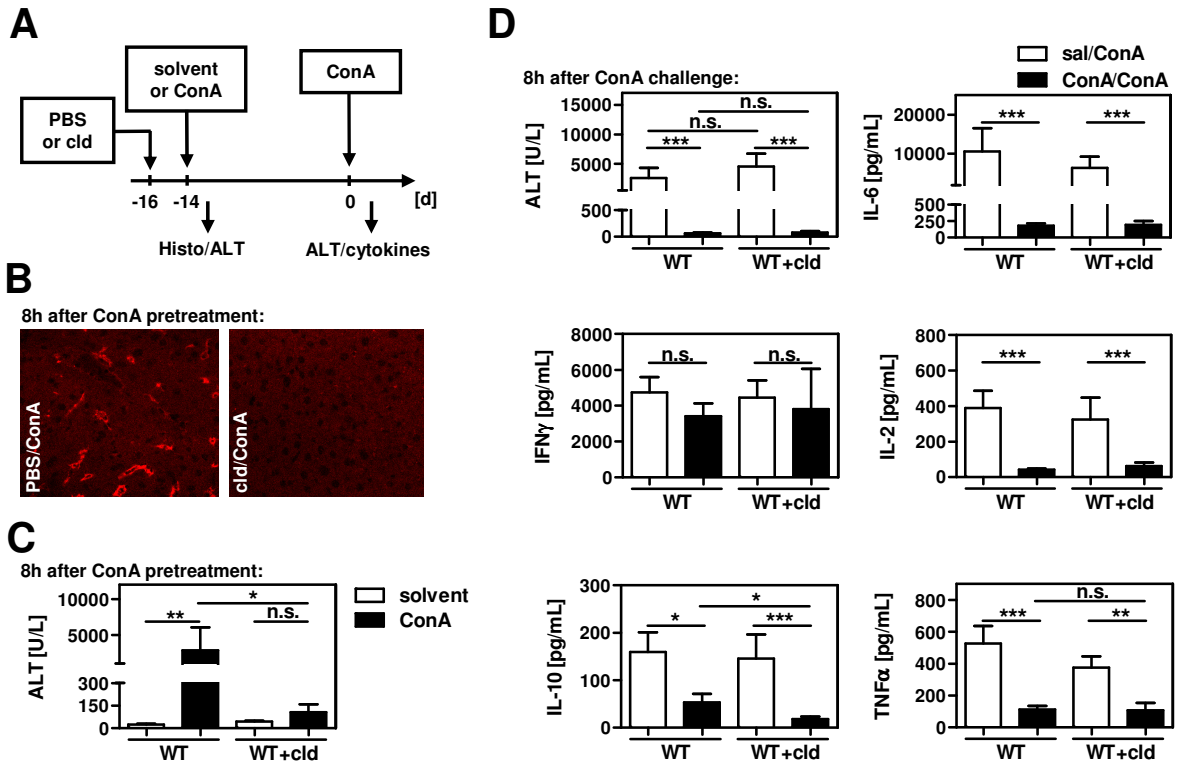

Figure 3.14: *Induction of resistance towards Con A induced liver injury in the absence of Kupffer cells and hepatitis during Con A pretreatment:* A) Injection scheme: Fourty-eight hours before solvent or Con A pretreatment, mice received PBS or clodronate liposomes. Eight hours after pretreatment, some mice were sacrificed (n=2 per group) for histological liver analysis and blood was drawn from the other mice. Fourteen days after pretreatment, mice were challenged with Con A and sacrificed. Liver damage as well as systemic plasma cytokine levels were determined 8 hours afterwards. B) Liver immunohistology from Cryosection. F4/80$^+$ cells are stained in red. C) ALT plasma activities 8 hours after solvent or Con A pretreatment. D) Plasma ALT activities and plasma cytokine levels 8 hours after Con A challenge. TNFα levels were determined 2 hours after Con A challenge. Data are presented as mean $\pm$ SD (n=4 per group). Statistical analysis was done by One-Way-ANOVA with Bonferroni's post-hoc test (* $p \leq 0.05$; ** $p \leq 0.01$; *** $p \leq 0.001$; n.s., not significant).

3.5.2 Resistance towards Con A induced liver injury despite depletion of potentially de novo differentiated KCs after Con A pretreatment

Acute liver injury results in secretion of monocyte-chemoattractant protein-1 (MCP-1, CCL2) and recruitment of large amounts of monocytes, the precursors of tissue macrophages like KCs [Zimmermann et al., 2012]. MCP-1 is also released from the liver after Con A challenge [Ajuebor et al., 2003]. This indicates that Con A challenge might result in de novo differentiation of KCs in the liver. To investigate if such de novo differentiated KCs have anti-inflammatory characteristics that protect from Con A-induced hepatitis, mice received PBS or clodronate liposomes for KC depletion five days after solvent or Con A pretreatment (8 mg/kg). Fourty-eight hours after PBS or clodronate treatment, some mice were sacrificed and KCs were stained in livers to verify depletion (fig. 3.15B). The remaining mice were restimulated with a second dose Con A (9 mg/kg) 14 days after depletion of KCs. Eight hours later, ALT activities and cytokine levels were analyzed in plasma. PBS and clodronate treated mice that had been pretreated with Con A showed significantly reduced plasma ALT activities compared to mice that received Con A for the first time. This indicates that monocytes that are recruited upon a single Con A injection and then differentiate into Kupffer Cells in the regenerating liver are negligible for suppression of liver inflammation upon a second Con A dose.

3.6 Resistance towards Con A induced hepatic injury - a liver specific process?

Depletion of KCs before Con A pretreatment inhibited the immediate hepatic injury after Con A pretreatment. However, this Con A pretreatment was still sufficient to induce resistance towards hepatic injury upon a second Con A challenge 14 days later. This finding raised the question if there was a liver-intrinsic mechanism of protection or if there was rather a central, possibly liver independent mechanism protecting against Con A induced liver injury. Because it was shown that one of the first events after Con A injection is binding of Con A itself to the liver sinusoids [Gantner et al., 1995; Knolle et al., 1996], it was analyzed if Con A binding to sinusoids was modulated in Con A pretreated mice and circumventing the liver as primary Con A target organ.

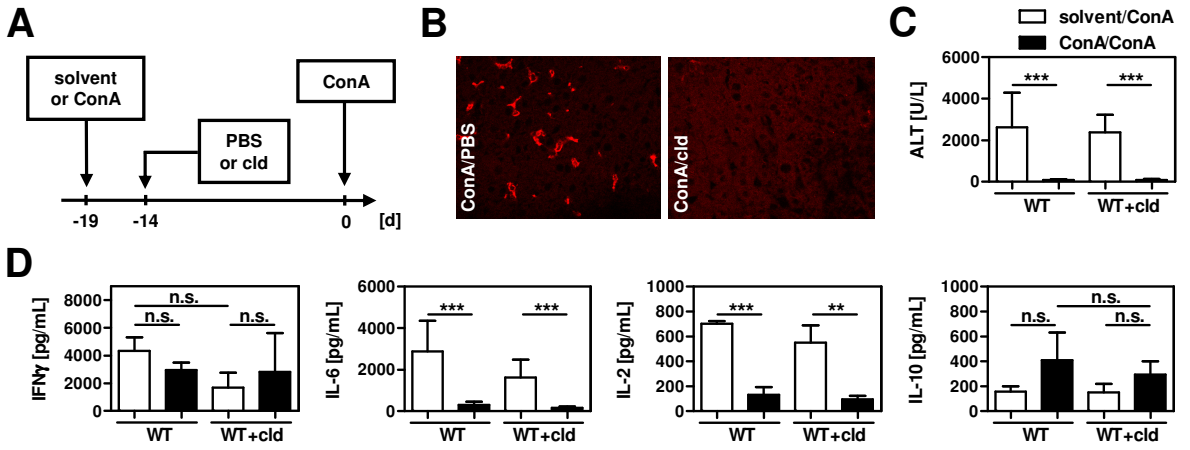

Figure 3.15: *Hepatic resistance towards Con A despite depletion of potentially de novo differentiated KCs after Con A pretreatment:* A) Treatment scheme: Mice received PBS or clodronate liposomes 5 days after solvent or Con A pretreatment (8 mg/kg). Fourteen days after cld administration mice were challenged with 9 mg/kg Con A. B) Seven days after Con A pretreatment and 48 hours after PBS or clodronate administration 2 control mice were sacrificed and their livers were stained for F4/80$^+$ KCs (red). C) Eight hours after Con A challenge mice were sacrificed and ALT plasma activities were determined. D) Plasma cytokines were also determined 8 hours after Con A challenge. Data are presented as mean ± SD (n=4 per group). Statistical analysis was done by One-Way-ANOVA with Bonferroni's post-hoc test (** $p \leq 0.01$; *** $p \leq 0.001$; n.s., not significant).

3.6.1 Accumulation of Con A in liver sinusoids of naïve and Con A protected mice

To examine a possible modulation of Con A binding to the sinusoidal cells after Con A i.v. injection, Con A-FITC was injected into mice that had been pretreated with solvent or Con A fourteen days earlier. FITC fluorescence in liver sinusoids was analyzed via histology 30 minutes after Con A-FITC treatment. As shown in figure 3.16, FITC fluorescence was detected along sinusoids of Con A-FITC treated solvent and Con A pretreated mice. FITC fluorescence was not completely overlapping with F4/80$^+$ KCs, suggesting that other cells, most likely endothelial cells, contribute to Con A binding to liver sinusoids. This demonstrates that Con A is also bound in liver sinusoids from Con A protected mice indicating that the liver might still be the primary organ targeted by Con A itself.

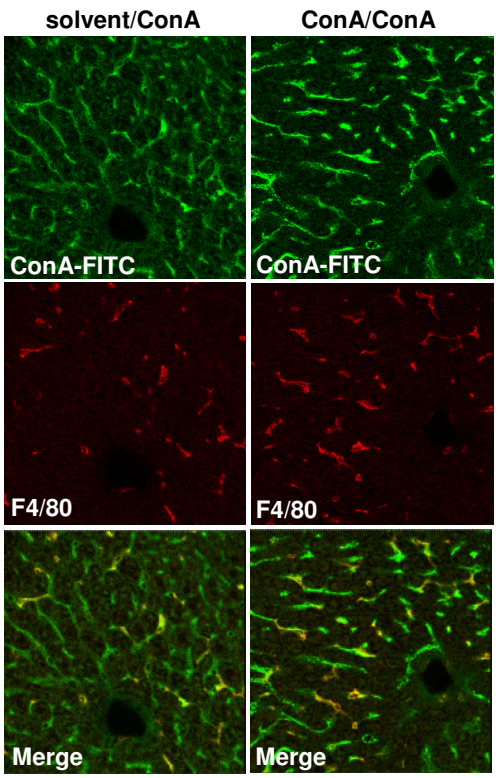

Figure 3.16: *Accumulation of Con A in liver sinusoids of naïve and Con A protected mice:* Mice were pretreated with solvent or 8 mg/kg Con A. Fourteen days later, mice were injected with Con A-FITC in a dose equivalent to about 3.5 mg/kg Con A. Thirty minutes after Con A-FITC injection mice were sacrificed and F4/80$^+$ KCs were stained in cryo-preserved liver tissue. Liver sections were subjected to confocal laser imaging.

3.6.2 Con A binding by LSECs of naïve and Con A protected mice

Con A-FITC accumulated in liver sinusoids of both, naïve and Con A pretreated mice. The efficiency of Con A binding by LSECs was then investigated in more detail. Therefore, solvent and Con A pretreated mice were challenged with Con A-FITC 14 days after pretreatment. 30 minutes after Con A-FITC administration mice were sacrificed and liver mononuclear cells (MNCs) were isolated via gradient centrifugation. FITC mean fluorescence intensity (MFI) was quantified via flow cytometry. As shown in fig. 3.17A, FITC MFI was highest in CD31$^+$ cells, suggesting that indeed endothelial cells are responsible for Con A binding to the liver. Compared to LSECs from solvent pretreated mice, LSECs from Con A pretreated mice showed significantly higher FITC fluorescence (fig. 3.17B). These results were confirmed by two similar experiments. This indicates, that LSECs from Con A protected mice might bind Con A more efficiently than LSECs from naïve mice. As it was demonstrated that Con A mainly accumulates in liver sinusoids and not in other organs after i.v. injection [Gantner et al., 1995] it was analyzed if efficient binding of Con A by LSECs leads to a faster decrease of Con A concentrations in

the circulation. Hence, Con A-FITC was injected into mice fourteen days after solvent or Con A pretreatment. Blood was drawn after 5, 15, 30 and 75 minutes and Con A plasma concentrations were determined by FITC fluorescence of plasma samples. The decline of Con A concentration was more pronounced in plasma from Con A pretreated mice if compared to solvent pretreated mice (fig. 3.17C) indicating that efficient Con A binding by the liver sinusoids might influence the levels of circulating Con A.

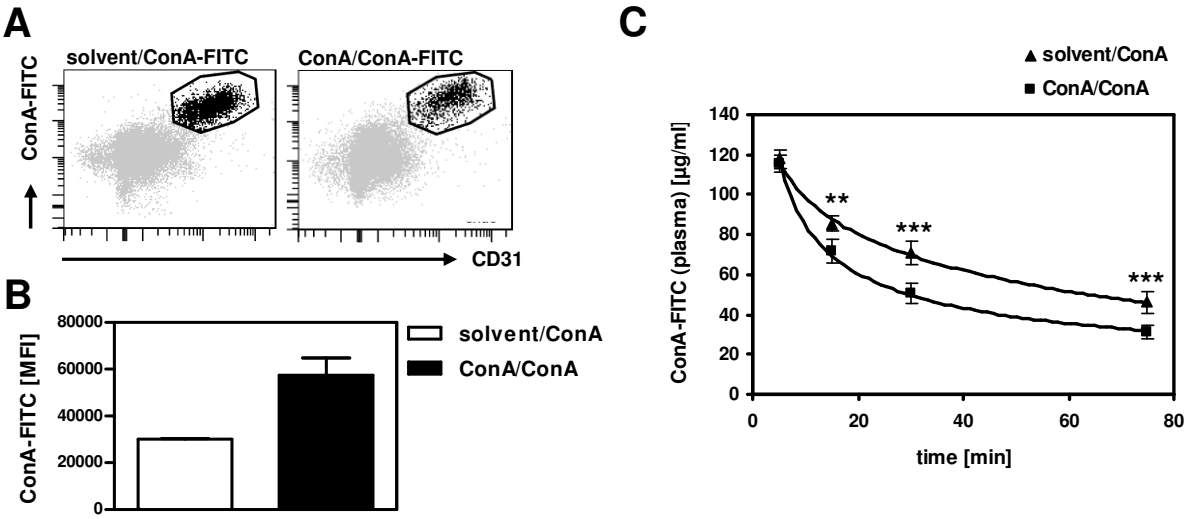

Figure 3.17: *Con A binding by LSECs of naïve and Con A protected mice:* A) and B) Mice were pretreated with solvent or 8 mg/kg and 14 days later challenged with Con A-FITC equivalent to 5 mg/kg Con A. Mice were sacrificed 30 minutes after Con A-FITC injection and liver mononuclear cells were isolated by gradient centrifugation using OptiPrep. A) FITC fluorescence was analyzed in $CD31^+$ endothelial cells via flow cytometry. B) FITC mean fluorescence intensity in $CD31^+$ endothelial cells. Data represent mean ± SD ($n \geq 2$ per group) C) Mice were pretreated with solvent or 7 mg/kg Con A. Fourteen days afterwards mice were challenged with Con A-FITC equivalent to 7 mg/kg Con A. Con A plasma concentrations were determined by FITC fluorescence in plasma 5, 15, 30 and 75 minutes after Con A-FITC injection. Data represent mean of four individuals per group ± SD ($n \geq 4$ per group). Statistics were analyzed by Two-Way-ANOVA with the variable treatment and matched time variable with Bonferroni's post-hoc test (** $p \leq 0.01$; *** $p \leq 0.001$).

3.7 Protection from liver microcirculatory dysfunction early after Con A challenge in Con A pretreated mice

LSECs are among the first liver resident cells coming into contact with Con A. Moreover, it was postulated that death of LSECs might be among the first events resulting in liver damage in the Con A hepatitis model [Knolle et al., 1996]. Indeed, a decrease in velocity of the intrahepatic blood flow and even hemorrhage into the liver parenchyma have been reported to occur early after Con A injection [Yang et al., 2010; Miyazawa et al., 1998]. Thus, impairment of the liver microcirculation seems to be involved in the generation of liver damage after Con A challenge of mice. In the following experiments, it was investigated if Con A pretreatment could abrogate impairment of liver microcirculation and thereby protect from hepatic damage.

3.7.1 Physiological blood flow after Con A challenge of protected mice

Impairment of liver microcirculation and decrease of velocity of hepatic blood flow might result in the accumulation of blood in the liver. Therefore, potential Con A induced blood accumulation in the liver was examined by MRI analysis. Mice were pretreated with solvent or 8 mg/kg Con A. Fourteen days later, mice of both groups were either treated with solvent or challenged with 9 mg/kg Con A. Four hours after solvent treatment or Con A challenge, T2* time was measured in livers of the animals by MRI analysis. In comparison to Con A challenged Con A pretreated mice, liver tissue of solvent pretreated Con A challenged mice appeared darker, indicating that T2* time was decreased in these livers (fig. 3.18A). Moreover, T2* time was only slightly reduced upon comparison of Con A challenged Con A pretreated mice and unchallenged mice (fig. 3.18B). Thus, heavily increased blood accumulation is seen after Con A challenge of solvent but not of Con A pretreated animals suggesting that dysfunction of the hepatic microcirculation after Con A challenge is inhibited in Con A pretreated animals.

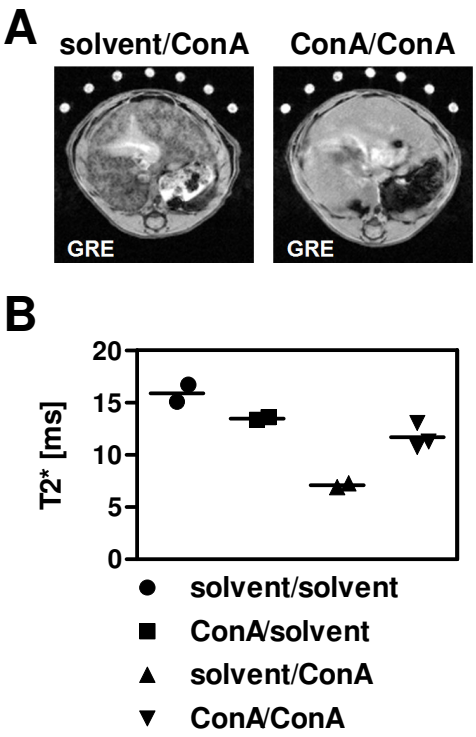

Figure 3.18: *Intact liver microcirculation after Con A challenge of protected mice:* Enhanced accumulation of blood was used as parameter to study impairment of liver microcirculation by MRI analysis. Mice were pretreated with solvent or Con A (8 mg/kg) and 14 days analyzed by MRI or challenged with 9 mg/kg Con A and 4 hours after challenge analyzed by MRI. Quantitative T2*-relaxometry was performed via gradient echo (GRE) sequence. In the GRE image, short T2* times provide a weaker signal and therefore, appear dark. A) Representative GRE images of livers from Con A challenged solvent pretreated (right) or Con A challenged Con A pretreated (left) mice. B) Quantification of T2* times from livers of solvent pretreated or Con A pretreated mice as well as from livers of Con A challenged solvent pretreated or Con A challenged Con A pretreated mice.

3.7.2 Inhibition of blood coagulation upon Con A challenge of Con A protected animals

The decreased presence of hemoglobin in livers of Con A challenged Con A pretreated mice when compared to Con A challenged solvent pretreated mice suggested that Con A pretreated animals might be protected from liver damage by inhibition of severe dysfunction of the liver microcirculation that might result in a detrimental lack of oxygen supply. Because Con A induced microcirculatory dysfunction in the liver was shown to involve hypercoagulation [Miyazawa et al., 1998], it was tested, if Con A pretreatment might inhibit hypercoagulation upon Con A challenge. To investigate this, the prothrombin time was determined after Con A challenge (8 mg/kg) of solvent pretreated or Con A pretreated (7 mg/kg) mice. Three hours after Con A challenge, the prothrombin time was reduced in mice that had been pretreated with Con A if compared to animals that had been pretreated with solvent 14 days before (fig. 3.19). In fact, the prothrombin time was equal to that of naïve control mice. Hence, Con A challenge of naïve mice seems to result in severe hypercoagulation as demonstrated by consumption of coagulation factors shown by elongated prothrombin time. Upon challenge of Con A pretreated

mice, however, prothrombin time is of physiological duration indicating that coagulation is suppressed upon Con A challenge of these animals.

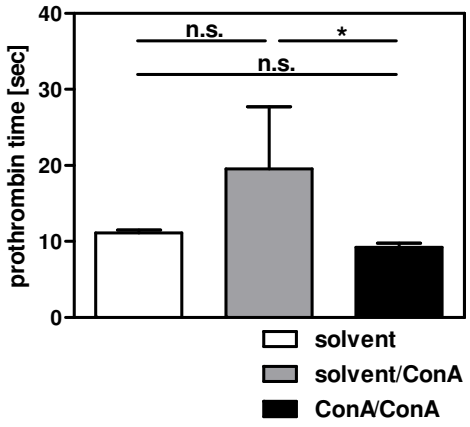

Figure 3.19: *Inhibition of blood coagulation upon Con A challenge of Con A protected animals:* Mice were pretreated with solvent or 7 mg/kg Con A. Fourteen days later, mice were challenged with 8 mg/kg Con A. After 3 hours, blood was taken and equally citrated. Coagulation of citrated blood was activated by Dade®Innovin® and time to fibrin clot formation was measured by a KC10 coagulometer instrument. Data are presented as mean ± SD. Statistical analysis was done by One-Way-ANOVA with Bonferroni's post-hoc test (* $p \leq 0.05$; n.s., not significant).

3.8 Analysis of Global Liver Gene Expression in Con A susceptible and Con A protected mice

Four hours after Con A challenge, liver damage is not yet detectable by ALT elevation in plasma. However, MRI analysis suggested, that increased blood accumulation and thus, a first sign of liver damage, was present in solvent pretreated but not or only slightly in Con A pretreated mice at this time point. To investigate potential differences in gene expression that might give a hint on the mechanism resulting in resistance of hepatic parenchyma, global liver gene expression was quantified via microarray analysis in mice 14 days after solvent or Con A pretreatment or four hours after Con A challenge of solvent or Con A pretreated mice.

3.8.1 Minor regulation in liver gene expression of Con A protected mice compared to Con A susceptible mice

Significantly regulated genes were not detected upon comparison of gene expression between groups 14 days after solvent or Con A pretreatment (see table 3.1, solvent/solvent vs. Con A/solvent). Similarly, significantly regulated genes were not detected in liver tissues when Con A challenged solvent pretreated mice were compared to Con A challenged Con A pretreated mice (solvent/Con A vs Con A/Con A). However, 2025 genes

were significantly regulated when Con A challenged solvent pretreated mice were compared to unchallenged solvent pretreated mice (solvent/solvent vs solvent/Con A) and 1680 genes were significantly regulated upon comparison of Con A challenged Con A pretreated mice and unchallenged Con A pretreated mice (Con A/solvent vs Con A/Con A). This suggests, that there are only minor differences in gene expression in response to Con A between livers of solvent and Con A pretreated mice indicating that the inflammatory response in livers is evoked by Con A in both situations.

Table 3.1: Microarray statistics: Quantities of significantly regulated genes upon group comparisons of microarray analysis by B&H corrected student's t-test

solvent/solvent vs Con A/solvent (comparison 1)	**solvent/solvent vs solvent/Con A** (comparison 2)	**solvent/Con A vs Con A/Con A** (comparison 3)	**Con A/solvent vs Con A/Con A** (comparison 4)
none	2025	none	1680

3.8.2 Expression analysis of cytokine and cytokine receptor genes

Expression levels of cytokine and cytokine receptor genes, that were significantly regulated upon at least one of the comparisons 2 (solvent/solvent vs solvent/Con A) and 4 (Con A/solvent vs Con A/Con A) were visualized by a median centered log2 scaled heatmap (see fig. 3.20). Samples from unchallenged solvent and unchallenged Con A pretreated mice (solvent/solvent and Con A/solvent) clustered together as well as samples from Con A challenged solvent pretreated and Con A challenged Con A pretreated mice (solvent/Con A and Con A/Con A). This indicated similar cytokine and cytokine receptor gene expression patterns in unchallenged susceptible and protected mice as well as in Con A challenged susceptible and protected mice, and is in line with the observation that significant gene regulations upon comparison between these groups, that clustered together, were not detectable(see table 3.1). In a second similar heatmap, the same cytokine and cytokine receptor genes were depicted by a median centered log2 scaled heatmap but only for comparison between Con A challenged solvent pretreated and Con A challenged Con A pretreated mice (solvent/Con A and Con A/Con A, fig. 3.21). In this case, Con A challenged Con A pretreated mice clustered together and Con A challenged solvent pretreated mice clustered together indicating that gene expression was

similar within one group and different from the other group. This indicated the existence of minor differences in cytokine and cytokine receptor genes between these two groups. However, only few cytokine/cytokine receptor genes showed clearly different patterns upon comparison between Con A challenged Con A pretreated or Con A challenged solvent pretreated mice. Among these were CXCL2 and IL-6, which were downregulated in samples from Con A pretreated mice.

3.8.3 Expression analysis of genes involved in apoptosis signaling

Similar median centered log2 scaled heatmaps of significantly regulated genes from comparisons 2 (solvent/solvent vs solvent/Con A) and 4 (Con A/solvent vs Con A/Con A) were created for genes involved in apoptosis signaling (fig. 3.22). Comparison between all 4 groups again showed clustering of samples from unchalleged susceptible and protected mice (solvent/solvent and Con A/solvent) as well as clustering of samples from challenged susceptible and protected mice (solvent/Con A and Con A/Con A). This was again in concordance with the finding that significant differences were not detectable upon comparison of these groups that clustered together (see table 3.1). However, a second median centered log2 scaled heatmap of these genes considering only Con A challenged samples of solvent and Con A pretreated mice (solvent/Con A and Con A/Con A) revealed again minor differences in gene expression of genes involved in apoptosis signaling between these two groups (fig. 3.23). Especially genes involved in NFκB signaling seemed to be downregulated in samples from Con A pretreated mice.

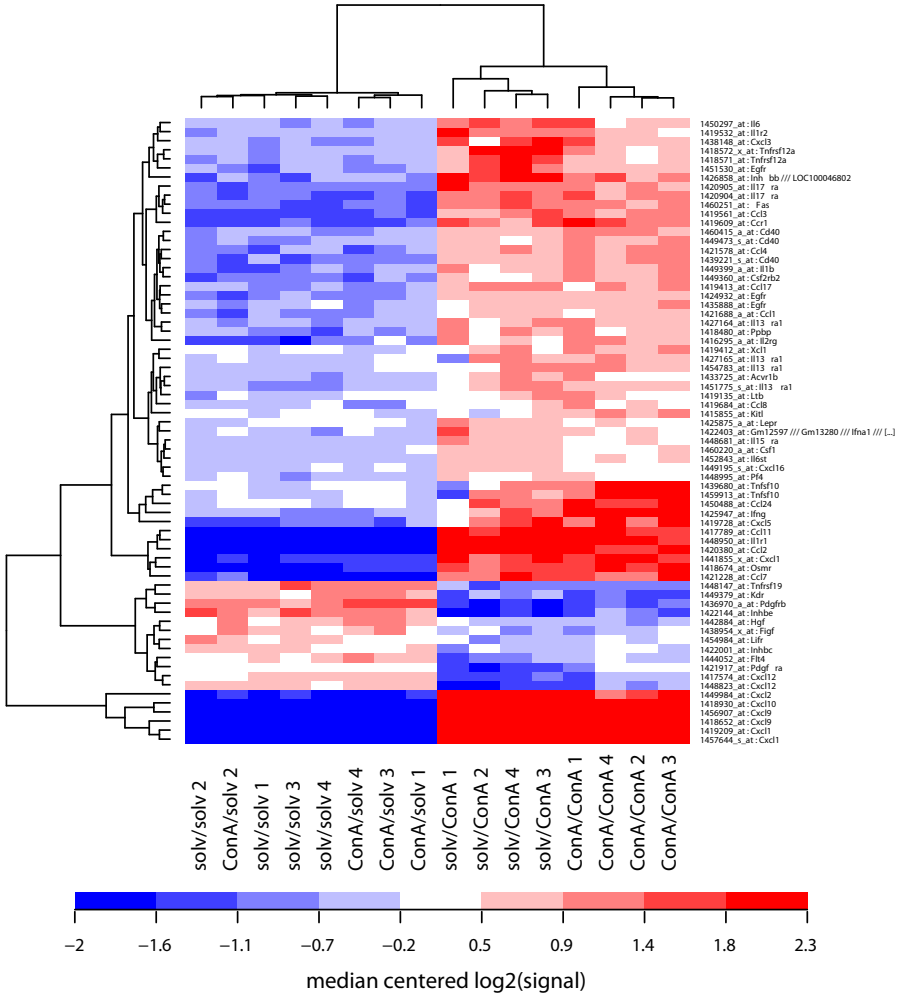

Figure 3.20: *Heatmap of regulated cytokine and cytokine receptor genes from healthy and Con A challenged livers of solvent or Con A pretreated animals:* Mice were injected with solvent or 8 mg/kg Con A. Fourteen days later, some solvent or Con A pretreated mice were sacrificed. Other solvent or Con A pretreated mice were challenged with 9 mg/kg Con A and sacrificed 4 hours after Con A challenge. RNA was isolated from liver tissue and microarray analysis were performed by Affimetrix GeneChip® according to the manufacturer's protocol. Depicted are cytokine and cytokine receptor genes (according to the KEGG database [KEGG, b]) that were significantly regulated upon at least one of the comparisons 2 and 4 from table 3.1 (BH corrected student's t test). For the generation of a heatmap, the median fluorescence intensity was calculated from all samples for every single gene spot. For every gene spot, aberrations (x-fold) from the median were calculated for every sample and were depicted color-coded as shown in the scale (median centered log2 scale). Genes were clustered regarding similar regulation within the different samples (left frame clusters). Samples that showed a similar gene regulation profile were clustered (top frame cluster).

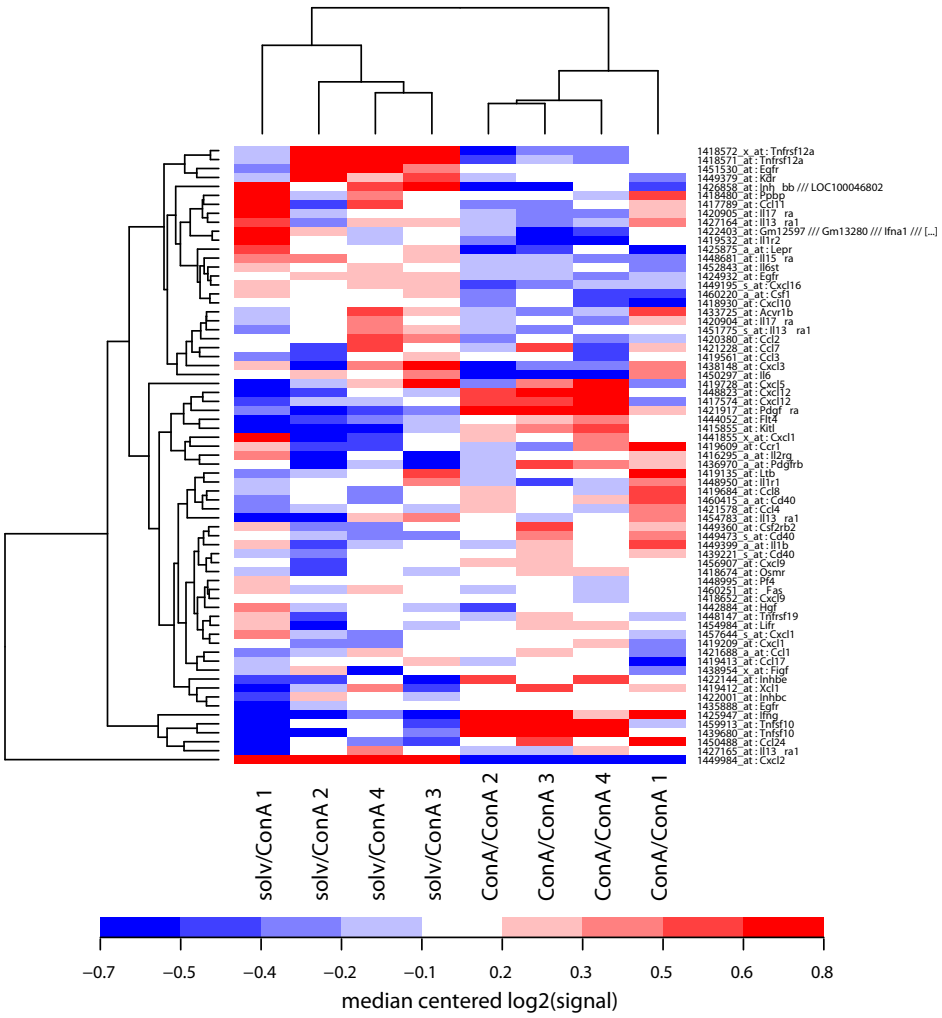

Figure 3.21: *Heatmap of regulated cytokine or cytokine receptor genes from Con A challenged livers of solvent or Con A pretreated animals:* Data were generated as described in fig. 3.20. Depicted are the same cytokine and cytokine receptor genes. For the generation of a heatmap, the median fluorescence intensity for every gene spot was calculated from samples of Con A challenged solvent pretreated or Con A challenged Con A pretreated mice. For every gene spot in a given sample, aberrations (x-fold) from the median are shown. Genes were clustered regarding similar regulation within the different samples (left frame clusters). Samples that showed a similar gene regulation profile were clustered (top frame cluster).

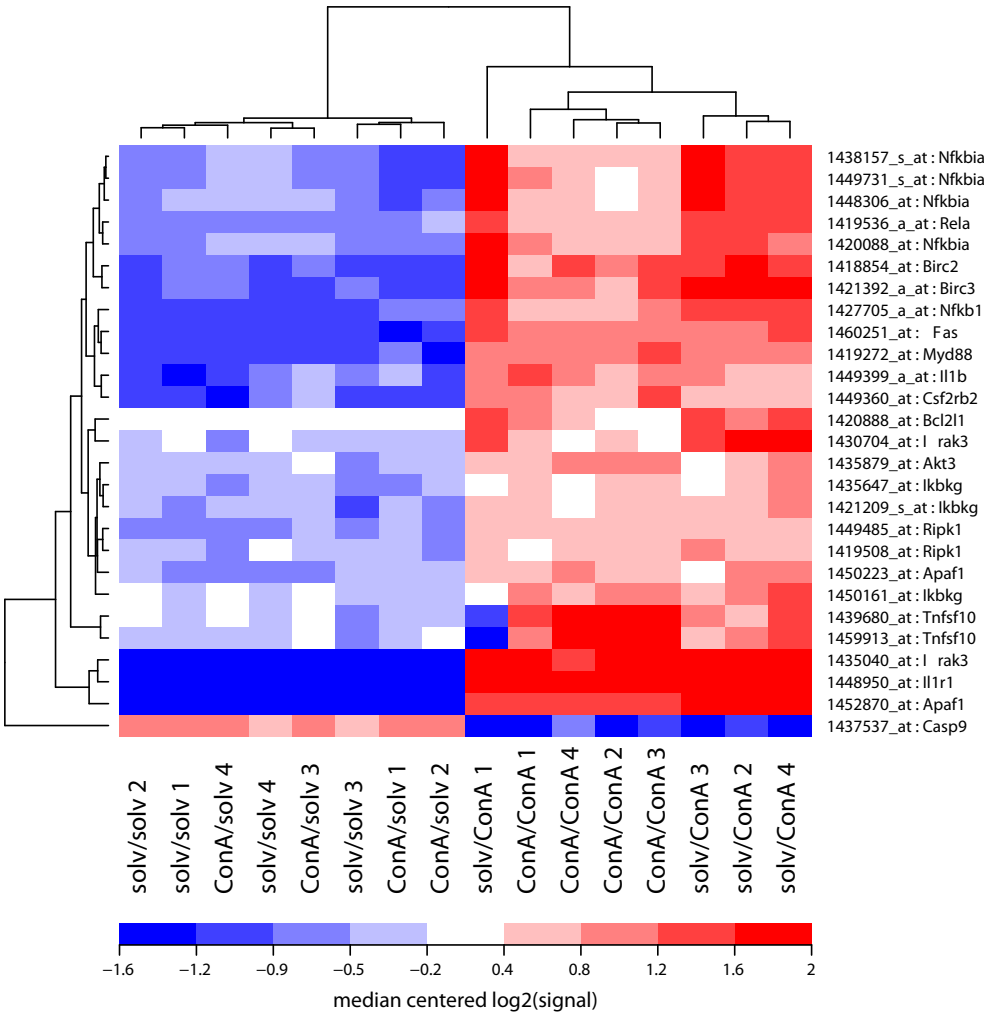

Figure 3.22: *Heatmap of regulated genes involved in cell death or cell survival from healthy and Con A challenged livers of solvent or Con A pretreated animals:* Data were generated as described in fig. 3.20. Depicted are genes involved in apoptosis signaling (according to the KEGG [KEGG, a]) that were significantly regulated upon at least one of the comparisons 2 and 4 from table 3.1 (BH corrected student's t test). For the generation of a heatmap, the median fluorescence intensities for every gene spot were calculated. For every gene spot in a given sample, aberrations (x-fold) from the median are shown. Genes were clustered regarding similar regulation within the different samples (left frame clusters). Samples that showed a similar gene regulation profile were clustered (top frame cluster).

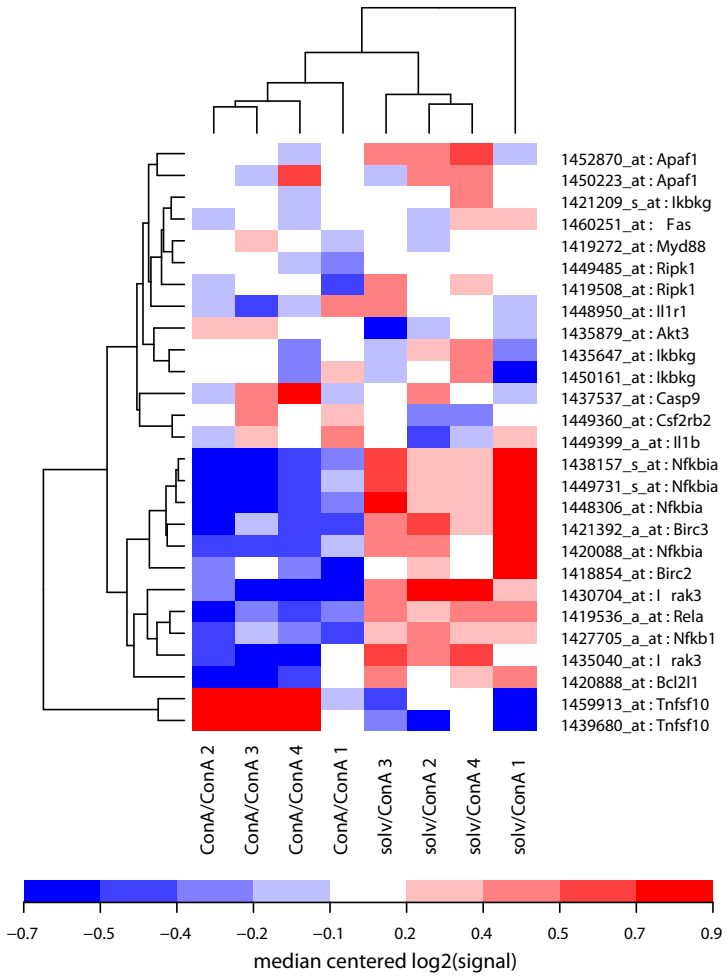

Figure 3.23: *Heatmap of regulated genes involved in cell death or cell survival from Con A challenged livers of solvent or Con A pretreated animals:*Data were generated as described in fig. 3.20. Depicted are the same genes involved in apoptosis signaling as described in fig. 3.22. For the generation of a heatmap, the median fluorescence intensity for every gene spot was calculated from samples of Con A challenged solvent pretreated or Con A challenged Con A pretreated mice. For every gene spot in a given sample, aberrations (x-fold) from the median are shown. Genes were clustered regarding similar regulation within the different samples (left frame clusters). Samples that showed a similar gene regulation profile were clustered (top frame cluster).

4 Discussion

The liver fulfills essential metabolic and detoxifying functions in the organism and pathology of the liver can be life-threatening. Liver inflammatory diseases can be the result of uncontrolled T cell responses. Polyclonal T cell activation by Con A culminates in T cell mediated liver disease. Here, the model of Con A induced hepatitis was used to analyze regulation of T cell responses in the liver.

4.1 Resistance towards hepatic injury despite aggravated Th1 conditioning upon a second Con A challenge 14 days after pretreatment

This study showed that protection of hepatocytes against Con A challenge can be induced by a sublethal Con A pretreatment 14 days earlier. Interestingly, this resistance occurred despite of liver inflammation because leukocytes were still recruited into the liver of Con A pretreated animals as shown by histology. Thus, a general suppression of liver inflammation including suppression of recruitment of leukocytes is excluded as a mechanism of protection. In line with that, IFNγ was not found to be regulated in plasma 2 hours after Con A challenge of pretreated mice and was even found to be upregulated 8 hours after Con A challenge. Interestingly, IFNγ is a critical upstream mediator of Con A induced liver damage because IFNγ was demonstrated to contribute to damage by stimulating TNFα secretion [Küsters et al., 1996; Nicoletti et al., 2000] and by recruiting leukocytes via stimulation of chemokine secretion and expression of adhesion molecules [Jaruga et al., 2004]. Thus, Th1 conditioning is not sufficient to induce liver damage, and protection against liver parenchymal damage can be induced without suppression of the Th1 response. This supposes a mechanism for protection that is different from the recently published mechanism 8 days after Con A pretreatment, where suppres-

sion of IFNγ was observed [Erhardt et al., 2007; Ye et al., 2009]. Most likely a different T cell response to Con A accounted for the modulated cytokine response. Therefore, cytokine production was investigated on a single cell level after in vitro restimulation of liver MNCs and splenocytes from solvent or Con A pretreated mice. NKT cells express high levels of the ART2 enzyme and thus, are highly prone to apoptosis after exposure to increased NAD^+ concentrations [Seman et al., 2003; Scheuplein et al., 2010]. Because increased NAD^+ concentrations might occur during cell isolation procedures, liver NKT cells isolated from the liver rapidly undergo apoptosis upon *in vitro* culture (see fig. 4.1). Therefore, ART2-inhibiting s+16a nanobody was injected before sacrification of mice to increase viability of NKT cells during *in vitro* restimulation. All analyzed hepatic T cell populations, i.e. $CD4^+$ T cells, $CD8^+$ T cells and NKT cells, produced less TNFα upon *in vitro* restimulation 14 days after *in vivo* Con A challenge of mice. Moreover, $CD4^+$ and $CD8^+$ T cells produced even more IFNγ suggesting that these cell populations contributed to the increased Th1 conditioned milieu upon *in vivo* Con A challenge 14 days after pretreatment. NKT cells showed the highest frequency of IFNγ^+ cells among the analyzed cell populations. Because NKT cells were reported to be enriched in livers 14 days after Con A treatment [Fujii et al., 2010], a finding that was also observed during the present study (data not shown), these cells might also contribute to enhanced IFNγ secretion upon the second Con A challenge. Importantly, modified cytokine expression patterns were more pronounced in T cells derived from the liver than from the spleen indicating that activation of T cells in presence of the tolerance-inducing liver milieu might have resulted in organ-specific long-lasting modulation of liver resident T cells. Taken together, a modulated T cell response indeed might contribute to protection against Con A induced hepatic parenchymal injury, since TNFα derived from T cells was shown to be essential for Con A induced hepatocye damage [Grivennikov et al., 2005].

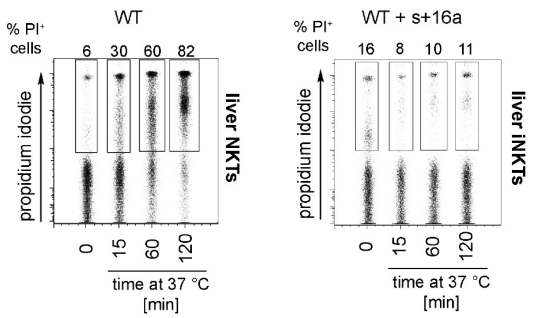

Figure 4.1: *Increase of iNKT cell vitality by ART2 inhibition:* Wt mice were sacrificed without or 15 minutes after s+16a i.v. treatment and liver MNCs were isolated by gradient centrifugation using Percoll. $CD3^+NK1.1^+$ NKT cells were FACS sorted and cultured at 37°C for indicated time periods. Propidium Iodide positive dead cells were quantified by flow cytometry. Unpublished data from Björn Rissiek.

4.2 Protection against hepatic injury is independent from IL-10

IL-10 was identified as a major immunosuppressive factor protecting against hepatitis 8 days after Con A pretreatment. [Erhardt et al., 2007; Ye et al., 2009]. This study, however, suggests that IL-10 is neglectable for protection against Con A induced hepatic damage 14 days after pretreatment because protection could not be abrogated by neutralizing IL-10 or by blocking IL-10R with monoclonal antibodies. Although postulated by two independent studies [Di Marco et al., 1999; Louis et al., 1997], an hepatitis exacerbating effect upon IL-10 neutralization or IL-10R blockade before a single Con A injection was not observed in these experiments. Louis et al. used an IL-10 monoclonal antibody derived from the same clone (JES5-2A5, IgG1κ) as in this study and injected 4 mg of antibody i.p. into C3H/HeJ mice 2 hours before Con A challenge. In contrast, di Marco et al. performed their experiments in C57Bl/6J mice and injected 2 mg of anti-IL-10 antibody (clone SXC.1, IgM) i.p. per mouse 2 hours before Con A challenge. As the dose administered here showed neutralization of IL-10 in plasma and because anti-IL-10R blockade showed accumulation of IL-10 in plasma 8 hours after Con A treatment, the antibody dose and route of injection seemed to be sufficient for neutralization of IL-10 signaling in experiments performed here. Consequently, strain differences might explain diverging observations between the present study and the study performed by Louis et al.. First of all, C3H/HeJ mice have a loss of function mutation in their TLR4 gene and thus, lipopolysaccharide (LPS) signaling is defective in these mice Poltorak et al. [1998]. LPS and TLR signaling, however, were shown to influence the outcome of ConA induced hepatitis [Ojiro et al., 2010; Nishikage et al., 1999]. Additionally, activation of TLR4 by LPS induces strong Th1 responses [Netea et al., 2005] and consequently, the Th1/Th2 balance might be shifted in TLR4 deficient C3H/HeJ mice. The proper Th immune response to a given pathogen is of high relevance for the host. For example, it has been shown that upon infection with *Leishmania major* T cells in C57Bl/6 mice produce IFNγ, which stimulates macrophages to clear the pathogen, whereas T cells in Balb/c mice instead produce more IL-4 which inhibits macrophages and results in fatal disease [Scott et al., 1988; Heinzel et al., 1989]. Interestingly, Th1-driven Con A induced hepatitis is more severe in C57Bl/6 mice, prone to Th1 responses, than in Balb/c mice, prone to Th2 responses [Mizuhara et al., 1998]. In a mouse model for food allergy, it has

been demonstrated, that C3H/HeJ mice show an even more pronounced IL-10 response after sensitization to an allergen than Balb/c mice which results in Th2 driven food allergy in C3H/HeJ but not Balb/c mice [Morafo et al., 2003]. Thus, indeed, C3H/HeJ mice might be rather prone to Th2 responses. Supporting this idea, Louis et al. found IL-10 levels of about 200 pg/ml in serum 2 hours after a single Con A treatment of C3H/HeJ mice, whereas in this study, IL-10 concentrations were below detection limit, i.e. $\leq$ 20 pg/ml. Taken together, IL-10 might indeed have a liver protective effect after a single Con A treatment but the ability to rapidly produce hepato-protective IL-10 might depend on the mouse strain or possibly also on animal housing. However, discrepancies remain between the present study and the study from di Marco et al., which could be possibly explained by the use of different antibody isotypes or different animal housing conditions. Additional experiments with recombinant IL-10 under animal housing conditions in Hamburg could provide further information on the protective role for IL-10 in Con A induced hepatitis.

4.3 Negligibility of Tregs for protection against hepatic injury

A protective role for Tregs has been shown in Con A induced hepatitis [Wei et al., 2008]. In that study, depletion of Tregs by a monoclonal antibody against CD25 exacerbated hepatitis after a single Con A injection and therefore, Tregs were proposed to protect against hepatitis in a TGFβ dependent mechanism. As mentioned before, Tregs were also suggested to protect against Con A induced hepatitis in an IL-10 dependent manner 8 days after Con A pretreatment [Erhardt et al., 2007]. Tregs were supposed to develop a T-bet expressing Th1-like phenotype after a single low dose Con A treatment enabling these cells to migrate very efficiently to the site of inflammation and suppress the local ongoing inflammation. [Erhardt et al., 2011]. Data from the present study suppose that Th1-like Tregs develop already 24 hours after a single Con A treatment. In DEREG mice, DT treatment before Con A pretreatment results in depletion of the entire Treg population 24 hours after Con A pretreatment. Thus, the occurence of Tbet$^+$ Tregs is completely abrogated 24 hours after Con A pretreatment. However, protection against hepatic damage was still observed in these animals upon Con A challenge 14 days after pretreatment. Additionally, protection was also observed if Tregs were depleted before

Con A challenge 14 days after pretreatment. Together, these data suggest that Tregs are not necessary for priming liver cells directly after Con A pretreatment and moreover, are not necessary as major suppressors upon Con A challenge 14 days after pretreatment indicating that Tregs might only play a minor role in protection from hepatic damage in this model.

4.4 Involvement of $CD4^+$ T cells in protection against hepatic injury

Con A induced hepatitis depends on $CD4^+$ T cells, which are most likely classical $CD4^+$ iNKT cells [Gisa Tiegs, 2003]. Interestingly, it has been shown that NKT cells become anergic after a single treatment of mice with hepatotoxic doses of α-galactosylceramide (α-GalCer) leading to liver protection against repeated α-GalCer stimulation 3 or 8 days afterwards [Biburger & Tiegs, 2008]. Moreover, it was shown recently that NKT cells develop hyporesponsiveness by noradrenergic neurotransmitter signaling in a murine stroke model leading to systemic immunosuppression after stroke [Wong et al., 2011]. Finally, Halder et al demonstrated that stimulation of Type II NKT cells by their natural ligand sulfatide induces recruitment of anergic classical iNKT cells by IL-12 expressing $CD11c^+$ DCs resulting in protection against Con A induced hepatic injury [Halder et al., 2007]. To investigate if modulation of $CD4^+$ T cells or NKT cells after Con A pretreatment might contribute to hepatic protection against Con A induced injury, a system involving reconstitution of $CD4^+$ cell populations in $RAG1^{-/-}$ was established. Transfer of $CD4^+$ cells from the spleen or liver into $RAG1^{-/-}$ mice resulted in reconstitution of the $CD4^+$ T cell compartment but most likely not of the NKT cell compartment. However, 14 days after $CD4^+$ T cell transfer $RAG1^{-/-}$ mice were highly susceptible towards Con A induced hepatitis indicating that $CD4^+$ T cells are sufficient to induce hepatic damage in this system. Con A pretreatment of $RAG1^{-/-}$ mice before $CD4^+$ T cell transfer could not protect from Con A induced hepatic damage 14 days after T cell transfer. In contrast, protection against Con A induced hepatic damage 14 days after Con A pretreatment seemed to be observable if pretreatment was performed 14 days after $CD4^+$ T cell transfer. In summary, these data indicate that $CD4^+$ T cells are involved in mediating protection against Con A challenge 14 days after pretreatment. $CD4^+$ T cells might either be modulated themselves or might be involved in modulating other cells like intrahepatic APCs.

Although the NKT cell compartment was only insufficiently reconstituted 14 days after $CD4^+$ cell transfer a role for NKT cells in protection against Con A hepatitis cannot be excluded completely. For example, transfer of NKT cells into $RAG1^{-/-}$ mice might have resulted in their activation and this might have resulted in downregulation of the NK1.1 marker in NKT cells which would have hindered their detection by NK1.1 antibodies.
In comparison to wt mice, protection against Con A induced hepatic damage was less robust in $RAG1^{-/-}$ mice adoptively transfered with $CD4^+$ cells. An explanation might be that the model of Con A induced hepatitis is different in $RAG1^{-/-}$ mice compared to wt mice: Severe hepatic damage was induced in $CD4^+$ cell transplanted $RAG1^{-/-}$ mice most likely in the absence of NKT cells, which were demonstrated to be essential in the wt system [Takeda et al., 2000; Kaneko et al., 2000]. Thus, lymphocyte populations in the liver of transplanted $RAG1^{-/-}$ mice, i.e. $CD4^+$ T cells and NK cells, are most likely of different characteristic with possibly higher cytotoxic potential upon activation than those in wt mice. Supporting this hypothesis, NK cells in $RAG1^{-/-}$ mice seem to develop from liver precursors and the liver was hypothesized as a possible pool for NK cells with special characteristics [Chambers & Ljunggren, 2010; Andrews & Smyth, 2010]. For example, liver derived NK cells show enhanced capability to kill tumor cells in a granzyme and perforin dependent manner [Vermijlen et al., 2002]. Despite the decreased robustness of liver protection, the finding that $CD4^+$ T cells are necessary for the induction of protection against Con A induced liver damage fits the finding of reprogrammed cytokine secretion patterns with more pronounced IFNγ and reduced TNFα secretion of $CD4^+$ T cells after Con A pretreatment of wt mice. IFNγ levels were not increased upon Con A challenge of Con A pretreated $RAG1^{-/-}$ mice in comparison to Con A challenge of solvent pretreated $RAG1^{-/-}$ mice, but IFNγ in $RAG1^{-/-}$ mice might mainly result from activated NK cells. Thus, it would be interesting to analyze if a reprogrammed cytokine expression pattern with pronounced IFNγ and reduced TNFα expression could be found in $CD4^+$ T cells from Con A pretreated transplanted $RAG1^{-/-}$ mice. In addition, RAG and common cytokine receptor gamma chain double knock-out mice lack all lymphoid cells including T, NKT, B and NK cells [Mazurier et al., 1999]. Therefore, reconstitution of these mice would provide a model for analysis of the role for $CD4^+$ T cells in Con A hepatitis and resistance towards it independent from NK cell activity.

4.5 Protection against hepatic injury without reprogramming of Kupffer cells

KCs play a critical role in the induction of hepatitis after Con A injection in mice. KCs start to secrete large amounts of TNFα after Con A challenge [Schümann et al., 2000; Hatano et al., 2008] and TNFα derived from myeloid cells including KCs is essential for the onset of Con A induced liver damage [Grivennikov et al., 2005]. Although KCs do not seem to contribute to systemic IL-10 levels upon a single Con A treatment [Hatano et al., 2008], they start to secrete large amounts of IL-10 upon Con A challenge 8 days after Con A pretreatment and this IL-10 secretion might be critical for liver protection 8 days after pretreatment [Erhardt et al., 2007]. In contrast, IL-10 does not contribute to protection against Con A induced injury 14 days after pretreatment. But KCs, however, might have been reprogrammed after Con A pretreatment and might thus be modulated in their IL-10-independent response upon Con A challenge 14 days later. This potential mechanism was investigated by depletion of KCs 48 hours before Con A pretreatment or 5 days after Con A pretreatment. According to the literature, complete KC repopulation of the liver after depletion of these cells by clodronate liposomes takes about 14 days [Yamamoto et al., 1996]. Consistent with findings from that report, hepatitis was inducible 16 or 14 days after KC depletion that was performed either before or after solvent pretreatment, respectively. This indicates that KCs had indeed repopulated the liver before mice were challenged with Con A. However, in neither of the two experiments resistance towards Con A challenge was abrogated by KC depletion performed before or after Con A pretreatment. This suggests that reprogramming of KCs might play a minor role for protection against Con A induced liver injury. However, modulation of the KC response by other cells, e.g. $CD4^+$ T cells, upon Con A challenge 14 days after pretreatment can not be excluded. Moreover, these findings were of particular interest, because depletion of KCs before Con A pretreatment abrogated liver disease immediately after Con A pretreatment but did not abrogate protection against Con A induced hepatitis 14 days later. This suggests that protection against Con A induced liver injury occurs even in the absence of liver disease after Con A pretreatment indicating that damage-associated reprogramming of the liver-resident cells, especially parenchymal cells, is not responsible for the induction of hepatoprotection against Con A challenge 14 days later.

4.6 Regulation of liver microcirculation

Liver specificity of Con A induced injury is thought to result from preferential binding of Con A to LSECs [Gantner et al., 1995]. Investigations from this study show that Con A is bound in the liver sinusoids in naïve and Con A pretreated mice indicating that the liver is still targeted by Con A 14 days after pretreatment. LSECs from pretreated mice might even bind Con A more efficiently and this might result in higher Con A accumulation in the liver and faster Con A clearance from the system in pretreated mice. It was suggested that binding of Con A by LSECs also predisposes these cells to Con A induced T cell toxicity and thus, that destruction of the endothelial barrier might represent one of the first detrimental events culminating in destruction of the liver microcirculation and finally liver disease [Knolle et al., 1996; Yang et al., 2010]. In this study, decreased accumulation of blood was observed in livers of Con A pretreated mice 4 hours after Con A challenge in comparison to naïve mice indicating inhibition of microcirculatory dysfunction upon Con A challenge 14 days after Con A pretreatment. Microcirculatory dysfunction occured before onset of liver parenchymal destruction, because reliable increase in ALT plasma activities did not appear at this time point (data not shown). Miyazawa et al. reported correlation of overshooting hemostasis with Con A damage and moreover, they suggested contribution of hemostasis to formation of liver damage because the thrombin inhibitor heparin protected from overshooting hemostasis and Con A induced liver injury [Miyazawa et al., 1998]. Interestingly, these authors showed that hypercoagulation and overshooting hemostasis and thus microcirculatory dysfunction, was dependent on IFNγ and TNFα which was recently confirmed by an additional study [Kato et al., 2013]. In the present study, a protective role for inhibition of hypercoagulation by inhibition of microcirculatory dysfunction was suggested by the finding that protection against Con A induced hepatic damage 14 days after pretreatment correlated with absence of elongated prothrombin time. Taken together, these experiments from the present study suggest that blood coagulation and microcirculatory dysfunction occur after Con A challenge of naïve mice but are inhibited after Con A challenge of pretreated mice indicating that this inhibition might protect these mice from Con A induced hepatic injury. Moreover, early TNFα regulation in these pretreated mice might be responsible for inhibition of coagulation and hemostasis.

4.7 Microarray analysis for detection of detrimental and protective pathways

Regulation of local inflammatory stimuli might be of major importance for resistance towards liver microcirculatory dysfunction and Con A induced liver damage 14 days after Con A pretreatment. A more global approach for such regulation was investigated by microarray analysis of liver gene expression. Interestingly, livers of naïve mice or livers of healthy mice 14 days after Con A pretreatment did not show any significant differences (B&H corrected t test) in gene expression suggesting complete recovery of liver tissue 14 days after low dose Con A induced hepatitis. However, due to low sensitivity of the statistical test system minor differences can not be excluded. Although significant differences in accumulation of blood low in oxygen and in consumption of coagulation factors were discovered upon comparison between naïve mice and pretreated mice early after Con A challenge, the same comparison failed to reveal significant differences in hepatic gene expression 4 hours after Con A challenge. This indicates either that genetic regulation plays a minor role in protection against onset of parenchymal damage or that minor alterations in gene expression account for protection against onset of parenchymal damage. To investigate the latter possibility gene expression was analyzed in more detail regarding cytokine signaling and apoptosis signaling. Some cytokine or cytokine receptor genes were indeed differently regulated after Con A challenge of naïve mice compared to Con A challenge of Con A pretreated mice. Among these genes were IL-6 and IFNγ confirming data obtained from serum analysis. The most obvious difference was found in expression of the chemokine CXCL2, which is also known as Macrophage Inflammatory Protein 2α (MIP-2α). CXCL2 belongs to the ELR-positive CXC chemokine family, which has a glutamic acid-leucine-arginine sequence (ELR) immediately in front of an N-terminal cysteine - any amino acid - cysteine motiv (CXC). ELR positive CXC chemokines bind the chemokine receptors CXCR1 and CXCR2 and are able to specifically induce migration of neutrophils. Indeed, it has been shown recently in a peritonitis model that CXCL2 is involved in the recruitment of neutrophils to the inflamed tissue [Filippo et al., 2013]. Additionally, it has been suggested that CXCL2 plays a key role in extravasation of neutrophils upon experimental endotoxemic liver injury [Li et al., 2004]. This hypothesis, however, has been doubted by Jaeschke et al. who could not reproduce these data [Jaeschke & Bajt, 2004]. Nevertheless, neutrophils play a detrimental

role in Con A induced liver injury [Bonder et al., 2004] and regulation of CXCL2 gene expression upon Con A challenge of pretreated mice might indicate that regulation of neutrophil recruitment or neutrophil activity might be important for protection against Con A induced liver damage.

Upon comparison of expression of apoptosis or survival associated genes between Con A challenged naïve or Con A challenged pretreated mice, the most obvious differentially regulated genes were a group of genes encoding for proteins involved in NFκB signaling, which were all less strongly induced in Con A preteated mice. Interestingly, genes involved in NFκB signaling, including most of the regulated apoptosis or survival associated genes here, are often gene targets of active NFκB signaling themselves [Pahl, 1999]. This indicates decreased NFκB signaling after Con A challenge of Con A pretreated mice. However, NFκB does not have a detrimental impact in Con A induced hepatitis [Streetz et al., 2001] and thus, inhibition of NFκB signaling is unlikely to account for resistance towards Con A induced injury in hepatocytes. On the contrary, NFκB induces anti-apoptotic survival factors upon death receptor ligation by e.g. TNFα [Papa et al., 2009]. This suggests, that decreased NFκB signaling might either be the result of a decreased stress response in hepatocytes soon after Con A challenge of pretreated mice or that NFκB signaling is decreased in other cells where it indeed induces liver detrimental pathways. Besides NFκB signaling associated genes, the genes c-jun and c-fos were less induced in Con A challenged pretreated mice compared to Con A challenged naïve mice (data not shown). Products of these genes form the transcription factor AP-1 upon activation, e.g. via JNK signaling and at least the former one can be induced by AP-1 itself in a positive feedback loop [Minet et al., 2001] suggesting that JNK signaling might be decreased in Con A challenged pretreated mice. Interestingly, the JNK pathway is another pathway that is activated by TNF receptor signaling and this pathway seems to be detrimental in liver injury [Papa et al., 2009]. Con A induced hepatitis has also been suggested to depend on activation of the JNK pathway [Streetz et al., 2001; Maeda et al., 2003]. Although this pathway might not directly be involved in death signaling in hepatocytes during Con A hepatitis [Ni et al., 2008; Das et al., 2009], decreased signaling via the JNK pathway in liver tissue again argues for an important role for down-regulation of TNFα upon Con A challenge of Con A pretreated mice because it is associated with inhibition of the hepato-destructive milieu in these mice.

5 Summary

The liver is an organ with a special immunologic milieu and hepatic T cell priming results rather in tolerance than in immunity. In contrast, autoimmune diseases, including autoimmune hepatitis (AIH), are characterized by loss of tolerance against self antigens. In consequential anti-self immune responses, TNFα often plays a detrimental role.
Experimental hepatitis in the mouse can be evoked by intravenous injection (i.v.) of the plant lectin Concanavalin A (Con A) that results in Th1 mediated activation of sessile innate immune cells in the liver, particularly in activation of Kupffer cells (KCs). In this model, T and NKT cell mediated cytotoxicity, the inflammatory cytokine TNFα and disruption of the hepatic microcirculation are most likely involved in damage to the hepatic parenchyma. A sublethal dose of Con A results in hepatic resistance towards a second Con A challenge 8 days later that is mediated by immunosuppression via secretion of the anti-inflammatory cytokine IL-10 by regulatory T cells (Tregs) and KCs. Fourteen days after a sublethal Con A dose resistance towards hepatic injury appears even more robust. Hallmarks of active immunosuppression, i.e. increased IL-10 and decreased IFNγ plasma cytokine levels, observed upon Con A challenge 8 days after Con A pretreatment, though, are lacking in this sustained hepatic resistance. This study was aimed to identify the protective mechanisms that inhibit damage of hepatocytes upon Con A challenge 14 days after Con A pretreatment.
The inflammatory milieu upon a second Con A challenge was examined by ELISA, T cell *in vitro* restimulation and hepatic gene expression. Experiments involving depletion or neutralization of immunosuppressive regulatory T cells (Tregs), KCs and the anti-inflammatory cytokine IL-10 were performed to investigate the role for these mediators in sustained resistance towards Con A induced hepatic injury. $CD4^+$ T cells were adoptively transfered into immunodeficient RAG1-/- mice to evaluate a role for these cells in induction of sustained liver resistance. Finally, blood accumulation in the liver was investigated via MRI and consumption of coagulation factors by prothrombin time to determine if inhibition of hepatic microcirculatory disruption is involved in sustained

resistance towards Con A induced hepatic injury.

Protection of the liver parenchyma was not the consequence of general immunosuppression because it was accompanied by high levels of the Th1 key effector cytokine IFNγ and was independent from immunosuppressive Tregs as well as from anti-inflammatory IL-10. Moreover, protection seemed to be independent from reprogramming of KCs, which are key mediators of Con A induced liver injury. Instead, TNFα plasma levels and expression of hepatic TNFα target genes were reduced upon a second Con A challenge. This correlated with decreased coagulation and maintenance of physiological microcirculation in Con A challenged protected livers. Hepatic T cells showed a sustained modified cytokine expression pattern with more pronounced IFNγ and reduced TNFα expression and might thus contribute to modulation of the hepatic immune response upon a second Con A challenge. Moreover, the pivotal role for $CD4^+$ T cells in hepatic resistance towards Con A challenge was supported by the fact that Con A pretreatment could only induce protection against a second Con A challenge in presence of $CD4^+$ T cells.

In conclusion, Con A induced hepatic polyclonal T cell priming might result in sustained modulation of the hepatic T cell cytokine response that might be beneficial for host tissue.

6 Deutschsprachige Zusammenfassung

In der Leber herrscht ein besonderes immunologisches Milieu, so resultiert aus dem Priming von T Zellen in der Leber z.B. eher Toleranz als Immunität gegenüber einem Antigen. Im Gegensatz dazu führt der Verlust von Toleranz gegenüber Selbstantigenen zu Autoimmunkrankheiten, einschließlich der Autoimmunhepatitis. In solchen Immunantworten gegen Selbstantigene kommt dem Zytokin TNFα oft eine Gewebe schädigende Rolle zu.

Experimentelle Hepatitis kann in der Maus durch intravenöse Applikation von dem Pflanzenlectin Concanavalin A (Con A) erzeugt werden, die zur Th1-abhängigen Aktivierung von ortsansässigen Zellen des angeborenen Immunsystems, vor allem Kupffer Zellen, führt. In diesem Modell sind höchstwahrscheinlich Zytotoxizität durch T und NKT Zellen, das inflammatorische Zytokin TNFα, und Störung der hepatischen Mikrozirkulation für die Schädigung des Leberparenchyms verantwortlich. Eine subletale Dosis Con A führt zum Schutz des Leberparenchyms gegenüber einer wiederholten Applikation von Con A 8 Tage später. Dieser Schutzeffekt beruht auf der antiinflammatorischen Wirkung von IL-10, das bei der zweiten Con A Applikation vermehrt von regulatorischen T Zellen (Tregs) und Kupffer Zellen ausgeschüttet wird. Wird eine zweite Con A Dosis 14 Tage nach Erstbehandlung appliziert, so erscheint der Schutzeffekt auf die Leber sogar noch robuster. Dieser langanhaltende Schutzeffekt tritt jedoch ohne die entscheidenden immunsuppressiven Merkmale, nämlich erhöhte IL-10 Plasmaspiegel und erniedrigte IFNγ Plasmaspiegel, auf. Die vorliegende Studie hatte das Ziel, die protektiven Mechanismen aufzuklären, die den Schaden der Hepatozyten nach Con A Gabe verhindern.

Um dies zu untersuchen, wurde das inflammatorische Milieu nach zweiter Con A Gabe mit Hilfe der ELISA Technik, *in vitro* Stimulation von T Zellen, und Genexpressionsanalysen bestimmt. In Depletions- oder Neutralisierungsexperimenten wurde die Bedeutung

von Tregs, von Kupffer Zellen und von dem anti-inflammatorischen Zytokin IL-10 für den langanhaltenden Schutzeffekt der Leber untersucht. Darüber hinaus wurden $CD4^+$ T Zellen in immundefiziente RAG1-/- Mäuse transferiert, um die Beteiligung dieser Zellen für die Induktion des langanhaltenden Leberschutzes zu evaluieren. Schließlich wurde durch Bestimmung von hepatischer Blutakkumulation mittels Magnetresonanztomographie und dem Verbrauch von Koagulationsfaktoren mittels Plasmaprothrombinzeit ein möglicher Schutz vor Schädigung der hepatischen Mikrozirkulation analysiert.
Der Schutz des Leberparenchyms folgte nicht aus einer generellen Immunsuppression, da zeitgleich eine starke Th1 Immunantwort mit hohen Plasmakonzentrationen von TNFα zu beobachten war und da der Schutzeffekt unabhängig von Tregs und anti-inflammatorischem IL-10 erfolgte. Darüber hinaus schien ein Umprogrammieren von Kupffer Zellen, also der Zellen die mitunter hauptverantwortlich für den Con A induzierten Leberschaden sind, nicht nötig für den Schutzeffekt zu sein. Stattdessen waren reduzierte TNFα Plasmakonzentrationen und reduzierte Expression von hepatischen TNFα Zielgenen zu beobachten. Dies korrelierte mit verminderter Koagulation und Aufrechterhaltung der physiologischen Mikrozirkulation nach Con A Stimulation von vorbehandelten, geschützten Tieren. Hepatische T Zellen von geschützten Tieren zeigten, deutlicher als Milz Zellen, eine anhaltende modifizierte Zytokinexpression nach *in vitro* Stimulation, die durch erhöhte IFNγ und erniedrigte TNFα Expression gekennzeichnet war. Dies legt eine Beteiligung der T Zellen bei der Modulation der hepatischen Immunantwort nach Con A Stimulation 14 Tage nach Con A Vorbehandlung nahe. Unterstützt wurde diese Hypothese dadurch, dass der Schutzeffekt gegenüber Con A induziertem Leberschaden in $RAG1^{-/-}$ Mäusen nur in Anwesenheit von $CD4^+$ T Zellen möglich war.
Zusammenfassend ergibt sich daraus die Hypothese, dass polyklonale T Zellaktivierung in der Leber zu einer anhaltenden Modulation der hepatischen T Zell Immunantwort führt, die zuträglich für das Instandhalten der Leberfunktion bei starken entzündlichen Reaktionen sein kann.

Bibliography

Adams, D. H., Ju, C., Ramaiah, S. K., Uetrecht, J., & Jaeschke, H. (2010). Mechanisms of immune-mediated liver injury. *Toxicological Sciences*, 115(2), 307–321. PMID: 20071422.

Afkarian, M., Sedy, J. R., Yang, J., Jacobson, N. G., Cereb, N., Yang, S. Y., Murphy, T. L., & Murphy, K. M. (2002). T-bet is a STAT1-induced regulator of IL-12R expression in naïve CD4+ T cells. *Nature Immunology*, 3(6), 549–557. PMID: 12006974.

Ajuebor, M. N., Hogaboam, C. M., Le, T., & Swain, M. G. (2003). C-C chemokine ligand 2/monocyte chemoattractant protein-1 directly inhibits NKT cell IL-4 production and is hepatoprotective in T cell-mediated hepatitis in the mouse. *Journal of Immunology*, 170(10), 5252–5259. PMID: 12734374.

Andrews, D. M. & Smyth, M. J. (2010). A potential role for RAG-1 in NK cell development revealed by analysis of NK cells during ontogeny. *Immunology and Cell Biology*, 88(2), 107–116. PMID: 19949422.

Barnes, M. J. & Powrie, F. (2009). Hybrid Treg cells: steel frames and plastic exteriors. *Nature Immunology*, 10(6), 563–564. PMID: 19448654.

Beraza, N., Malato, Y., Sander, L. E., Al-Masaoudi, M., Freimuth, J., Riethmacher, D., Gores, G. J., Roskams, T., Liedtke, C., & Trautwein, C. (2009). Hepatocyte-specific NEMO deletion promotes NK/NKT cell- and TRAIL-dependent liver damage. *The Journal of Experimental Medicine*, 206(8), 1727–1737. PMID: 19635861.

Berger, A. (2000). Th1 and Th2 responses: what are they? *BMJ : British Medical Journal*, 321(7258), 424. PMID: 10938051.

Biburger, M. & Tiegs, G. (2008). Activation-induced NKT cell hyporesponsiveness protects from alpha-galactosylceramide hepatitis and is independent of active transregulatory factors. *Journal of Leukocyte Biology*, 84(1), 264–279. PMID: 18407967.

Bonder, C. S., Ajuebor, M. N., Zbytnuik, L. D., Kubes, P., & Swain, M. G. (2004). Essential role for neutrophil recruitment to the liver in concanavalin A-induced hepatitis. *Journal of Immunology*, 172(1), 45–53. PMID: 14688308.

Bonneville, M., O'Brien, R. L., & Born, W. K. (2010). Gammadelta T cell effector functions: a blend of innate programming and acquired plasticity. *Nature Reviews Immunology*, 10(7), 467–478. PMID: 20539306.

Böttcher, J. P., Knolle, P. A., & Stabenow, D. (2011). Mechanisms balancing tolerance and immunity in the liver. *Digestive diseases*, 29(4), 384–390. PMID: 21894009.

Chambers, B. J. & Ljunggren, H.-G. (2010). Unique features of NK cell development during ontogeny revealed in studies of RAG-1-deficient mice. *Immunology and Cell Biology*, 88(2), 105–106. PMID: 20010913.

Chen, L. & Flies, D. B. (2013). Molecular mechanisms of T cell co-stimulation and co-inhibition. *Nature Reviews Immunology*, 13(4), 227–242. PMID: 23470321.

Cogger, V. C., Muller, M., Fraser, R., McLean, A. J., Khan, J., & Le Couteur, D. G. (2004). The effects of oxidative stress on the liver sieve. *Journal of Hepatology*, 41(3), 370–376. PMID: 15336438.

Couinaud, C. (1957). *Le foie: études anatomiques et chirurgicales*. Masson et Cie.

Crawford, J. M. & Burt, A. D. (2012). 1 - Anatomy, pathophysiology and basic mechanisms of disease. In *MacSween's Pathology of the Liver (Sixth Edition)* (pp. 1–77). Edinburgh: Churchill Livingstone.

Das, M., Sabio, G., Jiang, F., Rincon, M., Flavell, R. A., & Davis, R. J. (2009). Induction of hepatitis by JNK-mediated expression of TNFα. *Cell*, 136(2), 249–260. PMID: 19167327.

Di Marco, R., Xiang, M., Zaccone, P., Leonardi, C., Franco, S., Meroni, P., & Nicoletti, F. (1999). Concanavalin A-induced hepatitis in mice is prevented by interleukin (IL)-10 and exacerbated by endogenous IL-10 deficiency. *Autoimmunity*, 31(2), 75–83. PMID: 10680745.

Elvevold, K., Smedsrød, B., & Martinez, I. (2008). The liver sinusoidal endothelial cell: a cell type of controversial and confusing identity. *American Journal of Physiology. Gastrointestinal and Liver Physiology*, 294(2), G391–400. PMID: 18063708.

Erhardt, A., Biburger, M., Papadopoulos, T., & Tiegs, G. (2007). IL-10, regulatory T cells, and Kupffer cells mediate tolerance in concanavalin A-induced liver injury in mice. *Hepatology*, 45(2), 475–485. PMID: 17256743.

Erhardt, A., Wegscheid, C., Claass, B., Carambia, A., Herkel, J., Mittrücker, H.-W., Panzer, U., & Tiegs, G. (2011). CXCR3 deficiency exacerbates liver disease and abrogates tolerance in a mouse model of immune-mediated hepatitis. *Journal of Immunology*, 186(9), 5284–5293. PMID: 21441449.

Filippo, K. D., Dudeck, A., Hasenberg, M., Nye, E., Rooijen, N. v., Hartmann, K., Gunzer, M., Roers, A., & Hogg, N. (2013). Mast cell and macrophage chemokines CXCL1/CXCL2 control the early stage of neutrophil recruitment during tissue inflammation. *Blood*. PMID: 23645836.

Fujii, Y., Kawamura, H., Kawamura, T., Kanda, Y., Matsumoto, H., Kobayashi, T., Yamamoto, T., Aoyama, T., & Abo, T. (2010). Co-appearance of autoantibody-producing $B220^{low}$ B cells with NKT cells in the course of hepatic injury. *Cellular Immunology*, 260(2), 105–112. PMID: 19857863.

Gantner, F., Leist, M., Lohse, A. W., Germann, P. G., & Tiegs, G. (1995). Concanavalin A-induced T-cell-mediated hepatic injury in mice: the role of tumor necrosis factor. *Hepatology*, 21(1), 190–198. PMID: 7806154.

Gao, B., Jeong, W.-I., & Tian, Z. (2008). Liver: An organ with predominant innate immunity. *Hepatology*, 47(2), 729–736. PMID: 18167066.

Gisa Tiegs (2003). T cells, NKT cells, and NK cells in an experimental model of autoimmune hepatitis. In M. Eric Gershwin, John M. Vierling, & Michael P. Manns (Eds.), *Liver Immunology, Principles and Practice* (pp. 171–183). Philadelphia: Hanley & Belfus, Inc., 15 edition.

Godfrey, D. I., Stankovic, S., & Baxter, A. G. (2010). Raising the NKT cell family. *Nature Immunology*, 11(3), 197–206. PMID: 20139988.

Grivennikov, S. I., Tumanov, A. V., Liepinsh, D. J., Kruglov, A. A., Marakusha, B. I., Shakhov, A. N., Murakami, T., Drutskaya, L. N., Förster, I., Clausen, B. E., Tessarollo, L., Ryffel, B., Kuprash, D. V., & Nedospasov, S. A. (2005). Distinct and nonredundant in vivo functions of TNF produced by t cells and macrophages/neutrophils: protective and deleterious effects. *Immunity*, 22(1), 93–104. PMID: 15664162.

Halder, R. C., Aguilera, C., Maricic, I., & Kumar, V. (2007). Type II NKT cell-mediated anergy induction in type I NKT cells prevents inflammatory liver disease. *The Journal of Clinical Investigation*, 117(8), 2302–2312. PMID: 17641782.

Hatano, M., Sasaki, S., Ohata, S., Shiratsuchi, Y., Yamazaki, T., Nagata, K., & Kobayashi, Y. (2008). Effects of Kupffer cell-depletion on Concanavalin A-induced hepatitis. *Cellular Immunology*, 251(1), 25–30. PMID: 18374909.

Hegde, V. L., Hegde, S., Cravatt, B. F., Hofseth, L. J., Nagarkatti, M., & Nagarkatti, P. S. (2008). Attenuation of experimental autoimmune hepatitis by exogenous and endogenous cannabinoids: involvement of regulatory T cells. *Molecular Pharmacology*, 74(1), 20–33. PMID: 18388242.

Heinzel, F. P., Sadick, M. D., Holaday, B. J., Coffman, R. L., & Locksley, R. M. (1989). Reciprocal expression of interferon gamma or interleukin 4 during the resolution or progression of murine leishmaniasis. Evidence for expansion of distinct helper T cell subsets. *The Journal of Experimental Medicine*, 169(1), 59–72. PMID: 2521244.

Hong, F., Jaruga, B., Kim, W. H., Radaeva, S., El-Assal, O. N., Tian, Z., Nguyen, V.-A., & Gao, B. (2002). Opposing roles of STAT1 and STAT3 in T cell-mediated hepatitis: regulation by SOCS. *Journal of Clinical Investigation*, 110(10). PMID: 12438448.

Ian R. Mackay MD, F. (2007). Contemporary Liver Immunology and Immunopathology. In M. E. G. M. FACP, J. M. V. M. FACP, & M. P. M. MD (Eds.), *Liver Immunology* (pp. 1–11). Humana Press.

Jaeschke, H. (2011). Reactive oxygen and mechanisms of inflammatory liver injury: Present concepts. *Journal of Gastroenterology and Hepatology*, 26 Suppl 1, 173–179. PMID: 21199529.

Jaeschke, H. & Bajt, M. L. (2004). Critical role of CXC chemokines in endotoxemic liver injury in mice. *Journal of Leukocyte Biology*, 76(6), 1089–1090; author reply 1091–1092. PMID: 15331625.

Jaruga, B., Hong, F., Kim, W.-H., & Gao, B. (2004). IFN-gamma/STAT1 acts as a proinflammatory signal in T cell-mediated hepatitis via induction of multiple chemokines and adhesion molecules: a critical role of IRF-1. *American Journal of Physiology. Gastrointestinal and Liver Physiology*, 287(5), G1044–1052. PMID: 15246962.

Josefowicz, S. Z., Lu, L.-F., & Rudensky, A. Y. (2012). Regulatory T cells: mechanisms of differentiation and function. *Annual Review of Immunology*, 30, 531–564. PMID: 22224781.

Kaneko, Y., Harada, M., Kawano, T., Yamashita, M., Shibata, Y., Gejyo, F., Nakayama, T., & Taniguchi, M. (2000). Augmentation of Valpha14 NKT cell-mediated cytotoxicity by interleukin 4 in an autocrine mechanism resulting in the development of concanavalin A-induced hepatitis. *The Journal of Experimental Medicine*, 191(1), 105–114. PMID: 10620609.

Kanellopoulos, J. M., De Petris, S., Leca, G., & Crumpton, M. J. (1985). The mitogenic lectin from phaseolus vulgaris does not recognize the t3 antigen of human t lymphocytes. *European Journal of Immunology*, 15(5), 479–486. PMID: 3873340.

Kato, J., Okamoto, T., Motoyama, H., Uchiyama, R., Kirchhofer, D., Van Rooijen, N., Enomoto, H., Nishiguchi, S., Kawada, N., Fujimoto, J., & Tsutsui, H. (2013). Interferon-gamma-mediated tissue factor expression contributes to T-cell-mediated hepatitis through induction of hypercoagulation in mice. *Hepatology*, 57(1), 362–372. PMID: 22936459.

Kaufmann, T., Jost, P. J., Pellegrini, M., Puthalakath, H., Gugasyan, R., Gerondakis, S., Cretney, E., Smyth, M. J., Silke, J., Hakem, R., Bouillet, P., Mak, T. W., Dixit, V. M., & Strasser, A. (2009). Fatal hepatitis mediated by tumor necrosis factor TNFalpha requires caspase-8 and involves the BH3-only proteins bid and bim. *Immunity*, 30(1), 56–66. PMID: 19119023.

Kawada, N., Mizoguchi, Y., Kobayashi, K., Morisawa, S., Monna, T., & Yamamoto, S. (1991). Interferon gamma modulates production of interleukin 1 and tumor necrosis factor by murine kupffer cells. *Liver*, 11(1), 42–47. PMID: 1904523.

KEGG. Apoptosis pathway, mus musculus. `http://www.genome.jp/dbget-bin/www_bget?pathway+mmu04210`. Accessed: 30-05-2013.

KEGG. Cytokine-cytokine receptor interaction pathway, mus musculus. `http://www.genome.jp/dbget-bin/www_bget?pathway+mmu04060`. Accessed: 30-05-2013.

Kinoshita, M., Uchida, T., Sato, A., Nakashima, M., Nakashima, H., Shono, S., Habu, Y., Miyazaki, H., Hiroi, S., & Seki, S. (2010). Characterization of two F4/80-positive Kupffer cell subsets by their function and phenotype in mice. *Journal of Hepatology*, 53(5), 903–910. PMID: 20739085.

Knolle, P. A., Gerken, G., Loser, E., Dienes, H. P., Gantner, F., Tiegs, G., Meyer zum Buschenfelde, K. H., & Lohse, A. W. (1996). Role of sinusoidal endothelial cells of the liver in concanavalin A-induced hepatic injury in mice. *Hepatology*, 24(4), 824–829. PMID: 8855184.

Koch, M. A., Thomas, K. R., Perdue, N. R., Smigiel, K. S., Srivastava, S., & Campbell, D. J. (2012). T-bet(+) Treg cells undergo abortive Th1 cell differentiation due to impaired expression of IL-12 receptor β2. *Immunity*, 37(3), 501–510. PMID: 22960221.

Koch, M. A., Tucker-Heard, G., Perdue, N. R., Killebrew, J. R., Urdahl, K. B., & Campbell, D. J. (2009). The transcription factor T-bet controls regulatory T cell homeostasis and function during type 1 inflammation. *Nature Immunology*, 10(6), 595–602. PMID: 19412181.

Korn, T., Bettelli, E., Oukka, M., & Kuchroo, V. K. (2009). IL-17 and Th17 Cells. *Annual Review of Immunology*, 27(1), 485–517. PMID: 19132915.

Küsters, S., Gantner, F., Künstle, G., & Tiegs, G. (1996). Interferon gamma plays a critical role in T cell-dependent liver injury in mice initiated by concanavalin A. *Gastroenterology*, 111(2), 462–471. PMID: 8690213.

Küsters, S., Tiegs, G., Alexopoulou, L., Pasparakis, M., Douni, E., Künstle, G., Bluethmann, H., Wendel, A., Pfizenmaier, K., Kollias, G., & Grell, M. (1997). In vivo

evidence for a functional role of both tumor necrosis factor (TNF) receptors and transmembrane TNF in experimental hepatitis. *European Journal of Immunology*, 27(11), 2870–2875. PMID: 9394812.

Lahl, K., Loddenkemper, C., Drouin, C., Freyer, J., Arnason, J., Eberl, G., Hamann, A., Wagner, H., Huehn, J., & Sparwasser, T. (2007). Selective depletion of Foxp3+ regulatory T cells induces a scurfy-like disease. *The Journal of Experimental Medicine*, 204(1), 57–63. PMID: 17200412.

Lehmann, V., Freudenberg, M. A., & Galanos, C. (1987). Lethal toxicity of lipopolysaccharide and tumor necrosis factor in normal and D-galactosamine-treated mice. *The Journal of Experimental Medicine*, 165(3), 657–663. PMID: 3819645.

Leist, M., Gantner, F., Bohlinger, I., Germann, P. G., Tiegs, G., & Wendel, A. (1994). Murine hepatocyte apoptosis induced in vitro and in vivo by TNF-alpha requires transcriptional arrest. *Journal of Immunology*, 153(4), 1778–1788. PMID: 8046244.

Li, X., Klintman, D., Liu, Q., Sato, T., Jeppsson, B., & Thorlacius, H. (2004). Critical role of CXC chemokines in endotoxemic liver injury in mice. *Journal of Leukocyte Biology*, 75(3), 443–452. PMID: 14673016.

Liberal, R., Grant, C. R., Mieli-Vergani, G., & Vergani, D. (2013). Autoimmune hepatitis: A comprehensive review. *Journal of Autoimmunity*, 41, 126–139. PMID: 23218932.

Liedtke, C., Bangen, J.-M., Freimuth, J., Beraza, N., Lambertz, D., Cubero, F. J., Hatting, M., Karlmark, K. R., Streetz, K. L., Krombach, G. A., Tacke, F., Gassler, N., Riethmacher, D., & Trautwein, C. (2011). Loss of caspase-8 protects mice against inflammation-related hepatocarcinogenesis but induces non-apoptotic liver injury. *Gastroenterology*, 141(6), 2176–2187. PMID: 21878202.

Liu, Z. X., Govindarajan, S., Okamoto, S., & Dennert, G. (2000). NK cells cause liver injury and facilitate the induction of T cell-mediated immunity to a viral liver infection. *Journal of Immunology*, 164(12), 6480–6. PMID: 10843705.

Louis, H., Le Moine, A., Quertinmont, E., Peny, M. O., Geerts, A., Goldman, M., Le Moine, O., & Devière, J. (2000). Repeated concanavalin A challenge in mice

induces an interleukin 10-producing phenotype and liver fibrosis. *Hepatology*, 31(2), 381–390. PMID: 10655261.

Louis, H., Le Moine, O., Peny, M. O., Quertinmont, E., Fokan, D., Goldman, M., & Devière, J. (1997). Production and role of interleukin-10 in concanavalin A-induced hepatitis in mice. *Hepatology*, 25(6), 1382–1389. PMID: 9185757.

Maeda, S., Chang, L., Li, Z.-W., Luo, J.-L., Leffert, H., & Karin, M. (2003). IKKbeta is required for prevention of apoptosis mediated by cell-bound but not by circulating TNFalpha. *Immunity*, 19(5), 725–737. PMID: 14614859.

Malarkey, D. E., Johnson, K., Ryan, L., Boorman, G., & Maronpot, R. R. (2005). New insights into functional aspects of liver morphology. *Toxicologic Pathology*, 33(1), 27–34. PMID: 15805053.

Malchow, S., Thaiss, W., Jänner, N., Waetzig, G. H., Gewiese-Rabsch, J., Garbers, C., Yamamoto, K., Rose-John, S., & Scheller, J. (2011). Essential role of neutrophil mobilization in concanavalin A-induced hepatitis is based on classic IL-6 signaling but not on IL-6 trans-signaling. *Biochimica Et Biophysica Acta*, 1812(3), 290–301. PMID: 21130161.

Mazurier, F., Fontanellas, A., Salesse, S., Taine, L., Landriau, S., Moreau-Gaudry, F., Reiffers, J., Peault, B., Di Santo, J. P., & de Verneuil, H. (1999). A novel immunodeficient mouse model–RAG2 x common cytokine receptor gamma chain double mutants–requiring exogenous cytokine administration for human hematopoietic stem cell engraftment. *Journal of Interferon & Cytokine Research*, 19(5), 533–541. PMID: 10386866.

Minet, E., Michel, G., Mottet, D., Piret, J. P., Barbieux, A., Raes, M., & Michiels, C. (2001). c-JUN gene induction and AP-1 activity is regulated by a JNK-dependent pathway in hypoxic HepG2 cells. *Experimental Cell Research*, 265(1), 114–124. PMID: 11281649.

Miyazawa, Y., Tsutsui, H., Mizuhara, H., Fujiwara, H., & Kaneda, K. (1998). Involvement of intrasinusoidal hemostasis in the development of concanavalin A-induced hepatic injury in mice. *Hepatology*, 27(2), 497–506. PMID: 9462649.

Mizuhara, H., Kuno, M., Seki, N., Yu, W. G., Yamaoka, M., Yamashita, M., Ogawa, T., Kaneda, K., Fujii, T., Senoh, H., & Fujiwara, H. (1998). Strain difference in the induction of T-cell activation-associated, interferon gamma-dependent hepatic injury in mice. *Hepatology*, 27(2), 513–519. PMID: 9462651.

Mizuhara, H., O'Neill, E., Seki, N., Ogawa, T., Kusunoki, C., Otsuka, K., Satoh, S., Niwa, M., Senoh, H., & Fujiwara, H. (1994). T cell activation-associated hepatic injury: mediation by tumor necrosis factors and protection by interleukin 6. *The Journal of Experimental Medicine*, 179(5), 1529–1537. PMID: 8163936.

Mizuhara, H., Uno, M., Seki, N., Yamashita, M., Yamaoka, M., Ogawa, T., Kaneda, K., Fujii, T., Senoh, H., & Fujiwara, H. (1996). Critical involvement of interferon gamma in the pathogenesis of T-cell activation-associated hepatitis and regulatory mechanisms of interleukin-6 for the manifestations of hepatitis. *Hepatology*, 23(6), 1608–1615. PMID: 8675184.

Morafo, V., Srivastava, K., Huang, C.-K., Kleiner, G., Lee, S.-Y., Sampson, H. A., & Li, A. (2003). Genetic susceptibility to food allergy is linked to differential TH2-TH1 responses in C3H/HeJ and BALB/c mice. *The Journal of Allergy and Clinical Immunology*, 111(5), 1122–1128. PMID: 12743580.

Mullen, A. C., High, F. A., Hutchins, A. S., Lee, H. W., Villarino, A. V., Livingston, D. M., Kung, A. L., Cereb, N., Yao, T.-P., Yang, S. Y., & Reiner, S. L. (2001). Role of T-bet in Commitment of TH1 Cells Before IL-12-Dependent Selection. *Science*, 292(5523), 1907–1910. PMID: 11397944.

Nakashima, H., Kinoshita, M., Nakashima, M., Habu, Y., Shono, S., Uchida, T., Shinomiya, N., & Seki, S. (2008). Superoxide produced by Kupffer cells is an essential effector in concanavalin A-induced hepatitis in mice. *Hepatology*, 48(6), 1979–1988. PMID: 18942689.

Netea, M. G., Van der Meer, J. W. M., Sutmuller, R. P., Adema, G. J., & Kullberg, B.-J. (2005). From the Th1/Th2 paradigm towards a Toll-like receptor/T-helper bias. *Antimicrobial Agents and Chemotherapy*, 49(10), 3991–3996. PMID: 16189071.

Ni, H.-M., Chen, X., Ding, W.-X., Schuchmann, M., & Yin, X.-M. (2008). Differential

roles of JNK in ConA/GalN and ConA-induced liver injury in mice. *The American Journal of Pathology*, 173(4), 962–972. PMID: 18772342.

Nicoletti, F., Zaccone, P., Xiang, M., Magro, G., Di Mauro, M., Di Marco, R., Garotta, G., & Meroni, P. (2000). Essential pathogenetic role for interferon (IFN-)gamma in concanavalin A-induced T cell-dependent hepatitis: exacerbation by exogenous IFN-gamma and prevention by IFN-gamma receptor-immunoglobulin fusion protein. *Cytokine*, 12(4), 315–323. PMID: 10805211.

Nishikage, T., Seki, S., Toyabe, S., Abo, T., Kagata, Y., Iwai, T., & Hiraide, H. (1999). Inhibition of concanavalin A-induced hepatic injury of mice by bacterial lipopolysaccharide via the induction of IL-6 and the subsequent reduction of IL-4: the cytokine milieu of concanavalin A hepatitis. *Journal of Hepatology*, 31(1), 18–26. PMID: 10424279.

Ojiro, K., Ebinuma, H., Nakamoto, N., Wakabayashi, K., Mikami, Y., Ono, Y., Po-Sung, C., Usui, S., Umeda, R., Takaishi, H., Yamagishi, Y., Saito, H., Kanai, T., & Hibi, T. (2010). MyD88-dependent pathway accelerates the liver damage of Concanavalin A-induced hepatitis. *Biochemical and Biophysical Research Communications*, 399(4), 744–749. PMID: 20696131.

Pahl, H. L. (1999). Activators and target genes of Rel/NF-kappaB transcription factors. *Oncogene*, 18(49), 6853–6866. PMID: 10602461.

Papa, S., Bubici, C., Zazzeroni, F., & Franzoso, G. (2009). Mechanisms of liver disease: cross-talk between the NF-kappaB and JNK pathways. *Biological Chemistry*, 390(10), 965–976. PMID: 19642868.

Poltorak, A., He, X., Smirnova, I., Liu, M. Y., Van Huffel, C., Du, X., Birdwell, D., Alejos, E., Silva, M., Galanos, C., Freudenberg, M., Ricciardi-Castagnoli, P., Layton, B., & Beutler, B. (1998). Defective LPS signaling in C3H/HeJ and C57BL/10ScCr mice: mutations in Tlr4 gene. *Science*, 282(5396), 2085–2088. PMID: 9851930.

Pot, C., Apetoh, L., & Kuchroo, V. K. (2011). Type 1 regulatory T cells (Tr1) in autoimmunity. *Seminars in Immunology*, 23(3), 202–208. PMID: 21840222.

Quintáns, J., Yokoyama, A., Evavold, B., Hirsch, R., & Mayforth, R. D. (1989). Direct activation of murine resting T cells by con A or anti-CD3 Ig. *The Journal of Molecular and Cellular Immunology: JMCI*, 4(4), 225–237. PMID: 2532886.

Racanelli, V. & Rehermann, B. (2006). The liver as an immunological organ. *Hepatology*, 43(S1), S54–S62. PMID: 16447271.

Radaeva, S., Sun, R., Pan, H.-N., Hong, F., & Gao, B. (2004). Interleukin 22 (IL-22) plays a protective role in T cell-mediated murine hepatitis: IL-22 is a survival factor for hepatocytes via STAT3 activation. *Hepatology*, 39(5), 1332–1342. PMID: 15122762.

Rappaport, A. M., Borowy, Z. J., Lougheed, W. M., & Lotto, W. N. (1954). Subdivision of hexagonal liver lobules into a structural and functional unit; role in hepatic physiology and pathology. *The Anatomical Record*, 119(1), 11–33. PMID: 13180999.

Sass, G., Heinlein, S., Agli, A., Bang, R., Schümann, J., & Tiegs, G. (2002). Cytokine expression in three mouse models of experimental hepatitis. *Cytokine*, 19(3). PMID: 12242077.

Scheuplein, F., Rissiek, B., Driver, J. P., Chen, Y.-G., Koch-Nolte, F., & Serreze, D. V. (2010). A recombinant heavy chain antibody approach blocks ART2 mediated deletion of an iNKT cell population that upon activation inhibits autoimmune diabetes. *Journal of Autoimmunity*, 34(2), 145–154. PMID: 19796917.

Schmidt, A., Oberle, N., & Krammer, P. H. (2012). Molecular mechanisms of Treg-mediated T cell suppression. *Frontiers in Immunology*, 3, 51. PMID: 22566933.

Schümann, J., Wolf, D., Pahl, A., Brune, K., Papadopoulos, T., van Rooijen, N., & Tiegs, G. (2000). Importance of Kupffer cells for T-cell-dependent liver injury in mice. *The American Journal of Pathology*, 157(5), 1671–1683. PMID: 11073826.

Scott, P., Natovitz, P., Coffman, R. L., Pearce, E., & Sher, A. (1988). Immunoregulation of cutaneous leishmaniasis. T cell lines that transfer protective immunity or exacerbation belong to different T helper subsets and respond to distinct parasite antigens. *The Journal of Experimental Medicine*, 168(5), 1675–1684. PMID: 2903212.

Seino, K., Kayagaki, N., Takeda, K., Fukao, K., Okumura, K., & Yagita, H. (1997). Contribution of Fas ligand to T cell-mediated hepatic injury in mice. *Gastroenterology*, 113(4), 1315–1322. PMID: 9322527.

Seman, M., Adriouch, S., Scheuplein, F., Krebs, C., Freese, D., Glowacki, G., Deterre, P., Haag, F., & Koch-Nolte, F. (2003). NAD-induced T cell death: ADP-ribosylation of cell surface proteins by ART2 activates the cytolytic P2X7 purinoceptor. *Immunity*, 19(4), 571–582. PMID: 14563321.

Streetz, K., Fregien, B., Plümpe, J., Körber, K., Kubicka, S., Sass, G., Bischoff, S. C., Manns, M. P., Tiegs, G., & Trautwein, C. (2001). Dissection of the intracellular pathways in hepatocytes suggests a role for Jun kinase and IFN regulatory factor-1 in Con A-induced liver failure. *Journal of Immunology*, 167(1), 514–523. PMID: 11418690.

Sun, R., Tian, Z., Kulkarni, S., & Gao, B. (2004). IL-6 prevents T cell-mediated hepatitis via inhibition of NKT cells in CD4+ T cell- and STAT3-dependent manners. *Journal of Immunology*, 172(9), 5648–5655. PMID: 15100309.

Swain, M. G. (2010). Natural killer T cells within the liver: conductors of the hepatic immune orchestra. *Digestive diseases (Basel, Switzerland)*, 28(1), 7–13. PMID: 20460885.

Tagawa, Y., Kakuta, S., & Iwakura, Y. (1998). Involvement of Fas/Fas ligand system-mediated apoptosis in the development of concanavalin A-induced hepatitis. *European Journal of Immunology*, 28(12), 4105–4113. PMID: 9862346.

Tagawa, Y., Matthys, P., Heremans, H., Dillen, C., Zaman, Z., Iwakura, Y., & Billiau, A. (2000). Bimodal role of endogenous interleukin-6 in concanavalin A-induced hepatitis in mice. *Journal of Leukocyte Biology*, 67(1), 90–96. PMID: 10648002.

Takeda, K., Hayakawa, Y., Van Kaer, L., Matsuda, H., Yagita, H., & Okumura, K. (2000). Critical contribution of liver natural killer T cells to a murine model of hepatitis. *Proceedings of the National Academy of Sciences of the United States of America*, 97(10), 5498–5503. PMID: 10792025.

Thomson, A. W. & Knolle, P. A. (2010). Antigen-presenting cell function in the tolerogenic liver environment. *Nature Reviews Immunology*, 10(11), 753–766. PMID: 20972472.

Tiegs, G., Hentschel, J., & Wendel, A. (1992). A T cell-dependent experimental liver injury in mice inducible by concanavalin A. *The Journal of Clinical Investigation*, 90(1), 196–203. PMID: 1634608.

Tiegs, G. & Lohse, A. W. (2010). Immune tolerance: what is unique about the liver. *Journal of Autoimmunity*, 34(1), 1–6. PMID: 19717280.

Van Rooijen, N. & Sanders, A. (1994). Liposome mediated depletion of macrophages: mechanism of action, preparation of liposomes and applications. *Journal of Immunological Methods*, 174(1-2), 83–93. PMID: 8083541.

Vermijlen, D., Luo, D., Froelich, C. J., Medema, J. P., Kummer, J. A., Willems, E., Braet, F., & Wisse, E. (2002). Hepatic natural killer cells exclusively kill splenic/blood natural killer-resistant tumor cells by the perforin/granzyme pathway. *Journal of Leukocyte Biology*, 72(4), 668–676. PMID: 12377935.

Vollmar, B. & Menger, M. D. (2009). The hepatic microcirculation: mechanistic contributions and therapeutic targets in liver injury and repair. *Physiological Reviews*, 89(4), 1269–1339. PMID: 19789382.

Wajant, H., Pfizenmaier, K., & Scheurich, P. (2003). Tumor necrosis factor signaling. *Cell death and differentiation*, 10(1), 45–65. PMID: 12655295.

Watanabe, Y., Morita, M., & Akaike, T. (1996). Concanavalin A induces perforin-mediated but not Fas-mediated hepatic injury. *Hepatology*, 24(3), 702–710. PMID: 8781346.

Wei, H.-X., Chuang, Y.-H., Li, B., Wei, H., Sun, R., Moritoki, Y., Gershwin, M. E., Lian, Z.-X., & Tian, Z. (2008). CD4+ CD25+ Foxp3+ regulatory T cells protect against T cell-mediated fulminant hepatitis in a TGF-beta-dependent manner in mice. *Journal of Immunology*, 181(10), 7221–7229. PMID: 18981144.

Wolk, K., Witte, E., Witte, K., Warszawska, K., & Sabat, R. (2010). Biology of interleukin-22. *Seminars in Immunopathology*, 32(1), 17–31. PMID: 20127093.

Wong, C. H. Y., Jenne, C. N., Lee, W.-Y., Léger, C., & Kubes, P. (2011). Functional innervation of hepatic iNKT cells is immunosuppressive following stroke. *Science*, 334(6052), 101–105. PMID: 21921158.

Yamamoto, T., Naito, M., Moriyama, H., Umezu, H., Matsuo, H., Kiwada, H., & Arakawa, M. (1996). Repopulation of murine Kupffer cells after intravenous administration of liposome-encapsulated dichloromethylene diphosphonate. *The American Journal of Pathology*, 149(4), 1271–1286. PMID: 8863675.

Yang, M.-C., Chang, C.-P., & Lei, H.-Y. (2010). Endothelial cells are damaged by autophagic induction before hepatocytes in Con A-induced acute hepatitis. *International Immunology*, 22(8), 661–670. PMID: 20547544.

Ye, F., Yan, S., Xu, L., Jiang, Z., Liu, N., Xiong, S., Wang, Y., & Chu, Y. (2009). Tr1 regulatory T cells induced by ConA pretreatment prevent mice from ConA-induced hepatitis. *Immunology Letters*, 122(2), 198–207. PMID: 19200442.

Zimmermann, H. W., Trautwein, C., & Tacke, F. (2012). Functional role of monocytes and macrophages for the inflammatory response in acute liver injury. *Frontiers in Physiology*, 3, 56. PMID: 23091461.

Danksagung

Zunächst danke ich herzlich Frau Prof. Dr. Gisa Tiegs für das interessante Thema und für das Ermöglichen eigenständigen Arbeitens. Darüber hinaus danke ich ihr, dass ich meine Promotion im Graduiertenkolleg des SFB841 mit den damit verbundenen stetigen hilfreichen Diskussionen durchführen konnte.
Ebenfalls besonders bedanke ich mich bei Frau Dr. Annette Erhardt. Sie wies mich in die Durchflusszytometrie ein und stand mir immer für Diskussion und mit Ideen zur Weiterführung des Projekts zur Verfügung.
Mein Dank gilt auch Herrn PD Dr. Thomas Jacobs und Herrn Prof. Dr. Christoph Schramm, die als Betreuungskommission im Graduiertenkolleg meine Arbeit mit Diskussionen und Anregungen unterstützt haben.
Frau PD Dr. Minka Breloer danke ich für die Begutachtung der vorliegenden Arbeit.
Darüber hinaus möchte ich Thomas Ernst und Dr. Harald Ittrich für die Hilfe am MRT danken. Kristin Klätschke danke ich für die Hilfe beim Durchführen des Microarrays und Herrn Benjamin Otto für die Hilfe bei der komplexen Auswertung der Daten. Bei Dr. Björn Rissiek bedanke ich mich für die Diskussion bezüglich der Kultivierung von NKT Zellen und danke ihm sowie Prof. Dr. Friedrich Koch-Nolte für das Bereitstellen des s+16a Antikörpers. Bei Frau Dr. Mareike Sandmann, Herrn Dr. Artur Gontarewicz und Herrn Dr. Alexander Quaas bedanke ich mich für das Anfertigen und die Beurteilung der H&E gefärbten histologischen Schnitte.
Ich danke den Kollegiaten sowie den Projektleitern des Graduiertenkollegs für die motivierenden, gemeinschaftlichen Veranstaltungen im Rahmen des Graduiertenkollegs.
Dankbar bin ich all meinen aktuellen und ehemaligen Kollegen für das angenehme, freundschaftliche Arbeitsklima. Claudia Wegscheid, Sven Burghardt und Fabian Flottman, die auch mit dem Con A Mausmodell arbeiteten, möchte ich für Diskussion und für tatkräftige Unterstützung bei größeren Versuchen, Elena Tasika und Carsten Rothkegel für technische Unterstützung danken. Auch den BTA Schülerinnen Imke, Lisa-Marie, Magdalena, Mareike, Kristin und Carolina danke ich für technische Unterstützung. Katie

Tungatt danke ich dafür, dass sie mich und meine Arbeit als Praktikantin im Rahmen des DAAD RISE Programms unterstützt hat. Ellen Gardner danke ich für das Korrekturlesen.
Schließlich danke ich meiner Familie und meinen Freunden, insbesondere meinen Mitbewohnern und meinem Bruder, fürs Aufrichten in enttäuschenden Momenten. Meinen Eltern danke ich für ihre immerwährende Unterstützung. Und meiner Freundin Ioanna danke ich für all die Energie, die sie mir verleiht.

Eidesstattliche Versicherung

Hiermit erkläre ich an Eides statt, dass ich die vorliegende Dissertationsschrift selbst verfasst und keine anderen als die angegebenen Quellen und Hilfsmittel benutzt habe.

Unterschrift: Hamburg, 24.7.13 B. Cl